DEVELOPMENT AND CHARACTERIZATION OF STABLE GLYCOENZYME CONJUGATES

A Dissertation

by

DUSTIN WAYNE RITTER

Submitted to the Office of Graduate and Professional Studies of
Texas A&M University
in partial fulfillment of the requirements for the degree of

DOCTOR OF PHILOSOPHY

Chair of Committee,	Michael J. McShane
Committee Members,	Kenith E. Meissner
	Melissa A. Grunlan
	Christie M. Sayes
Head of Department,	Gerard L. Coté

December 2014

Major Subject: Biomedical Engineering

ABSTRACT

Optical glucose biosensors are being developed for long-term monitoring in diabetic individuals. These sensors rely upon the enzyme glucose oxidase, and loss of enzymatic activity leads to a need for frequent recalibration and eventually sensor replacement. Current enzyme stabilization strategies are effective, but generally result in a large increase in size and exclusion from the solution-phase. This sacrifice of native properties precludes the stabilized enzyme from incorporation into the aforementioned sensing platform, which requires that the enzyme be homogenously distributed and entrapped within a hydrogel. It is this incompatibility which provides the motivation for the development of new non-traditional enzyme stabilization strategies.

Toward that end, this work focuses on the development and characterization of three enzyme modification strategies, all of which are intended to stabilize enzyme activity while permitting incorporation into an optical biosensing hydrogel. The first approach involves glycosylation site-targeted covalent attachment of poly(ethylene glycol) to glucose oxidase, which improves storage stability by 60%. The second approach builds upon the first, but subsequent modification of the poly(ethylene glycol)-modified glucose oxidase is performed to further stabilize the enzyme. This approach improves long-term storage stability by an order of magnitude. The final approach involves encasement of the glycoenzyme within a shell of albumin, wherein the inert protein is attached at the glycosylation sites in an orthogonal manner. This technique

result in highly thermostable enzyme, retaining greater than 25 times more activity than native glucose oxidase following exposure to buffer at 60 °C.

In summary, enzyme deactivation is expected to be a major barrier in the realization of long-term glucose sensing with fully implantable optical glucose biosensors, and this work represents a step towards overcoming that hurdle. Each enzyme modification strategy yields a stabilized enzyme under certain conditions, whether it be long-term storage, elevated temperature, or exposure to various solvents/additives. This work enables the stabilized enzymes to be incorporated into hydrogels for evaluation under simulated *in vivo* conditions, followed by *in vivo* evaluation. Finally, it is expected that these enzyme stabilization approaches will be advantageous in other applications as well, including *in vitro* diagnostics, tissue engineering, and therapeutic biologicals.

DEDICATION

I would like to dedicate this work to my amazing wife, Sarah, for her patience, love, and tireless support—especially through the tougher times of graduate school! I feel so lucky to have had someone by my side who experienced everything in parallel with me. I am sure that I would not be who I am today if she was not in my life. As this chapter of our lives comes to a close, I look forward to the future that we will make together.

ACKNOWLEDGEMENTS

I would like to thank my committee chair, Dr. Michael McShane, for fostering my interest in biomedical research when I was an undergraduate student and for helping me grow as an independent researcher. Dr. McShane also taught me what it means to be driven toward a goal. I am grateful to my committee members, Dr. Kenith Meissner, Dr. Melissa Grunlan, and Dr. Christie Sayes, for their guidance and support throughout the course of this research. I would also like to thank Dr. Gerard Coté and Dr. Kristen Maitland for their mentorship and their role in my starting down a path toward improving global health; also, thanks to Dr. Coté for keeping Sarah and I company in Rwanda for a month! Dr. Duncan Maitland and Dr. Saurabh Biswas are acknowledged for their valuable advice and mentorship along the way. Finally, thanks to the rest of the awesome faculty and staff of the Biomedical Engineering Department.

I've had the opportunity to work alongside so many great researchers, and for that, I am so very grateful. As an undergraduate student, I worked in Dr. McShane's lab under the mentorship of Dr. Erich Stein; this early experience taught me a great deal about research and heavily influenced my decision to pursue a doctoral degree. During my first few years of graduate school, I continued to learn from the more senior students, particularly Dr. Huiguang Zhu and Dr. Saurabh Singh. However, all of the members of the McShane group—past and present—are acknowledged for enriching my experience at Texas A&M University. In particular, I would like to thank Dr. Jason Roberts and Jared Newton, both of whom have made significant contributions toward the completion

of this work. Jason is acknowledged for his part in the concept generation of BSA-GOx, as well as the planning and completion of some of the PEG-GOx and BSA-GOx work. Jared has performed or assisted in the completion of a number of the experiments included throughout this work.

Dr. Larry Dangott, Director of the Protein Chemistry Laboratory at Texas A&M University, is gratefully acknowledged for providing technical expertise, comments, and suggestions. I would also like to thank the team at Spectrum Labs, specifically Cassidy Markee, for "going the extra mile" to provide the experimental apparatus which permitted completion of the glucose exposure experiments.

I would like to extend my heartfelt gratitude to the National Science Foundation for providing me with funding in the form of a Graduate Research Fellowship. I also wish to acknowledge the Dwight Look College of Engineering at Texas A&M University for support through the Barclay/Willson National Excellence Fellowship.

Finally, I could not have made it to this point without a strong support system of family and friends. In particular, I would like to thank my mother and father for their guidance, support, and encouragement in everything I have done. Early on, they made my education a priority, which helped me to recognize its importance, and for that I am very grateful.

NOMENCLATURE

AG	Albuminated glycoenzyme
BMPH	*N*-(β-maleimidopropionic acid) hydrazide
BSA	Bovine serum albumin
BSA-Cat	Bovine serum albumin-modified catalase
BSA-GOx	Bovine serum albumin-modified glucose oxidase
Cat	Catalase
CLEA	Crosslinked enzyme aggregate
CLEC	Crosslinked enzyme crystal
DLS	Dynamic light scattering
DMSO	Dimethyl sulfoxide
EtOH	Ethanol
FAD	Flavin adenine dinucleotide
GA	Glutaraldehyde
GFC	Gel filtration chromatography
GOx	Glucose oxidase
MALDI-TOF	Matrix-assisted laser desorption/ionization time-of-flight
PBS	Phosphate-buffered saline
PEG	Poly(ethylene glycol)
PEG-GOx	PEGylated glucose oxidase
PEG-Hz	Hydrazide-functionalized poly(ethylene glycol)

pHEMA	Poly(2-hydroxyethyl methacrylate)
pHEMA-*co*-AAm	Poly[(2-hydroxyethyl methacrylate)-*co*-acrylamide]
pHEMA-*co*-AEMA	Poly[(2-hydroxyethyl methacrylate)-*co*-(2-aminoethyl methacrylate)]

TABLE OF CONTENTS

Page

LIST OF FIGURES

Page

LIST OF TABLES

Page

1. INTRODUCTION

Enzymes are employed across a wide variety of fields, ranging from industrial applications like food processing to more research-focused applications such as molecular biology. In biomedical engineering, enzymes play a particularly significant role in certain types of biosensors. A well-known and critically important example is the glucose biosensor, the most common of which relies upon the glycoenzyme glucose oxidase (GOx). Glucose biosensors can and should be used by individuals with diabetes to monitor blood glucose levels, allowing appropriate measures to be taken if glucose levels deviate from the euglycemic range; this is vital as intensive therapy has been shown to delay the onset and slow the progression of diabetic complications.[1]

Glucose test strips, which are used in conjunction with point-of-care blood glucose meters, utilize GOx immobilized on an electrode within the strip. The enzyme reacts with glucose in a patient's blood sample and produces a proportional amount of hydrogen peroxide, which can be detected electrochemically and related back to the patient's blood glucose level. A similar technique is employed in current commercially available continuous glucose monitoring systems, which incorporate a percutaneous electrode that dwells within a patient's tissue.[2]

As an alternative to the current continuous glucose monitoring systems, our lab is developing optical glucose biosensors, which are also intended for long-term monitoring, but are luminescent and therefore do not require a physical connection between the sensor and the reader.[3-7] In these sensors, GOx is used to catalyze a reaction

between oxygen and glucose within the interstitial fluid. The decrease in oxygen resulting from the enzymatic reaction can be monitored using a luminophore that is collisionally quenched by oxygen and allows for calculation of the glucose concentration. The enzyme catalase (Cat) can also be incorporated to convert hydrogen peroxide—produced by the GOx-induced reduction of oxygen—back into oxygen and water;[6] this is important as hydrogen peroxide has been shown to deactivate GOx.[8]

Regardless of the application (biomedical or otherwise), enzymes are valued for their ability to convert substrate to product with high selectivity. This is only possible for as long as the enzyme maintains its catalytic activity. At minimum, loss of enzymatic activity can translate to financial losses—the cost of replacing deactivated enzyme or decreased revenue resulting from decreased yield of a product. However, in applications such as implantable glucose biosensors where replacement of deactivated enzyme is not trivial, the implications are far worse. Loss of enzymatic activity can drastically affect sensor response, leading to a need for frequent recalibration and eventually sensor replacement. If glucose prediction errors are permitted to exceed 20% (*e.g.*, resulting from failure to recalibrate or from improper recalibration), incorrect therapeutic decisions can be made, which can have severe consequences in terms of patient outcomes.[9]

When evaluating the stability of an enzyme, loss of activity over time and throughout normal operating conditions is certainly important, but should not be the only factor that is considered or assessed. In an enzyme-containing device, there are a number of factors that can lead to enzyme deactivation—during fabrication, processing,

distribution, and operation under extreme or abnormal conditions—to which an enzyme should ideally be stabilized. Depending upon the application, a long shelf-life, the ability to withstand harsh sterilization procedures, extreme temperatures (high and/or low), multiple freeze-thaw cycles, and exposure to various additives might be desirable.

Given the ubiquity of enzymes, myriad enzyme stabilization approaches have emerged over time. Many of these techniques—including those based on crosslinking,[10-15] chemical modification,[16-19] and immobilization on a solid support[20]—are quite effective. However, they often render the enzymes orders of magnitude larger than their native size, which can significantly limit diffusion, and the enzyme is no longer in the solution phase. In some cases, initial activity is significantly reduced upon stabilization (*e.g.*, due to random modification of groups involved in catalysis). These properties are requisite or desirable for incorporation of enzymes into our optical glucose biosensing platform; therefore, current enzyme stabilization approaches have some incompatibility issues with our current glucose biosensors.

Therefore, to realize our lab's goal of long-term fully implantable optical glucose biosensors, non-traditional enzyme stabilization strategies must be considered. Toward that end, this dissertation focuses on three enzyme stabilization strategies. The first approach involves the covalent attachment of poly(ethylene glycol) (PEG) chains to GOx, but rather than random multi-site PEGylation, glycosylation sites on the enzyme are targeted for attachment of the PEG. This approach was originally proposed by Zalipsky and co-workers,[21, 22] but the work presented herein represents the first full physical and functional characterization of the stability of GOx PEGylated in this

manner. The second and third approaches are novel and were inspired by the GOx immobilization strategy used in current glucose biosensors; however, a higher level of refinement has been achieved, in that these approaches are much more controlled and applicable on the level of a single enzyme. The second approach utilizes the glycosylation site-targeted PEGylation strategy, but subsequent modification of the PEGylated GOx (PEG-GOx) is performed in an effort to further stabilize the enzyme. The third and final approach involves encasement of two types of glycoenzymes (*i.e.*, GOx and Cat) within a shell of bovine serum albumin (BSA), wherein the inert protein is attached at the glycosylation sites in an orthogonal manner to form the albuminated glycoenzyme (AG).

The content of this dissertation is organized to facilitate presentation of the findings in the clearest and most logical manner possible. Several of the sections contained herein have been submitted for publication or are available in print. In Section 2, the background for this work is provided, with an emphasis on existing approaches to achieve enzymatic stability. The following three sections describe the synthesis, physical characterization, and functional characterization of PEG-GOx (Section 3), chemically modified PEG-GOx (Section 4), and AGs (Section 5). Some of the results and associated methods presented in Section 3 were published in *Enzyme and Microbial Technology*,[23] and some of the results and associated methods presented in Section 4 were published in *RSC Advances*.[24] Finally, Section 6 presents the conclusions drawn from this work, and future directions are proposed.

2. BACKGROUND

2.1. Current Enzyme Stabilization Strategies

The utility of an enzyme is often limited by its lifespan, which is determined by natural processes such as denaturation and degradation. An enzyme's useful lifespan can be shortened when it is exposed to harsh environmental conditions or industrial processing.[25, 26] Many enzyme stabilization approaches have emerged as a result of enzymes' widespread usage across various fields, and a vast number of recent reviews have been dedicated to the subject.[20, 26-34] In the sections that follow, some of the more common enzyme stabilization strategies will be considered in detail. Specifically, carrier-bound and carrier-free immobilization techniques, physical entrapment, gel formation, and PEGylation will be discussed.

2.1.1. Immobilization

Perhaps the most preferred and most commonly employed strategy to prepare industrial biocatalysts,[20] immobilization represents an entire class of enzyme stabilization approaches. One of the main advantages of immobilization is that expensive enzymes can be converted to heterogeneous biocatalysts, allowing for repeated recovery and reuse, which drives down costs.[20, 30, 32, 34] Additionally, immobilization has also been shown to protect enzyme from inactivation by air bubbles[35] and prevent enzyme inhibition.[36, 37]

2.1.1.1. Carrier-Bound Techniques

Attachment to a rigid support can dramatically stabilize an enzyme's tertiary structure, thereby stabilizing its enzymatic activity. Various methods by which the enzyme can be bound to the carrier range from strong covalent bonds to intermediate ionic bonds to weaker van der Waals and hydrophobic interactions.[34] Moreover, the enzyme can be attached to the carrier at a single point, or multi-point attachment can be utilized. The latter is especially useful for immobilization of multimeric enzymes, where attachment to a support prevents subunit dissociation.[20, 28-30, 32] Additionally, multi-point attachment to a support has been shown to result in much greater rigidity of the immobilized enzyme. In some cases, even the orientation of the enzyme can be controlled (i.e., oriented randomly or with the active site directed outwardly).

While immobilization on a support is often very effective in stabilizing enzymatic activity, one must not use these techniques indiscriminately. As will become obvious in the sections that follow, different immobilization methods can affect various enzymes differently, and in some cases, may induce conformational changes in the structure which lead to partial loss of activity. Moreover, the support matrix can present a significant transport barrier, and the enzyme is no longer in the solution phase.

2.1.1.1.1. Covalent Attachment to Carrier

Immobilization *via* covalent attachment to a carrier is often the most utilized technique, as it provides the strongest and generally the most stable attachment to the carrier. A number of activated resins are commercially available and offer a wide variety of surface chemistries. Epoxy-activated resins allow for stable enzyme attachment

through reaction with primary amines, thiols, or hydroxyls on the protein surface.[38] Due to the high reactivity of these activated resins, multi-point attachment is typically achieved.[39] Amino-functionalized resins are also readily available, and can be activated immediately before exposure to the enzyme using a dialdehyde or other bifunctional crosslinker.[40] The imine linkages that are formed between the enzyme's amines and the resin's aldehydes can be reduced for stability. Finally, polysaccharide-based hydrogel beads (*e.g.*, Sepharose) can be activated using cyanogen bromide, which forms amine-reactive functionalities.[41] Unfortunately, the toxicity of cyanogen bromide has limited this technique's adoption outside of research labs.

2.1.1.1.2. Electrostatic Attachment to Carrier

Commercially available ion-exchange resins are well-suited for immobilization of charged enzymes *via* electrostatic interactions, and both anion[42] and cation[43] resins can be employed. While this approach is often simpler and milder as compared to covalent attachment to a carrier, initial protocol development can sometimes be troublesome; determining the proper conditions to permit the enzyme to adhere tightly to the support while remaining active can be a challenge. Even after attachment, exposure to conditions such as high salt concentrations will result in detachment of the enzyme. Finally, anomalies can be observed if enzyme substrates or products are charged, as they could also interact with the support through electrostatics.

2.1.1.1.3. Physical Adsorption to Carrier

Physical adsorption is generally considered to be the easiest and least expensive means by which to immobilize an enzyme.[42] However, as in the case of electrostatic

attachment to a support, this advantage comes at a cost. Because this approach relies upon weaker van der Waals and hydrophobic interactions, displacement of the immobilized enzyme can occur under certain conditions (*e.g.*, non-polar solvents or in the presence of surfactant). Therefore, this technique is best suited for immobilizing lipophilic molecules such as lipases in polar solutions devoid of surfactant. A variety of hydrophobic carriers (*e.g.*, polypropylene, acrylic, and styrene) with a range of hydrophobicities can be employed. Additionally, other types of supports can be modified with hydrophobic functional groups.

2.1.1.2. Carrier-Free Techniques

While the carrier-bound immobilization strategies can be effective, it is often difficult to obtain high concentrations of the enzyme, as the carrier constitutes the majority of the mass (*ca.* 90–99.9%).[44] Carrier-free immobilization techniques overcome this limitation by eliminating the need for a carrier altogether. These approaches do not rely upon a rigid support, but rather use chemical crosslinkers such as glutaraldehyde (GA) to crosslink neighboring enzymes to one another. In this way, the intermolecular crosslinking that takes place serves to stabilize the tertiary and quaternary structures of the enzymes (*i.e.*, preventing denaturation and subunit dissociation) without "diluting" the activity.[10-15] As with the previously discussed techniques, these methods can be quite effective for stabilizing enzymatic activity; however, the resulting particles are large and polydisperse (*ca.* 5-50 μm), thus transport barriers are still expected.

2.1.1.2.1. Crosslinked Enzyme Crystals

As the name suggests, crosslinked enzyme crystals (CLECs) are prepared *via* initial crystallization of an enzyme, followed by crosslinking of the enzyme crystal.[10] Enzymes remain highly active following crystallization, so this technique seeks to "lock" the enzyme in this active conformation. The resulting microparticles are relatively polydisperse and have been shown to be more thermally stable, solvent tolerant, and resistant to proteolytic attack.

Quiocho and others first demonstrated the formation of CLECs in 1964 using crystallized carboxypeptidase A.[10] In the following couple of decades, this technique was only applied to a handful of other enzymes, mostly due to practical issues associated with the formation of the CLECs.[27] The main drawback of this approach is the requirement to start with the enzyme in the crystalline state. Crystallization requires highly purified enzyme and can often be a time-intensive process (on the order of months), even for an expert in enzyme crystallography. Moreover, some enzymes have eluded researchers' attempts at crystallization altogether. It is primarily for this reason that this strategy is not commonly employed to produce heterogeneous biocatalysts. Another inherent disadvantage is that only one type of enzyme can be crystallized and thus stabilized using this technique. While this might not be an issue in many cases, there are examples where co-stabilization might be desirable (*e.g.*, coupled reactions like GOx and Cat).

2.1.1.2.2. Crosslinked Enzyme Aggregates

The mechanism of stabilization for crosslinked enzyme aggregates (CLEAs) is very similar to that of CLECs. The major advantage of CLEAs is that their preparation does not require that an enzyme crystallization protocol be developed initially. Rather, the enzyme is initially exposed to conditions which cause it to precipitate (*e.g.*, addition of miscible organic solvents, non-ionic polymers such as PEG, or high concentrations of salt such as ammonium sulfate); this leads to a decrease in the intermolecular spacing (high effective concentration), which allows for efficient crosslinking upon addition of a chemical crosslinker.

This technique has been demonstrated for a wide variety of enzymes, and typically through screening of multiple aggregation media and crosslinkers, a protocol can be developed that provides adequate stabilization without unacceptable loss in enzymatic activity.[11-15] Unlike CLECs, the initial enzyme solution need not be highly purified—in fact, under appropriate conditions, contaminating proteins can be excluded from the CLEAs during formation. So-called "combi-CLEAs" have also been demonstrated, wherein CLEAs comprising two or more types of enzymes are formed to drive multiple cascade[45] or non-cascade[46] reactions forward.

While the stabilized enzymes that are produced using this technique are usually smaller than CLECs, they are at least an order of magnitude larger than the native enzymes. Therefore, diffusional limitations are still expected for enzyme which is not located near the surface of the particle. Furthermore, applications requiring solution-phase enzyme of near-native size are incompatible with this approach.

2.1.1.3. Physical Entrapment

In this immobilization technique, enzyme is entrapped within a polymeric network—typically organic polymers or a sol-gel.[47] Some of the more commonly used polymers for enzyme entrapment include polyacrylamide,[48] alginate,[49] and gelatin,[50] although more complex multi-component matrices have been demonstrated as well. Silica sol-gels are quite commonly employed for *in situ* entrapment of enzyme,[51] but other silicon-based sol-gels can be used as well.[52]

As with other immobilization strategies, stabilization of the tertiary structure by the polymer matrix helps to confer stability. The main disadvantages of this approach are mass transfer limitations, low enzyme loading,[53] and the requirement that substrates and products be capable of diffusing throughout the polymeric network while retaining enzymes. Due to the relatively small difference in size between enzymes and their substrates, this level of tunability is often difficult to achieve in practice. Therefore, physical entrapment has found its niche in whole-cell immobilization,[54-56] in which much looser polymeric networks with larger mesh sizes can be employed.

2.1.1.4. Gel Formation

A hybrid immobilization technique that is routinely employed for amperometric glucose biosensors involves the crosslinking of GOx directly on the surface of an electrode. In some cases, an inert macromolecule such as BSA is mixed with the enzyme to avoid excess crosslinking and to facilitate gel formation.[57] This approach has the advantage of extreme simplicity; however, limitations on diffusion are imposed, lack of

repeatability is common, and significant losses in initial activity can occur due to random modification of groups involved in catalysis.

2.1.2. PEGylation

Protein PEGylation is often performed to increase a protein's hydrodynamic volume, and this technique has been widely employed to increase circulation time of therapeutic biologicals.[58, 59] A given mass of PEG has a much larger hydrodynamic size than an equivalent mass of protein, so even attachment of a modest amount of PEG to a protein can drastically alter the protein's hydrodynamic size.[60] PEGylation with higher-molecular-weight PEGs has also been shown to discourage protein aggregation, as the larger PEG molecules tend to repel one another.[61, 62] In some cases, improvements in thermostability have even been demonstrated.[63]

Given these desirable characteristics, enzyme PEGylation offers a means to stabilize enzymes while preserving their near-native size and residence in the solution phase. While some studies report that PEGylation of a protein does not affect its secondary or tertiary structure, there have been other studies that report on activity loss of an enzyme following PEGylation. In the latter case, the commonly employed random multi-site PEGylation approaches can lead to activity loss due to blocking of the binding site and/or disruption of the protein's tertiary structure.[16-19] Site-selective PEGylation—targeting a protein's N-terminus, thiol groups (cysteine), or disulfide bridges, to name a few—can help to mitigate the issue of reduced activity due to blocking of the binding site.

2.2. Enzymes Employed in Glucose Biosensors

2.2.1. Glucose Oxidase

GOx is an enzyme that is used widely in the food industry to produce gluconic acid, act as a food preservative, and determine the glucose content in foodstuffs.[64] Many of the properties that make GOx ideal for use in the food industry—high selectivity for glucose, high turnover rate without the need for a soluble cofactor, and relative stability under certain conditions—also make it the most suitable choice for incorporation into glucose biosensors for biomedical applications.[65]

GOx is a homodimeric oxidoreductase that catalyzes β-D-glucose oxidation by diatomic oxygen to form δ-gluconolactone and hydrogen peroxide. The redox reaction scheme (excluding the reverse rate constants k_{-1} and k_{-3}) can be represented as

$$\begin{gathered} E_{ox} + G \overset{k_1}{\rightarrow} E_{red}P_1 \overset{k_2}{\rightarrow} E_{red} + \delta\text{-lactone} \\ E_{red} + \mathrm{O_2} \overset{k_3}{\rightarrow} E'_{ox}P_2 \overset{k_4}{\rightarrow} E_{ox} + \mathrm{H_2O_2}, \end{gathered} \tag{2.1}$$

where E_{ox} is the oxidized enzyme, G is glucose, $E_{red}P_1$ is the reduced enzyme-substrate complex, E_{red} is the reduced enzyme, $E'_{ox}P_2$ is the oxidized enzyme-substrate complex, and k_1, k_2, k_3, and k_4 are all rate constants.[66]

GOx can be purified from a variety of sources; however, GOx from *Aspergillus niger* is the most commonly used and most highly characterized form.[67] GOx from *A. niger* has a molecular mass of approximately 160 kDa and is highly glycosylated, with a total carbohydrate content of 18.8 ± 0.6% of its molecular mass (16.4 ± 0.3% neutral sugar and 2.4 ± 0.5% amino sugar).[68, 69] Each monomer has one active site and one

tightly bound flavin adenine dinucleotide (FAD) cofactor associated with it, which gives GOx its yellow color ($\varepsilon_{450\,nm}$ = 1.41 x 10^4 M^{-1} cm^{-1}).[70]

Monomeric GOx is a compact spheroid approximately 6 nm x 5.2 nm x 3.7 nm in size; the dimer measures approximately 6 nm x 5.2 nm x 7.7 nm.[71] The quaternary structure of GOx is quite stable, retaining its dimeric conformation under normal conditions, when exposed to heat, and even at low concentrations of chemical denaturants.[72] It is due to this surprising stability that O'Malley and Weaver incorrectly reported in 1972 that GOx comprises two polypeptide chains covalently linked by disulfide bonds.[73] Since that report, there have been multiple follow-up studies that have shown that the dimer contains two disulfide bonds and two free thiols, but no evidence of a covalent linkage between the two subunits.[74]

2.2.2. Catalase

Cat is a tetrameric enzyme which acts upon hydrogen peroxide, decomposing it into water and oxygen. The reaction scheme is shown below:

$$\begin{aligned} \mathrm{H_2O_2} + \mathrm{Cat} &\overset{k_5}{\rightarrow} I + \mathrm{H_2O} \\ \mathrm{H_2O_2} + I &\overset{k_6}{\rightarrow} \mathrm{Cat} + \mathrm{H_2O} + \mathrm{O_2}, \end{aligned} \tag{2.2}$$

where I is the intermediate form of the enzyme and k_5 and k_6 are rate constants (distinct from the rate constants given above for GOx).[75]

Each monomer of Cat has one active site and one protohematin group, giving it both UV and strong visible absorbance ($\varepsilon_{406\,nm}$ = 3.6 x 10^5 M^{-1} cm^{-1}).[76] Like GOx, Cat can also be purified from a variety of sources; however, bovine liver Cat is the most common. Though not as common, Cat from *A. niger* is commercially available, and

multiple groups have shown that this form of Cat exhibits greater stability to high concentrations of peroxide compared to bovine liver Cat.[75, 77] With a molecular mass of approximately 385 kDa according to Kikuchi-Torii and others, Cat from *A. niger* is also larger than other Cat macromolecules (*e.g.*, bovine liver Cat is 250 kDa).[76] Finally, while Cat from bovine liver is not glycosylated, *A. niger* Cat is glycosylated, with a total carbohydrate content of 10.2% of its molecular mass (8.3% neutral sugar and 1.9% glucosamine).[76] Not only is the glycosylation of *A. niger* Cat likely responsible for the greater stability (compared to Cat from bovine liver), the glycosylation sites also permit the same modification strategies that are employed for GOx to be applied to Cat.

2.2.3. Enzyme Inactivation

Both GOx and Cat are susceptible to enzyme inactivation during storage and operation. As discussed in Section 1, this inactivation causes issues with the sensor response, requiring recalibration and ultimately replacement. In their 1987 paper, Tse and Gough described these processes in detail.[8] Spontaneous inactivation resulting from enzyme denaturation is governed by first-order kinetics, in which the enzyme inactivation rate is directly proportional to the concentration of enzyme:

$$\frac{dc_e}{dt} = -k_o c_e, \tag{2.3}$$

where c_e is the active enzyme concentration, t is time, and k_o is the spontaneous inactivation rate constant. For immobilized GOx and Cat from *A. niger*, the spontaneous inactivation rate constants were determined to be 9.2 x 10^{-8} s^{-1} and 1.5 x 10^{-7} s^{-1}, respectively.

Conversely, hydrogen peroxide-mediated inactivation follows second-order kinetics, and the enzyme inactivation rate can be approximated as

$$\frac{dc_e}{dt} = -k_i c_h c_e, \tag{2.4}$$

where k_i is the hydrogen peroxide-mediated inactivation rate constant and c_h is the concentration of hydrogen peroxide. For immobilized Cat, the hydrogen peroxide-mediated inactivation rate constant was determined to be 1.5 x 10^{-2} M^{-1}/s. For GOx, both hydrogen peroxide-mediated inactivation of the reduced enzyme (k_i = 2.0 x 10^{-2} M^{-1}/s) and the oxidized enzyme–hydrogen peroxide complex (k_i = 7.6 x 10^{-1} M^{-1}/s) were shown to be significant. The oxidized enzyme–hydrogen peroxide complex was 38 times more susceptible to inactivation than the reduced form of the enzyme; however, at low oxygen concentrations, inactivation was mainly due to hydrogen peroxide interaction with the latter form, and the total inactivation rate was reduced.[8] This is significant for implantable glucose sensors, as tissue oxygen levels are expected to be quite low.[78] No dependence of the GOx oxidation state on the spontaneous inactivation rate was observed, and both Cat and its intermediate form appear to be equally susceptible to both types of inactivation.[8]

For our sensors, which will continuously be exposed to physiological levels of glucose, it is expected that hydrogen peroxide-mediated inactivation will dominate—at least during operation. Nevertheless, spontaneous deactivation will also be an issue, especially during processing and storage. Other deactivating factors such as elevated temperature and exposure to non-ideal solvents can be targeted as well and present an opportunity to even further stabilize the enzymes. However, the application of the

enzyme stabilization techniques discussed earlier in this section are either not adequate to accomplish these goals or not compatible with our sensing system; thus, new stabilization strategies have been developed and are presented herein.

3. GLYCOSYLATION SITE-TARGETED PEGYLATION OF GLYCOENZYME*

3.1. Introduction

Protein PEGylation—the covalent attachment of PEG to a protein or peptide—has been widely employed for therapeutic purposes since its introduction in 1977 by Abuchowski and others.[79] A number of reviews outline the benefits that PEGylation can impart upon therapeutic proteins, such as enhanced circulation half-life *in vivo* and decreased immunogenicity.[21, 80-82] Until recently, modification of the ε-amino group of superficial lysine residues with an amine-reactive PEG has been most commonly employed due to the large number of these reactive groups (lysine residues comprise 10% of a typical protein[83]); however, conjugates prepared using this technique are typically heterogeneous and often require purification to isolate the preferred isoform.[80, 81, 84] Furthermore, in enzymes, activity loss can be an issue when random multi-site PEGylation is applied, which has been partially attributed to lower substrate binding affinity due to steric hindrance of the binding site and disruption of the protein tertiary structure.[16-19] To overcome this issue, Zalipsky and co-workers designed a methoxy-PEG-hydrazide (PEG-Hz) derivative that could be used to target oligosaccharides on glycoproteins, allowing for PEGylation without disruption of the primary structure of the enzyme.[21, 22]

---

* Parts of this section are reprinted with permission from "Glycosylation site-targeted PEGylation of glucose oxidase retains native enzymatic activity" by D. W. Ritter, J. R. Roberts and M. J. McShane, *Enzyme Microb. Technol.*, 2013, **52**, 279-285. Copyright 2013 by Elsevier Inc.

As discussed previously, our group has developed optical glucose biosensors that are based on GOx,[3-5] and recent work has focused on extending the operating lifetime of these biosensors.[6] Effective and appropriate enzyme stabilization strategies are absolutely critical in moving these implantable devices toward the ultimate goal of long-term monitoring. Loss of enzymatic activity of GOx can result in undesirable changes in sensor response characteristics, necessitating frequent recalibration and decreasing operational lifetime.

Given that PEG has been shown to stabilize enzymes and does not drastically alter size or residence in the solution phase, PEGylation of GOx was considered as a strategy to stabilize enzyme activity. As GOx is highly glycosylated, with a total carbohydrate content of 18.8 ± 0.6% of its molecular mass,[68] attachment of PEG-Hz is an attractive option to avoid blocking the binding site or affecting the protein conformation. Therefore, I hypothesized that PEGylation of GOx with PEG-Hz would provide stability against enzyme deactivation without a significant reduction in initial activity. To test this hypothesis, GOx was modified with PEG-Hz to target glycosylation sites (Fig. 3-1), followed by physical characterization of the resulting modified enzyme, and finally a comparison of the functional properties (*i.e.*, initial activity, storage stability, and operational stability) of native GOx and PEG-GOx. This work represents the first full characterization (*i.e.*, physical and functional) of GOx modified with PEG-Hz.

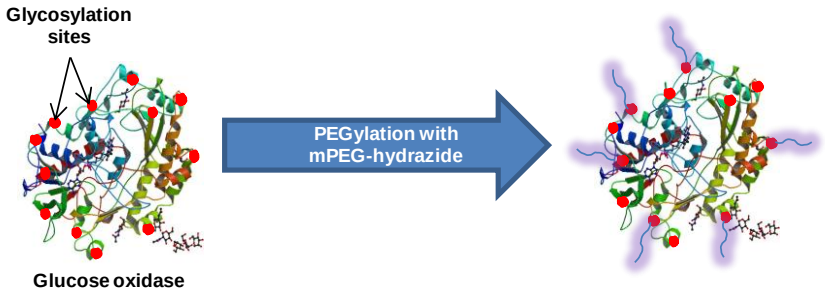

Fig. 3-1 Cartoon illustrating attachment of PEG to glycosylation sites of GOx (not drawn to scale).

3.2. Experimental

3.2.1. Materials

GOx from *Aspergillus niger* (type VII, 168.8 U/mg solid, 80% protein by biuret) and peroxidase from *Amoracia rusticana* (type II, 188 U/mg solid) were obtained from Sigma. PEG-Hz (4.5 kDa by gel permeation chromatography) was obtained from Laysan Bio.

3.2.2. Preparation of PEGylated GOx

A modification of Zalipsky's PEGylation protocol[85] was used to prepare the PEG-GOx and is illustrated below in Fig. 3-2. GOx (6 mg, **1**) was dissolved in 1.8 mL of 10 mM sodium phosphate containing 154 mM NaCl (pH 7.2). Separately, 8.6 mg of $NaIO_4$ was dissolved in 200 µL of deionized water *via* alternating sonication and vortexing, and the $NaIO_4$ solution was protected from light. The $NaIO_4$ solution was immediately added to the GOx solution, and the sample was slowly agitated on a nutating mixer. The mixture was reacted in the dark for 1 h at room temperature to yield **2**.

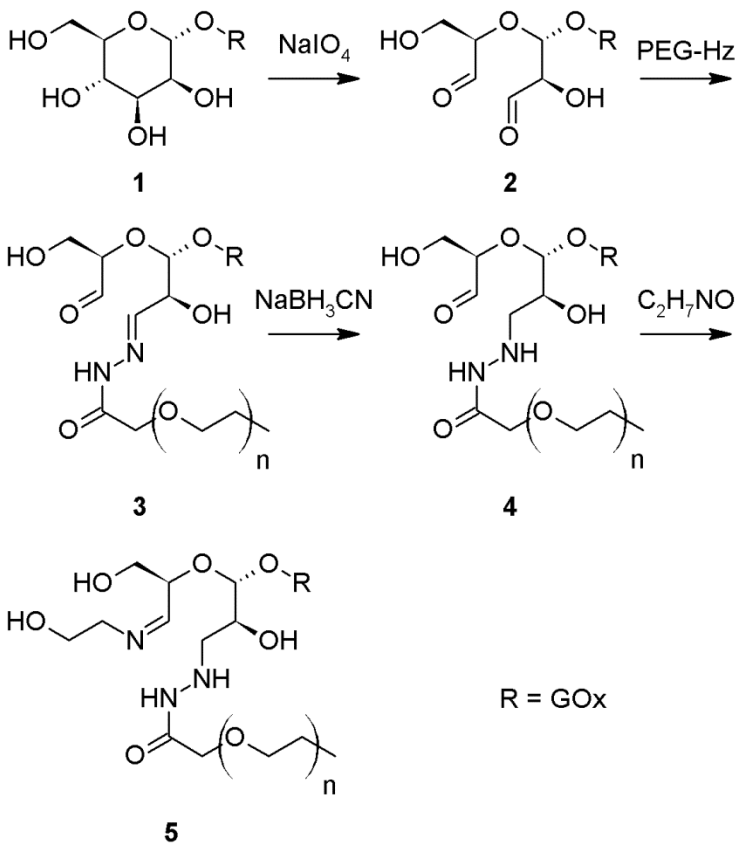

Fig. 3-2 Glycosylation site-targeted PEGylation of GOx. Oxidation of glycosylation sites on GOx yields reactive aldehydes, to which the hydrazide functionality on PEG-Hz can be covalently bound. The resulting hydrazone linkages are reduced for stability, and unreacted aldehydes are blocked with ethanolamine.

It is important to note that proteins exposed to oxidants such as $NaIO_4$ have been reported to form higher-order oligomers in certain cases due to intermolecular crosslinking; however, Nakamura and others exposed GOx from *A. niger* to a five-fold higher concentration of $NaIO_4$ for 5 h and found that the size and shape of the oxidized GOx was essentially the same as the native GOx.[86] Nevertheless, a small amount of aggregated GOx might be observed and should not be a cause for concern as it will be removed during subsequent desalting or purification.

The reaction was quenched by the addition of 2.5 µL of glycerol, corresponding to a 20-fold molar excess of glycerol to $NaIO_4$. The oxidized GOx was purified using a desalting column equilibrated with 100 mM sodium phosphate containing 154 mM NaCl (pH 6.0) to remove excess $NaIO_4$, glycerol, and degradation products from glycerol quenching (*i.e.*, formaldehyde and formic acid).

PEG-Hz (33.8 mg) was added to the oxidized GOx solution, yielding a 200-fold molar excess of PEG-Hz to GOx. The extremely low pK_a of the hydrazide reactive group (pK_a = 3), paired with its smaller size and large molar excess as compared to the GOx, makes attachment of PEG more favorable than intermolecular crosslinking between oxidized sugars and superficial amines on GOx. The reaction solution was reacted in the dark for 2 h at room temperature under gentle agitation to yield **3**. In a fume hood, 20 µL of 5 M $NaBH_3CN$ in 1 N NaOH was added. **Caution: $NaBH_3CN$ is extremely toxic; as such, all operations should be performed with care in a fume hood**. The $NaBH_3CN$ was reacted with PEG-GOx for 30 min at room temperature under gentle agitation to yield **4**. Unreacted aldehydes were blocked by addition of 100 µL of 1 M ethanolamine (pH 9.6) and reaction for 30 min at room temperature under gentle agitation to yield **5**. The PEG-GOx was purified from low-molecular-weight contaminants using a desalting column equilibrated with 10 mM sodium phosphate containing 154 mM NaCl (pH 7.2).

3.2.3. Physical Characterization

3.2.3.1. Liquid Chromatography

Gel filtration chromatography (GFC) was performed to separate the PEG-GOx from unattached PEG-Hz (*i.e.*, purify the conjugate), but it also provided information about the physical characteristics of the conjugate. The samples were injected into a liquid chromatography system (GE Healthcare Life Sciences model ÄKTAexplorer 10) equipped with a gel-filtration column (GE Healthcare Life Sciences model HiLoad Superdex 200 PG) equilibrated with 10 mM sodium phosphate containing 150 mM NaCl (pH 7.2). Absorbance at 280 nm was monitored and 2 mL fractions were collected.

3.2.3.2. Gel Electrophoresis

Reducing sodium dodecyl sulfate polyacrylamide gel electrophoresis was performed to test for an increase in the hydrodynamic size of GOx as a result of the PEGylation process. Protein samples were combined with sample buffer (containing 54 mg/mL DL-dithiothreitol), vigorously agitated, and loaded onto a 10-well, 10% precast polyacrylamide gel (Bio-Rad model 456-1033); all samples were duplicated symmetrically on the gel (*i.e.*, the first sample was loaded onto lane 1 and lane 10, *etc.*). Following electrophoresis, the gel was rinsed three times with deionized water and cut between lanes 5 and 6 so that half of the lanes could be stained for protein and the other half for PEG. To stain for protein, one half of the gel was placed in 30 mL of the Coomassie staining solution for 1 h, followed by rinsing with deionized water overnight. To stain for PEG, the other half of the gel was placed in 30 mL of perchloric acid for 15 min, and then 10 mL of 5% w/v barium chloride and 4 mL of 0.1 N iodine were added.

The gel was stained for 10 min, followed by extensive rinsing with deionized water.[87] Both stained halves of the gel were imaged separately using a gel imaging system (Bio-Rad model 170-8270).

3.2.3.3. Mass Spectrometry

Mass spectra were acquired with a matrix-assisted laser desorption/ionization time-of-flight (MALDI-TOF) mass spectrometer (Shimadzu model Axima-CFR) operating in linear mode to determine the extent of PEGylation (*i.e.*, the number of PEG chains attached per GOx). Protein samples (3 mg/ml) in 10 mM sodium phosphate containing 154 mM NaCl (pH 7.2) were concentrated and desalted (Millipore model $ZipTip_{C4}$ Pipette Tips); the eluate was spotted directly onto a steel sample plate, where it was combined with an equal volume of saturated sinapinic acid solution and air-dried.

3.2.3.4. Particle Sizing

A photon correlation spectrometer (Malvern model Zetasizer Nano ZS) was used to acquire size distributions of the GOx and PEG-GOx samples. This was necessary to determine the change in size after modification, as well as to gauge the extent of oligomerization during oxidation or subsequent PEGylation. Disposable 3.5 mL cuvettes were filled with enzyme (1 mL, 0.6 mg/mL) in 10 mM sodium phosphate containing 154 mM NaCl (pH 7.2).

3.2.4. Functional Characterization

3.2.4.1. Enzymatic Activity Assays

Enzymatic assays of PEG-GOx and native GOx were performed to determine activity.[88] The enzyme is added to a reaction cocktail comprising an excess of D-glucose

(to fix GOx at V_{max}), horseradish peroxidase, and *o*-dianisidine dihydrochloride. The consumption of glucose results in an equimolar production of H_2O_2, which is directly proportional to the concentration of GOx in the solution. In the presence of H_2O_2, peroxidase will oxidize *o*-dianisidine to form a product that absorbs at 500 nm (ε = 7.5 $mM^{-1}cm^{-1}$), and the rate of formation of this colored product is a measure of the enzymatic activity of the solution. In all cases, enzymatic activity measurements were performed in triplicate at pH 5.1 and 35 °C using a UV/Vis spectrophotometer (PerkinElmer model LAMBDA 45); these conditions are utilized for activity measurements primarily because it is standard to define GOx activity under these conditions (*i.e.*, 1.0 U of GOx will oxidize 1.0 μmol of β-D-glucose to D-gluconolactone and H_2O_2 per minute at pH 5.1 and 35 °C). To calculate specific activity, the enzyme concentration must be known. All enzyme concentrations were determined by UV/Vis spectroscopy using a molar extinction coefficient of 2.672 x 10^5 $M^{-1}cm^{-1}$ (λ = 280 nm).

3.2.4.2. Long-Term Storage Stability

To observe the effect that PEGylation has on the spontaneous denaturation of GOx, PEG-GOx and native GOx were stored at 37 °C (elevated temperature to accelerate deactivation and simulate physiological conditions) in the absence of glucose and assayed over the course of 29 days. Sealed vials (one per sample per timepoint) containing 0.3 mL of enzyme solution (50 μg/mL in 10 mM phosphate-buffered saline [PBS] containing 0.02% NaN_3 as a preservative) were stored in an incubator until the appropriate time to test for enzymatic activity. To reduce the possibility for sample

contamination, samples were not opened until the day they were assayed for enzymatic activity.

3.2.4.3. Operational Stability

To compare the rates of deactivation for PEG-GOx and native GOx under operating conditions, a study of activity during continuous exposure to glucose was performed. Enzyme solution (0.25 mL, 0.25 mg/mL) was injected into a dialysis cassette (10 kDa molecular-weight cutoff, 0.5 mL capacity) and placed into 1 L of 10 mM sodium phosphate containing 154 mM NaCl and 5% w/v glucose (pH 7.2). Both solutions were stirred and air-equilibrated by bubbling air through a gas diffuser. After 24 h at room temperature, the dialysis cassettes were transferred into 1 L of 10 mM sodium phosphate containing 154 mM NaCl (pH 7.2). The dialysate was tested for the presence of glucose using a biochemical analyzer (YSI Life Sciences model 2700 SELECT Biochemistry Analyzer) and exchanged for fresh buffer until glucose levels were undetectable. At that point, protein samples were removed from the dialysis cassettes and assayed for enzymatic activity. As a control, PEG-GOx and native GOx samples not exposed to glucose were also assayed for enzymatic activity.

3.3. Results and Discussion

3.3.1. Physical Characterization

It is important to note that of the various analytical techniques used to characterize the PEG-GOx and native GOx, mass spectrometry is the only one expected to provide actual molecular mass of the samples. In contrast, liquid chromatography, gel electrophoresis, and dynamic light scattering (DLS) can only provide apparent molecular

mass of the samples based on calibration curves constructed using non-PEGylated protein molecular mass standards. These apparent molecular masses can differ greatly from the actual molecular masses.

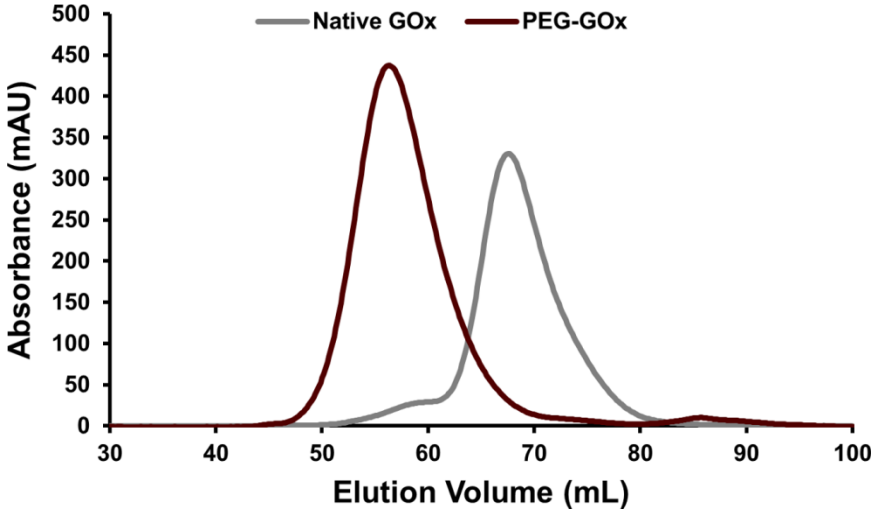

Fig. 3-3 Overlaid chromatograms of PEG-GOx (maroon line) and native GOx (gray line). Native GOx eluted at 67.52 mL and is estimated to be 140 kDa, while PEG-GOx eluted at 56.33 mL (molecular mass cannot be estimated as it is out of the calibration range).

3.3.1.1. Liquid Chromatography

Fig. 3-3 contains the overlaid chromatograms of PEG-GOx (maroon line) and native GOx (gray line) subjected to GFC. A calibration curve was compiled using seven proteins over a wide range of molecular masses within the column's fractionation range (*i.e.*, 10–600 kDa) and was used to convert elution volume to molecular mass (Fig. 3-4). Native GOx (elution volume of 67.52 mL) is estimated to be 140 kDa, while the apparent molecular mass of PEG-GOx (elution volume of 56.33 mL) could not be estimated because it eluted before the largest calibrant (*i.e.*, thyroglobulin with a

molecular mass of 669 kDa and an elution volume of 60.3 mL). Therefore, while the column that was chosen for GFC was appropriate to separate the bioconjugate from the native GOx, the only conclusion that can be drawn concerning the bioconjugate's apparent molecular mass is that it is larger than thyroglobulin.

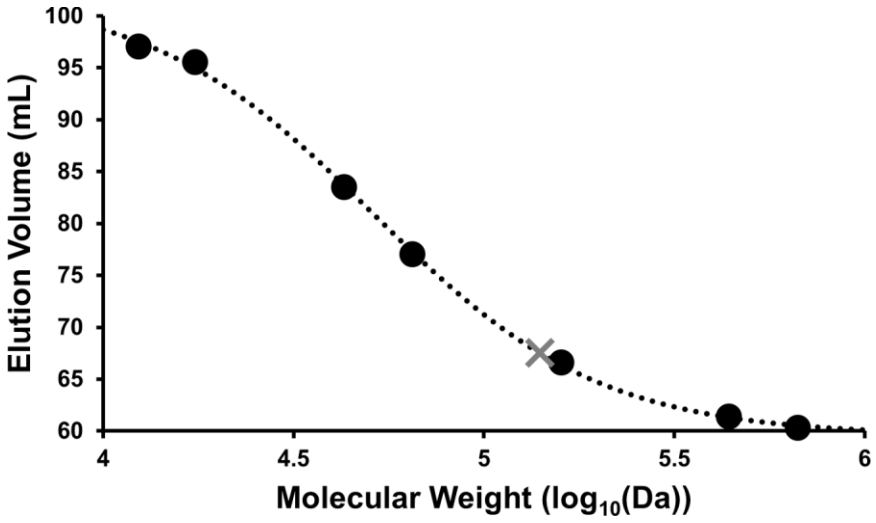

Fig. 3-4 Calibration curve for HiLoad Superdex 200 PG gel-filtration column. Calibrants are shown as black circles and fitted with a sigmoidal curve (dotted line). The point on the curve corresponding to the GOx elution volume is depicted as a gray cross.

3.3.1.2. Gel Electrophoresis

Fig. 3-5 shows a composite image of the gel on which PEG-GOx and native GOx were electrophoresed. The left half of Fig. 3-5, which depicts the half of the gel that was stained and imaged for the presence of protein, clearly shows an increase in the apparent monomer molecular mass upon PEGylation of GOx; lane 2 containing native GOx displays a band at 86.4 kDa, while lane 4 containing the PEG-GOx displays a band at 182.2 kDa. It is obvious that the sample bands corresponding to the native and the PEG-

GOx are quite diffuse. However, this is to be expected given that 1) GOx is a glycoenzyme and therefore has a distribution of molecular masses; 2) it has been shown that glycoproteins run anomalously in denaturing polyacrylamide gel electrophoresis, typically with an apparent molecular mass that is higher than the actual molecular mass due to suppressed binding of sodium dodecyl sulfate;[89, 90] and 3) the PEG has its own molecular mass distribution, which serves to further broaden the PEG-GOx band.

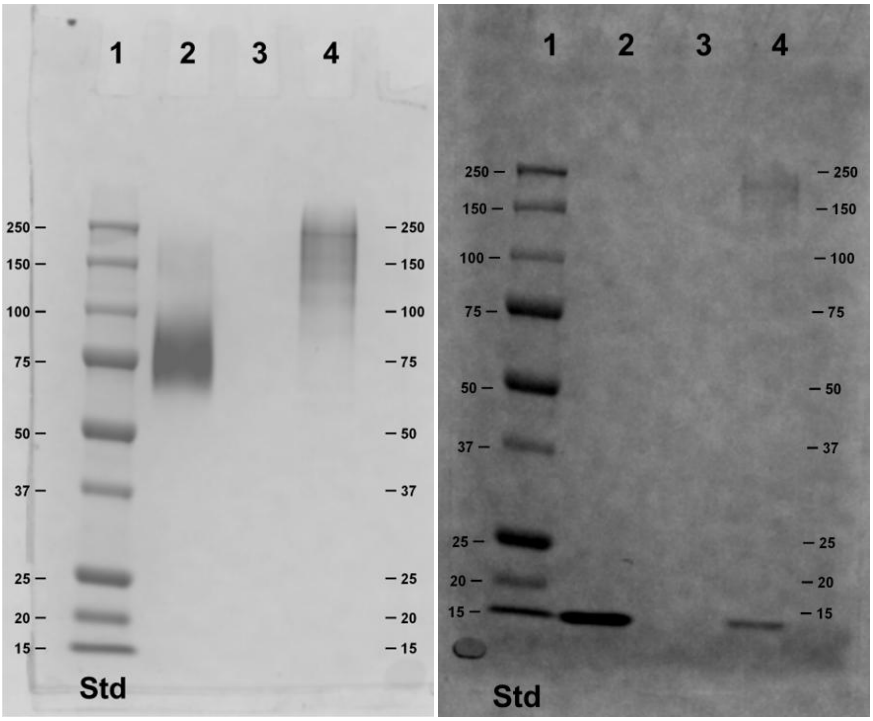

Fig. 3-5 Gel electrophoresis of PEG-GOx and native GOx. Protein samples were combined with sample buffer containing a reducing agent to break the GOx dimer into monomeric subunits and loaded onto a 10% polyacrylamide gel. Lane 1: prestained molecular weight marker; Lane 2: native GOx; Lane 3: blank; Lane 4: PEG-GOx. The left half of the image was stained for protein, while the right half was stained for PEG.

Upon inspection of the right half of Fig. 3-5, which depicts the half of the gel that was stained and imaged for the presence of PEG, one finds the absence of a band in close proximity to the protein band in lane 2. In contrast, lane 4 containing the PEG-GOx displays a faint band nearly coincident (apparent molecular mass of 175.7 kDa) with the protein band, which indicates that the PEG has been successfully attached to the GOx.

Gel electrophoresis and liquid chromatography data indicate complete modification of GOx, as evidenced by the lack of a band in the gel image or a peak in the chromatogram corresponding to the presence of unmodified GOx in the PEG-GOx sample. Furthermore, the presence of a single bioconjugated specie suggests that the chosen PEG:GOx molar ratio of 200:1 results in saturation of the available conjugation sites. However, to further confirm that a PEG:GOx molar ratio of 200:1 results in saturation, GOx was PEGylated using higher PEG:GOx molar ratios in the reaction solution (*i.e.*, 500:1 and 2000:1), and the bioconjugate was subjected to GFC equipped with a column that has a fractionation range of 5 kDa to 5 MDa (GE Healthcare Life Sciences model Superose 6 HR). The three bioconjugates, which are all well within the fractionation range of the column, have similar elution volumes (Fig. 3-6). The chromatogram corresponding to the PEG-GOx prepared using a 500:1 molar ratio of PEG:GOx (blue line) is broader and slightly shifted to higher elution volume as compared to that of the PEG-GOx prepared using the standard 200:1 molar ratio of PEG:GOx (maroon line). On the other hand, PEG-GOx prepared using a 2000-fold molar excess of PEG:GOx (orange line) has a broader chromatogram, but is shifted to

lower elution volume. However, the absence of a trend between PEG:GOx molar ratio and elution volume suggests that these small changes are insignificant random fluctuations, and the peak broadening might indicate that aggregation is present at higher ratios. Therefore, the lowest PEG:GOx molar ratio of 200:1 appears to be ideal.

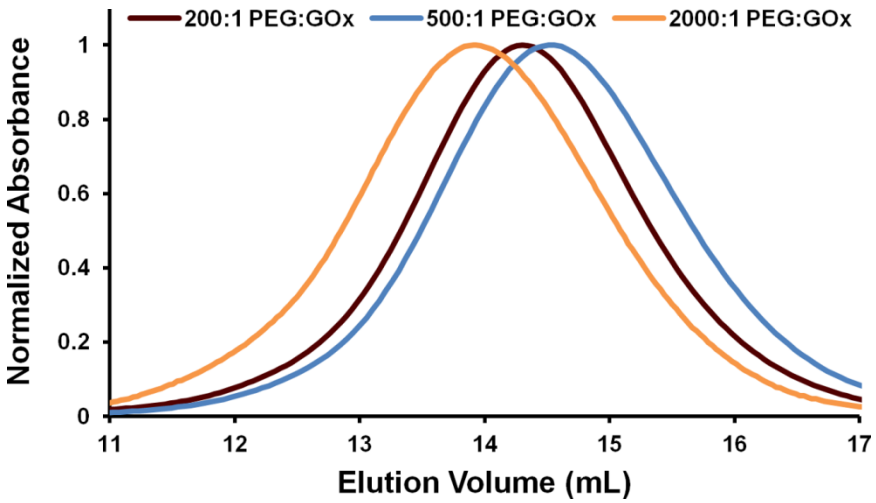

Fig. 3-6 Effect of PEG:GOx molar ratio on the extent of PEGylation. As the PEG:GOx molar ratio in the reaction solution is varied from 200 to 2000, the chromatogram of the bioconjugate changes in an unpredictable manner.

3.3.1.3. Mass Spectrometry

Fig. 3-7 shows the mass spectra of PEG-GOx (maroon line) and native GOx (gray line) collected using MALDI-TOF mass spectrometry. The spectrum collected from the native GOx sample depicts a broad peak centered at approximately 72 kDa, while the spectrum collected from the PEG-GOx sample depicts an even broader peak centered at approximately 85 kDa; this shift corresponds to a mass change of approximately 13 kDa per monomer as a result of GOx PEGylation.

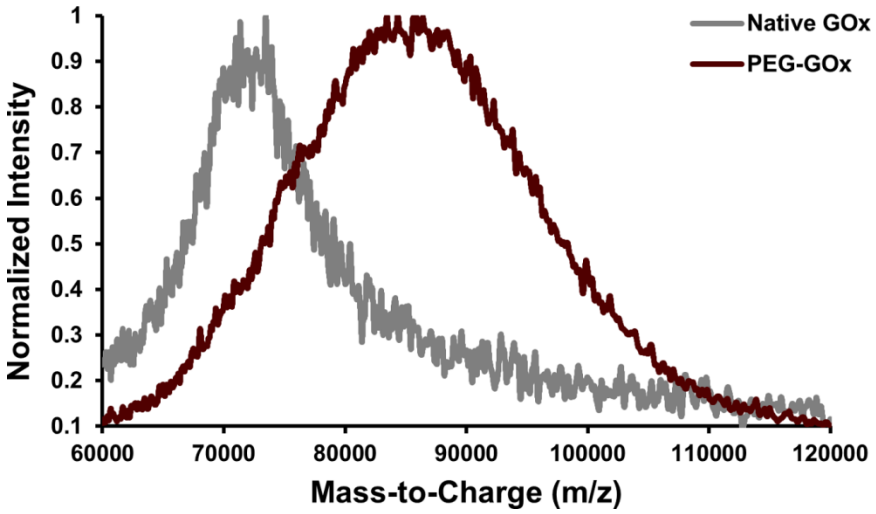

Fig. 3-7 Mass spectra of PEG-GOx (maroon line) and native GOx (gray line). The peak for the native GOx sample corresponds to 72 kDa, while the peak for the PEG-GOx sample corresponds to 85 kDa.

The peaks in the mass spectra above are relatively broad; as explained in Section 3.3.1.1, this is expected from a glycoprotein due to the existence of multiple glycoforms with various molecular masses. The peak from the PEG-GOx sample is broader than the native GOx peak, which is also expected as the PEG's molecular mass distribution will be convolved with the molecular mass distribution of the bioconjugate; this effect has been reported by other groups as well.[91] The monomeric molecular mass for native GOx by mass spectrometry matches well with the dimeric molecular mass for native GOx estimated by liquid chromatography, while the monomeric molecular mass for native GOx estimated by gel electrophoresis is slightly higher (likely due to glycosylation; see Section 3.3.1.1). The mass change of approximately 13 kDa per monomer as a result of GOx PEGylation corresponds to approximately three 4.5 kDa

PEG chains; therefore, our PEGylation protocol is believed to result in the attachment of approximately *six PEG chains per GOx dimer*.

3.3.1.4. Particle Sizing

Fig. 3-8 contains the size distributions of PEG-GOx (maroon bars) and native GOx (gray bars) as estimated from DLS. The PEG-GOx has a mean hydrodynamic diameter of 17.13 nm, while the native GOx has a mean hydrodynamic diameter of 11.48 nm, corresponding to an approximate 50% increase in the hydrodynamic size upon PEGylation. The size distributions have approximately equivalent widths (as determined by measuring the full width at half of the maximum).

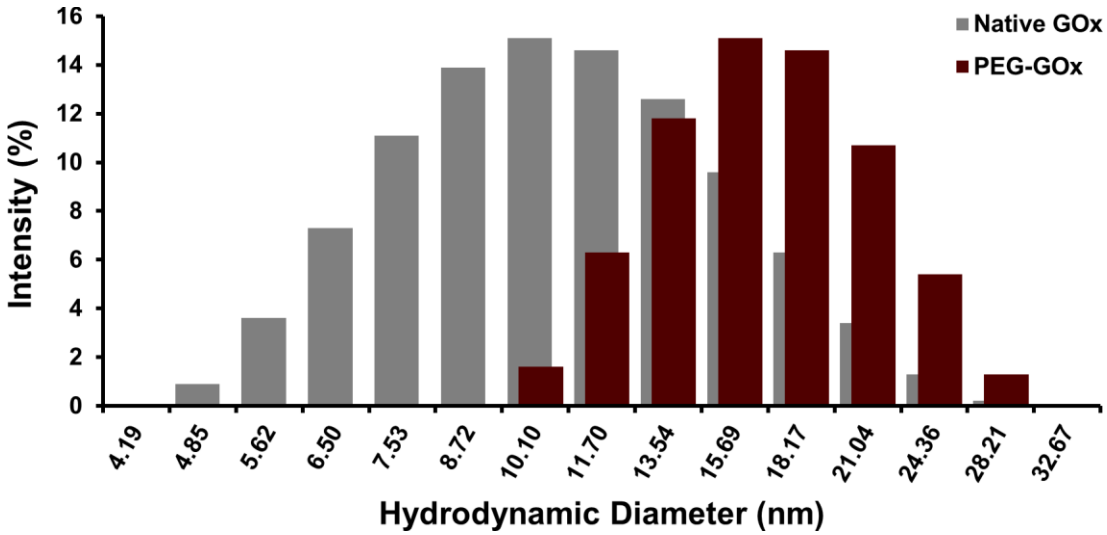

Fig. 3-8 Size distributions of PEG-GOx (maroon bars) and native GOx (gray bars). Native GOx has a mean hydrodynamic diameter of 11.48 nm, while PEG-GOx has a mean hydrodynamic diameter of 17.13 nm.

In 2004, Fee and Van Alstine proposed a model that was shown to accurately predict the hydrodynamic radius of various PEGylated proteins, which was related to the

bioconjugate's behavior in GFC.[60] By applying this model to our system, we find that despite the modest increase in molecular mass upon GOx PEGylation (*ca.* 26 kDa), the hydrodynamic diameter of the bioconjugate is estimated to increase from 8.6 nm (unmodified dimeric GOx; 144 kDa by mass spectrometry) to 14.3 nm (144 kDa GOx + 26 kDa PEG). This 66% increase in hydrodynamic diameter results in an approximate five-fold increase in the apparent molecular mass upon GOx PEGylation (from 144 kDa to 667 kDa), which agrees with our earlier observation that the bioconjugate's apparent molecular mass exceeds the column's exclusion limit of 600 kDa. Furthermore, this agrees well with the 50% increase in hydrodynamic size that was observed by DLS.

The particle sizing data do not support the presence of higher-order oligomers in the PEG-GOx sample, which would broaden the peak or present as slightly larger secondary peaks (corresponding to dimers, trimers, *etc.*). Although a secondary peak exists at 526 nm (not visible on graph as shown), it represents only 0.3% of the sample by volume (the primary peak accounts for the remaining 99.7% by volume), and is much larger than one would expect for an oligomer formed by intermolecular crosslinking of GOx during oxidation or PEGylation; it likely represents a small fraction of aggregated denatured protein or a contaminant.

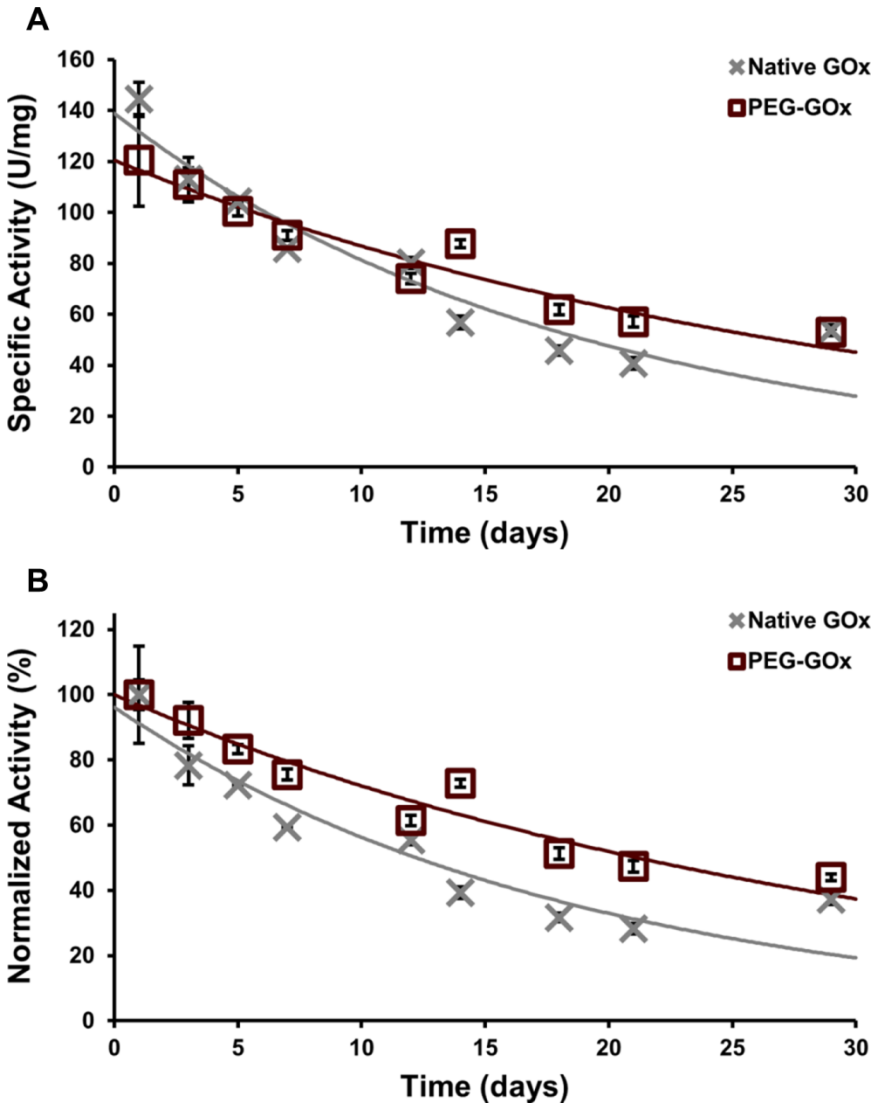

Fig. 3-9 Specific activity (A) and normalized activity (B) of PEG-GOx (maroon squares) and native GOx (gray crosses) in the absence of glucose over four weeks at 37 °C. Error bars represent 95% confidence intervals (n = 3). The data were fit with first-order exponential decays; the maroon lines correspond to the PEG-GOx data and the gray lines correspond to the native GOx data.

3.3.2. Functional Characterization

3.3.2.1. Long-Term Storage Stability

Fig. 3-9 depicts the loss in specific activity of PEG-GOx (maroon squares) and native GOx (gray crosses) in the absence of glucose and at 37 °C. Data points represent the average specific activities at each time point, and error bars represent 95% confidence intervals (n = 3). Fig. 3-9A shows the absolute specific activities over time, while Fig. 3-9B shows the same data which has been normalized to the initial specific activity value within each data set. The data were fit with a first-order exponential decay; the maroon line corresponds to the PEG-GOx data and the gray line corresponds to the native GOx data. Although the specific activities for PEG-GOx and native GOx are statistically different at intermediate time points, they are not statistically distinct at the initial two time points and the final time point (Fig. 3-9A). From Day 1 to Day 29, the activity retention for PEG-GOx and native GOx is 44.0 ± 6.64% and 37.2 ± 2.29%, respectively.

As shown in Fig. 3-9B, fitting reveals that native GOx loses its activity at a faster rate than PEG-GOx over four weeks. Half-life values are given by $t_{1/2} = (\ln 2)/\lambda$, where $t_{1/2}$ is the half-life and λ is the decay constant from the fitted exponential decay. Half-life values for PEG-GOx and native GOx stored for four weeks at 37 °C in the absence of glucose are 21.1 days and 12.9 days, respectively, which represents a 60% increase in half-life for GOx upon PEGylation.

3.3.2.2. Operational Stability

Table 3-1 compares the activity retention of PEG-GOx and native GOx following glucose exposure for 24 h; data represent 95% confidence intervals (n = 3). Although GOx apparently has greater specific activity before and after glucose exposure as compared to PEG-GOx before and after glucose exposure, the activity retention of GOx and PEG-GOx following glucose exposure for 24 h is statistically equivalent.

Table 3-1 Activity retention following glucose exposure for 24 h (95% confidence intervals, n = 3)

	Specific Activity (U/mg)		
Sample	Pre-glucose exposure	Post-glucose exposure	Activity retention (%)
GOx	237 ± 12	159 ± 15	67.3 ± 7.3
PEG-GOx	195 ± 4.1	122 ± 5.8	62.6 ± 3.2

Although half-life values are dependent upon many variables (*e.g.*, temperature, pH, substrate concentration, enzyme concentration, enzyme immobilization), our measurements for long-term storage stability and glucose stability are consistent with previous reports in the literature.[8, 92-95] For example, Krishnaswamy and Kittrell reported that solution-phase GOx (citrate-phosphate buffer, pH 5.5, air-equilibrated) exposed to 10 mM glucose has a half-life of 23.1 h,[95] which is slightly lower than what we observed for native GOx; similarly, Fortier and Belanger showed that GOx entrapped in a polypyrrole matrix and exposed to 250 mM glucose (*ca.* 5% w/v glucose) at room temperature had a half-life of approximately 18.7 h. The same group demonstrated that

solution-phase GOx has a half-life of 6 h at 50 °C in the absence of glucose,[93] which is significantly lower than what we observed at 37 °C. However, Tse and Gough reported a much higher half-life (*i.e.*, 87.2 days) for immobilized GOx stored in the absence of glucose at 37 °C in 0.1 M phosphate buffer (pH 7.3).[8]

Our findings agree well with work reported by Unterweger and others[91] on a PEGylated S218C mutant of L-lactate oxidase. Wild-type L-lactate oxidase from *Aerococcus viridans* is a homotetrameric enzyme with a molecular mass of 164 kDa and a flavin mononucleotide prosthetic group.[96] This group showed that site-specific PEGylation of a mutated L-lactate oxidase with one or two maleimide-activated PEGs caused a small decrease (*ca.* 30%) in specific activity and did not alter the enzymatic stability of the mutant.[91] Conversely, Slavica and others[97] showed that orthogonal maleimide-thiol coupling of D-amino acid oxidase from *Trigonopsis variabilis* (a non-glycosylated homodimeric FAD-dependent oxidase of 76 kDa)[98] with three maleimide-activated PEGs resulted in a marked decrease in substrate catalytic efficiency for the dioxygen-dependent reaction. Finally, there have been mixed reports concerning post-PEGylation activity when amine-reactive PEGs are employed, with some studies demonstrating complete retention of enzymatic activity[99, 100] and others indicating partial loss of enzymatic activity.[16-19]

3.4. Conclusions

PEG-Hz was covalently coupled to periodate-oxidized glycosylation sites of GOx from *A. niger*. Liquid chromatography and gel electrophoresis data indicate that the PEGylation protocol resulted in a drastic increase in the apparent molecular mass of

GOx, with complete conversion to the bioconjugate. Mass spectrometry data prove that the extent of PEGylation was three PEG chains per GOx subunit (*i.e.*, six PEG chains per GOx dimer). Particle sizing data do not support the presence of higher-order oligomers in the PEG-GOx sample. Enzymatic activity assays of PEG-GOx and native GOx revealed that the bioconjugate's performance was statistically equivalent to native GOx in terms of activity retention over the 29 day time period and following the 24 h glucose exposure, although a 60% increase in half-life was realized upon PEGylation. However, coupling of other potentially stabilizing molecules (*e.g.*, other synthetic or natural polymers, proteins, *etc.*) to GOx *via* its glycosylation sites can now be explored as it is likely that targeted attachment to these sites will not have a detrimental effect on enzymatic activity.

4. CHEMICAL MODIFICATION OF PEGYLATED GLYCOENZYME*

4.1. Introduction

As discussed in Section 2, many enzyme stabilization approaches have been demonstrated. Of these, carrier-free crosslinking-based techniques such as CLECs and CLEAs stand out for their ability to effectively stabilize an enzyme's tertiary and quaternary structure (*i.e.*, preventing denaturation and subunit dissociation) without "diluting" the activity.[10, 11, 15] However, the resulting particles are large and polydisperse (*ca.* 5-50 μm), they no longer reside in the solution phase, and significant transport barriers are expected. If these types of techniques could be reduced to the *single-enzyme level*, stabilization might still be possible, and some of the undesirable properties associated with CLECs and CLEAs could be avoided.

In this section, a novel approach to enzyme stabilization is demonstrated, which offers marked advantages over previously reported techniques. In Section 3, glycosylation site-targeted PEGylation of GOx was shown to have little effect on the functional properties of the enzyme. However, the polymeric shell substantially increased the radius of the conjugate (by *ca.* 50–66%), and PEGylation did not involve reaction of the enzyme's superficial amine groups; the technique presented herein leverages these two properties of GOx PEGylated in this manner. I hypothesized that this inert buffering layer deposited on the surface of each GOx molecule would permit

---

* Parts of this section are reprinted from D. W. Ritter, J. M. Newton and M. J. McShane, *RSC Adv.*, 2014, **4**, 28036-28040 – Reproduced by permission of The Royal Society of Chemistry. Available online at http://pubs.rsc.org/en/Content/ArticleLanding/2014/RA/c4ra03809f.

subsequent chemical modification to be performed to stabilize the enzyme, while preventing GOx molecules from reacting with one another. Such intermolecular crosslinking results in irreversible, large-scale aggregate formation,[25] which can lead to a decrease in apparent enzyme activity resulting from substrate inaccessibility to its binding site. Aggregate formation would also preclude the use of the stabilized enzyme in applications which require the macromolecule to be in solution phase and/or near-native size. Furthermore, preservation of the enzyme's reactive primary amines *via* this PEGylation route is key to permit effective modification by an amine-reactive dialdehyde such as GA.[25]

This straightforward approach combines two well-established modification strategies: 1) initial PEGylation of an enzyme to provide steric protection, followed by 2) chemical modification with GA in an effort to stabilize the enzyme's tertiary and quaternary structures (Fig. 4-1). The intention was to stabilize GOx in a way that permits subsequent homogenous distribution and entrapment within an optical biosensing hydrogel; however, this approach could in principle be applied to a myriad of other proteins for different applications, which might include tissue engineering and therapeutic biologicals. It is demonstrated that this technique results in dramatic increases in long-term storage stability for GOx, while avoiding undesirable aggregate formation.

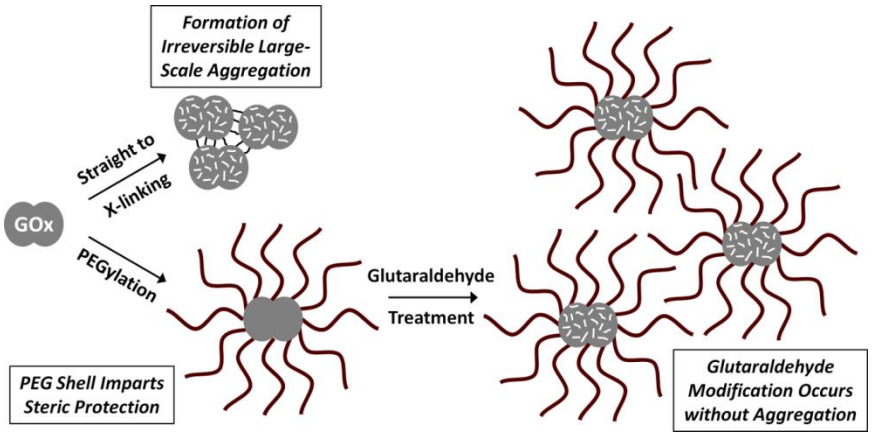

Fig. 4-1 PEGylation of the enzyme and subsequent chemical modification allows for enzyme stabilization. Covalently bound PEG chains sterically protect against intermolecular crosslinking.

4.2. Experimental

4.2.1. Materials

GOx from *A. niger* (338 U/mg solid, 82% protein) was obtained from BBI Enzymes, and peroxidase from *Amoracia rusticana* (type II, 188 U/mg solid) was obtained from Sigma. PEG-Hz (4.5 kDa by gel permeation chromatography) was obtained from Laysan Bio.

4.2.2. Synthesis of Modified Glucose Oxidase and PEGylated Glucose Oxidase

The procedure used in this work to synthesize PEG-GOx, which is depicted schematically in Fig. 4-2, is slightly modified from previous work detailed in Section 3.[23] Additionally, the supplier from which the GOx is purchased has been changed between these two studies. The reason for the change in supplier is that the GOx purchased from BBI Enzymes has a specific activity twice that of GOx purchased from Sigma. Since a higher quality enzyme with higher activity is more desirable for use

in our group's sensors, we began to incorporate the more active GOx once we became aware of its availability. Therefore, the change in supplier was justified to ensure that our findings remained relevant to our group's current glucose biosensors.

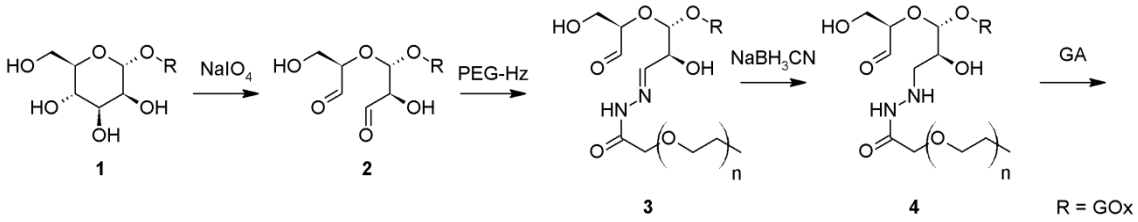

Fig. 4-2 Synthesis of PEG-GOx followed by GA modification. Glycosylation sites on GOx are oxidized by $NaIO_4$ to yield reactive aldehydes. The hydrazide group of the PEG is covalently attached at the glycosylation sites, and the resulting hydrazone linkages are reduced with $NaBH_3CN$ for stability.

GOx (6.6 mg, **1**) was dissolved in 1.8 mL of 100 mM sodium phosphate containing 154 mM NaCl (pH 7.2). Separately, $NaIO_4$ (8.6 mg) was dissolved in 200 µL of deionized water *via* sonication and vortexing (protected from light). Immediately following dissolution, the $NaIO_4$ solution was added to the GOx solution, and the container was wrapped in foil and placed on a nutating mixer to provide gentle agitation for 1 h at room temperature to yield **2**. As discussed in Section 3.2.2, proteins exposed to oxidants have been reported to form higher-order oligomers in certain cases due to intermolecular crosslinking; however, Nakamura and others exposed GOx from *A. niger* to a five-fold higher concentration of $NaIO_4$ for 5 h and found the size and shape of oxidized GOx similar to that of native GOx.[86] Nevertheless, using our protocol, a small amount of aggregated GOx could be observed after oxidation, but it will be removed during subsequent desalting or purification. Glycerol (20:1 molar ratio of glycerol to

$NaIO_4$) was added to quench the reaction. The oxidized GOx was immediately purified using a desalting column equilibrated with 100 mM sodium phosphate containing 154 mM NaCl (pH 7.2) to remove excess $NaIO_4$, glycerol, and degradation products from glycerol quenching (*i.e.*, formaldehyde and formic acid).

PEG-Hz (37.18 mg) was then added to the oxidized GOx solution (200:1 molar ratio of PEG to GOx). These conditions favor attachment of PEG rather than intermolecular crosslinking between oxidized sugars and superficial amines on GOx because of the hydrazide group's low pK_a (*ca.* 3), along with the smaller size and large molar excess of PEG as compared to GOx. The solution containing PEG and GOx was reacted in the dark for 2 h at room temperature under gentle agitation to yield **3**. In a fume hood, 20 µL of $NaBH_3CN$ (5 M, in 1 N NaOH) was added to the mixture. **Caution: $NaBH_3CN$ is extremely toxic; as such, all operations should be performed with care in a fume hood**. The $NaBH_3CN$ was reacted with the PEG-GOx for 30 min at room temperature under gentle agitation to yield **4**. PEG-GOx was then purified from low-molecular-weight contaminants using a desalting column equilibrated with 10 mM sodium phosphate containing 154 mM NaCl (pH 7.2).

GFC was performed to further purify PEG-GOx (*i.e.*, remove unattached PEG) and analyze products. Sample was injected into a liquid chromatography system (GE Healthcare Life Sciences model ÄKTAexplorer 10) equipped with a gel-filtration column (GE Healthcare Life Sciences model HiLoad Superdex 200 PG) equilibrated with 10 mM sodium phosphate containing 150 mM NaCl (pH 7.2). Absorbance at 220

nm, 280 nm, and 450 nm was monitored, 2 mL fractions were collected, and protein-containing fractions were pooled and concentrated to 6 mg/mL (relative to GOx).

To initiate chemical modification, equal volumes of enzyme solution (GOx or PEG-GOx, 6 mg/mL in 10 mM sodium phosphate containing 150 mM NaCl, pH 7.2) and GA solution (ranging from 7.5e-4 wt% to 25 wt%) were combined and reacted for 1 h at room temperature. The final GA concentrations in the reaction solution ranged from 3.75e-4 wt% to 12.5 wt%, corresponding to a molar excess of GA (relative to GOx monomer) ranging from 1 to 3.33e4, respectively. Excess GA was removed using a centrifugal device (Pall model Nanosep 30K), and the modified enzyme was transferred back into 10 mM sodium phosphate containing 154 mM NaCl (pH 7.2).

4.2.3. Physical and Chemical Characterization

4.2.3.1. Particle Sizing

A photon correlation spectrometer (Malvern model Zetasizer Nano ZS) was used to acquire size distributions of the modified and unmodified PEG-GOx and native GOx samples (n = 5). This was necessary to determine the change in size after GA modification, as well as the extent of oligomerization during oxidation, subsequent PEGylation, and GA exposure. Disposable 3.5 mL cuvettes were filled with enzyme (1 mL, 0.6 mg/mL) in 10 mM sodium phosphate containing 154 mM NaCl (pH 7.2).

4.2.3.2. Primary Amine Content

A fluorescamine assay was used to determine the presence of free primary amines on GA-modified and unmodified PEG-GOx and native GOx samples as an indication of the extent of modification (n = 4). In a 96-well solid black flat bottom

polystyrene microplate, enzyme (200 µL, 25 µg/mL) in 10 mM sodium phosphate containing 154 mM NaCl (pH 7.2) was mixed with 1 mM fluorescamine (50 µL, 0.3 mg/mL) in acetone for 60 s. Fluorescence was excited from samples at 405 nm and fluorescamine emission was collected at 485 nm using a multimode microplate reader (Tecan model Infinite M200 PRO series).

4.2.3.3. Temperature Ramp

A photon correlation spectrometer (Malvern model Zetasizer Nano ZS) was used to determine the effect of heating on the size of the modified and unmodified PEG-GOx and native GOx samples (n = 3). Standard 3.5 mL glass cuvettes were filled with enzyme (1 mL, *ca.* 0.735 mg/mL) in 10 mM sodium phosphate containing 154 mM NaCl (pH 7.2). The temperature of the cuvette holder was incrementally increased from 25 °C to 90 °C in steps of 5 °C, and the enzyme solution was allowed to equilibrate to each temperature for 2 min prior to collection of sizing data. Due to the large amount of sample required to test each enzyme type, only the most extreme GA concentrations (0 wt% and 2.5 wt% GA) were tested.

4.2.4. Functional Characterization

4.2.4.1. Enzymatic Activity Assays

Enzymatic assays of GA-modified and unmodified PEG-GOx and native GOx samples were performed to determine activity following exposure to various challenges.[88] In all cases, enzymatic activity measurements were performed in triplicate at pH 5.1 and 35°C using a UV/Vis spectrophotometer (Agilent model Cary 300) equipped with a water-thermostatted multicell holder to maintain the appropriate

temperature. Absorbance data were collected at approximately 30 Hz for approximately 2.5 min. Data were fit *via* linear regression using the maximum number of points to obtain a norm of residuals less than 0.025. This procedure was adopted to minimize the effects of nonlinearities present at later time points in absorbance data collected for samples of high catalytic activity.

4.2.4.2. Long-Term Storage Stability

To observe the effects of PEGylation and GA modification on the spontaneous denaturation of GOx, enzymatic activity was assayed over a period of four weeks with the enzyme samples stored at 37 °C (elevated temperature to accelerate deactivation and simulate physiological conditions) in the absence of glucose. To limit sample contamination, multiple samples were prepared for each enzyme type and each time point to prevent the need for samples to be repeatedly opened; that is, samples were only opened on the day they were assayed for enzymatic activity.

4.2.4.3. Operational Stability

To test for the effect of glucose on GA-modified and unmodified PEG-GOx and native GOx, samples were continuously exposed to PBS containing glucose at room temperature for up to 24 h. For these experiments, a dynamic dialysis system in a microplate format (10-well MicroDialyzer) was obtained from Spectrum Labs (Note: this product has been discontinued). The MicroDialyzer has ten wells, each of which can be filled with up to 500 µL of sample that is in direct contact with a 12-14 kDa regenerated cellulose dialysis membrane (Spectrum Labs model Spectra/Por 2). Beneath the dialysis membrane, a stirred dialysate solution is pumped through the dialysis

chamber. For our purposes, enzyme solutions (250 µL, *ca.* 0.25 mg/mL) were added to the wells (n = 3), and PBS containing glucose (100 mg/dL) was pumped through the dialysis chamber at 4 mL/min using a peristaltic pump. Fig. 4-3 (*left*) shows the assembled MicroDialyzer on top of a magnetic stir plate in the foreground with the peristaltic pump shown in the background. Fig. 4-3 (*right*) illustrates the flow and diffusion path for glucose to enter the enzyme-containing wells while product (*i.e.*, H_2O_2 and gluconic acid) is also removed from the system.

After the appropriate glucose exposure time (6 h, 12 h, or 24 h), glucose-containing PBS was removed from the dialysis chamber, and 1 L of fresh PBS (no glucose) was pumped through the system at 4 mL/min (*ca.* 4 h) to remove excess glucose and product from the sample wells. Because the samples may change volume due to osmotic and hydrostatic forces—and because there is a possibility for the membrane to be compromised during testing—the samples were transferred to a standard microplate and analyzed for concentration using a multimode microplate reader (Tecan model Infinite M200 PRO series). Finally, the samples were assayed for enzymatic activity as described in Section 4.2.4.1.

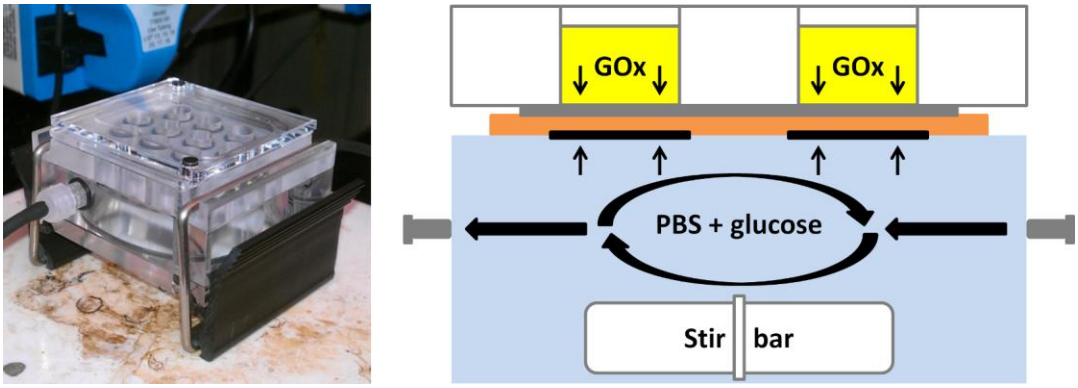

Fig. 4-3 Apparatus used for glucose exposure experiments. The photograph on the left depicts the MicroDialyzer during operation, while the schematic on the right illustrates how the MicroDialyzer is utilized for these experiments.

4.2.4.4. Thermostability

To determine if PEGylation and GA modification provides stabilization of the enzyme at elevated temperatures (*i.e.*, where thermally-induced denaturation dominates), enzyme samples (0.73 mg/mL) were immersed into a 60 °C water bath for up to 1 h. Separate replicate samples (n = 3) were prepared for each time point (5 min, 15 min, and 1 h). Upon removal from the water bath, samples were immediately cooled to 4 °C, then assayed for enzymatic activity as described in Section 4.2.4.1.

4.2.4.5. Solvent/Additive Stability

Solvents and additives to which the GA-modified and unmodified PEG-GOx and GOx might be expected to be exposed (*e.g.*, during sensor fabrication or sterilization) were tested for their effect on enzymatic activity. Enzymes (0.25 mg/mL) were exposed to 70% ethanol (EtOH) and 50% dimethyl sulfoxide (DMSO) for 10 min. Additionally, enzymes were exposed to three multi-component polymer precursor solutions: poly(2-hydroxyethyl methacrylate) (pHEMA), poly[(2-hydroxyethyl methacrylate)-*co*-(2-

aminoethyl methacrylate)] (pHEMA-*co*-AEMA), and poly[(2-hydroxyethyl methacrylate)-*co*-acrylamide] (pHEMA-*co*-AAm). The composition of each of the precursor solutions is provided in Table 4-1, and the final enzyme concentrations were approximately 0.215 mg/mL. Following exposures, samples were transferred back into PBS using centrifugal devices (Pall model Nanosep 30K). Samples were then transferred to a microplate and concentration was determined using a multimode microplate reader (Tecan model Infinite M200 PRO series). Finally, the samples were assayed for enzymatic activity as described in Section 4.2.4.1.

Table 4-1 Composition of polymer precursor solutions

Component	Volume of Component (µL)		
	pHEMA	pHEMA-*co*-AEMA	pHEMA-*co*-AAm
2-Hydroxyethyl methacrylate	122.5	122.5	93.75
2-Aminoethyl methacrylate (25 mM in H_2O)	—	5	—
Acrylamide (67 wt% in H_2O)	—	—	31.25
Tetraethylene glycol dimethacrylate	2.5	2.5	2.5
Ethylene glycol	45	45	45
DMSO	25	25	25
Enzyme (1 mg/mL in H_2O)	54	54	54

4.3. Results and Discussion

4.3.1. Physical and Chemical Characterization

4.3.1.1. Particle Sizing

DLS reveals that PEG-GOx has a hydrodynamic diameter of 16.98 ± 2.68 nm, as compared to native GOx, which has a hydrodynamic diameter of 10.76 ± 0.95 nm (Fig. 4-4). Subsequently, PEG-GOx was modified with GA at various concentrations ranging from 3.75e-4 wt% to 12.5 wt%. DLS was used to determine the hydrodynamic size of the modified PEG-GOx (n = 5), which provides insight into the extent of intermolecular crosslinking at various GA concentrations. As hypothesized, there was no statistically significant change in the size of the initially PEGylated GOx across the range of GA concentrations (Fig. 4-4). In a control experiment, native GOx exposed to GA concentrations of 2.5 wt% or higher was determined to be larger than native GOx, indicating formation of multi-enzyme aggregates (Fig. 4-4). Upon visual inspection, the GOx samples exposed to the two highest GA concentrations (*i.e.*, 6.25 wt% and 12.5 wt%) contained easily identifiable large-scale aggregates. These GA concentrations were omitted for the remainder of the study to prevent possible misrepresentation of enzymatic activity due to inaccurate estimates of protein concentrations or significant apparent activity reduction due to blockage of substrate diffusion to active sites.

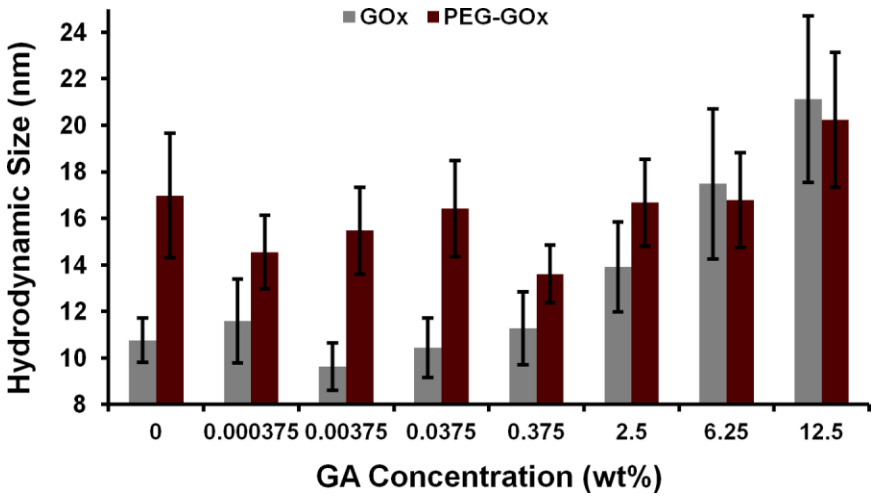

Fig. 4-4 Mean hydrodynamic size of native GOx (gray bars) and PEG-GOx (maroon bars) exposed to various GA concentrations. Error bars represent 95% confidence intervals (n = 5).

4.3.1.2. Primary Amine Content

A fluorescamine assay was employed to test for free primary amines (*e.g.*, ε-amino group of superficial Lys residues)[101] as an indication of the extent of GA modification of PEG-GOx and native GOx (n = 4). The data clearly show that with increasing GA concentration, the amine content of both PEG-GOx and native GOx is decremented (indicated by a decrease in fluorescamine emission)—attributable to modification of the enzyme by GA (Fig. 4-5). Further, the decrease in amine content of the PEG-GOx with increasing GA concentration appears to be similar to that of native GOx; thus, the presence of PEG does not appear to interfere with the reaction between GA and PEG-GOx. Finally, because the fluorescamine emission from PEG-GOx is initially and persistently lower than that of native GOx, this might suggest that PEG-GOx contains fewer primary amines than native GOx. However, we believe this is more likely due to the steric hindrance of PEG: a portion of the amines on PEG-GOx are

inaccessible by fluorescamine, which is more bulky and has a molecular mass nearly three times that of GA.

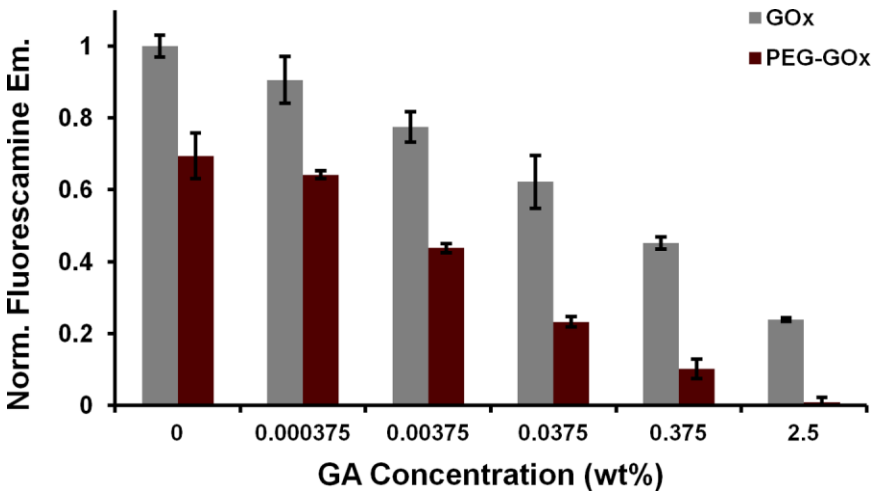

Fig. 4-5 Free primary amine content of native GOx (gray bars) and PEG-GOx (maroon bars) exposed to various GA concentrations. Error bars represent 95% confidence intervals (n = 4).

4.3.1.3. Temperature Ramp

To further characterize the modified and unmodified enzymes, DLS was employed to investigate the effect of heating on size distribution (n = 3). The hydrodynamic diameter of each form of enzyme was monitored while incrementally increasing the temperature of the sample from 25 °C to 90 °C. Fig. 4-6 shows the size distributions for each type of enzyme as a function of temperature. Clearly, all sample types exhibit one primary peak at all tested temperatures; however, the GA-modified samples show evidence of higher-molecular-weight species at some temperatures. Because DLS measurements are scattering-based, they are particularly sensitive to large particles. While this increased sensitivity facilitates identification of aggregation and

contamination and permits better comparison among the samples, it should be noted that the primary peak accounted for at least 99.0% of the sample by volume in all cases.

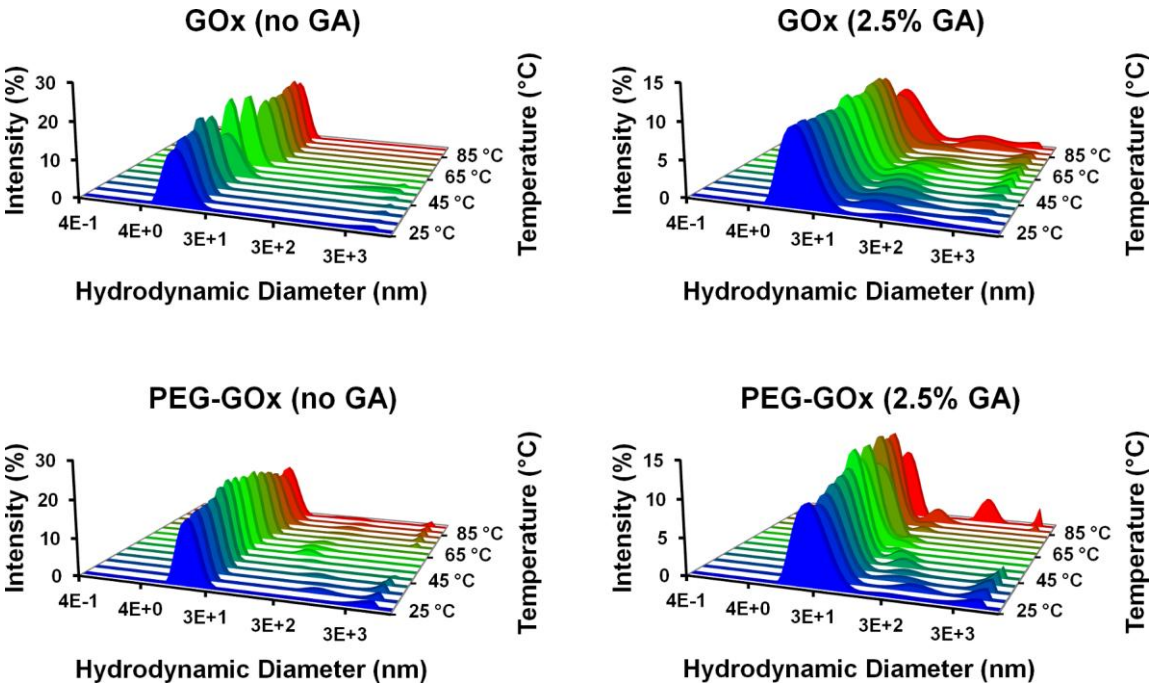

Fig. 4-6 Size distributions of GA-modified and unmodified PEG-GOx and native GOx as a function of temperature (n = 3).

As it is difficult to compare the different enzyme types in Fig. 4-6, the percent change in the size of the primary peak from its initial size was plotted as a function of temperature (Fig. 4-7). The size distribution of native GOx begins to drastically shift toward larger size at 60 °C (*ca.* 150% change at 75 °C), which is indicative of thermal denaturation and subsequent aggregation of the enzyme at these temperatures. This is consistent with reports from other groups that place the melting temperature for GOx between approximately 56 °C and 58 °C.[72, 100, 102] Moreover, GOx is reported to form

primarily trimers and tetramers upon thermal denaturation, which is supported by the magnitude of the size increase as well.[72] For the GA-modified GOx, the size distribution still shifts toward larger size at elevated temperature; however, the onset is delayed until about 80 °C is reached and the size change is attenuated by a factor of two. Reduced aggregation from the GA-modified GOx could indicate reduced thermal denaturation, possibly due to increased rigidity resulting from GA crosslinking. In the case of both unmodified and GA-modified PEG-GOx, no significant increase in size was observed across the range of exposure temperatures. This could signal an increase in thermal stability, but it could be that the presence of PEG merely prevents thermally denatured enzyme from aggregating.

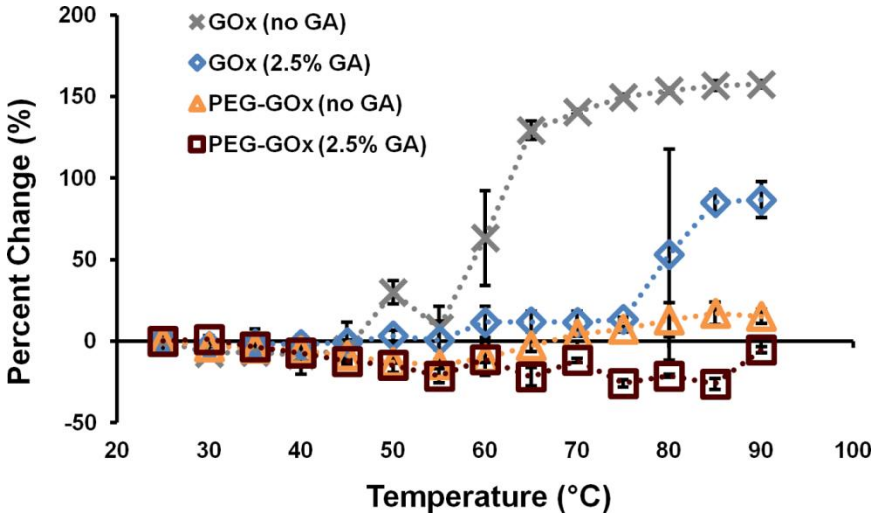

Fig. 4-7 Effect of heating on the mean hydrodynamic size of GA-modified and unmodified PEG-GOx and native GOx. Error bars represent 95% confidence intervals (n = 3), and dotted lines are intended to be a guide for the eyes.

4.3.2. Functional Characterization

4.3.2.1. Long-Term Storage Stability

To investigate the effect of GA modification on the long-term retention of enzymatic activity, samples of PEG-GOx and native GOx—either unmodified or modified with GA concentrations ranging from 3.75e-4 wt% to 2.5 wt%—were stored in PBS for four weeks at 37 °C. Enzymatic activity was assayed at various points in time. The initial time point reveals that GOx modified with 2.5 wt% GA has only 87.6% the specific activity of unmodified GOx, whereas there is no statistically significant difference between the specific activities of PEG-GOx modified with 2.5 wt% GA and its unmodified counterpart (Fig. 4-8A). Also, no statistically significant difference is observed between the specific activities of GOx modified with 0.375 wt% GA and unmodified GOx after 1 day. The data show that after four weeks, PEG-GOx modified with 2.5 wt% GA retains more than twice its initial specific activity compared to unmodified PEG-GOx (273 U/mg *vs.* 112 U/mg or 73.1% *vs.* 30.0% retention, respectively). Similarly, Fig. 4-8B shows that GOx modified with 2.5 wt% GA retains 70.3% specific activity after four weeks, which is greater than GOx modified with 0.375 wt% GA (40.8% retention) and greater still than unmodified GOx (8.19% retention).

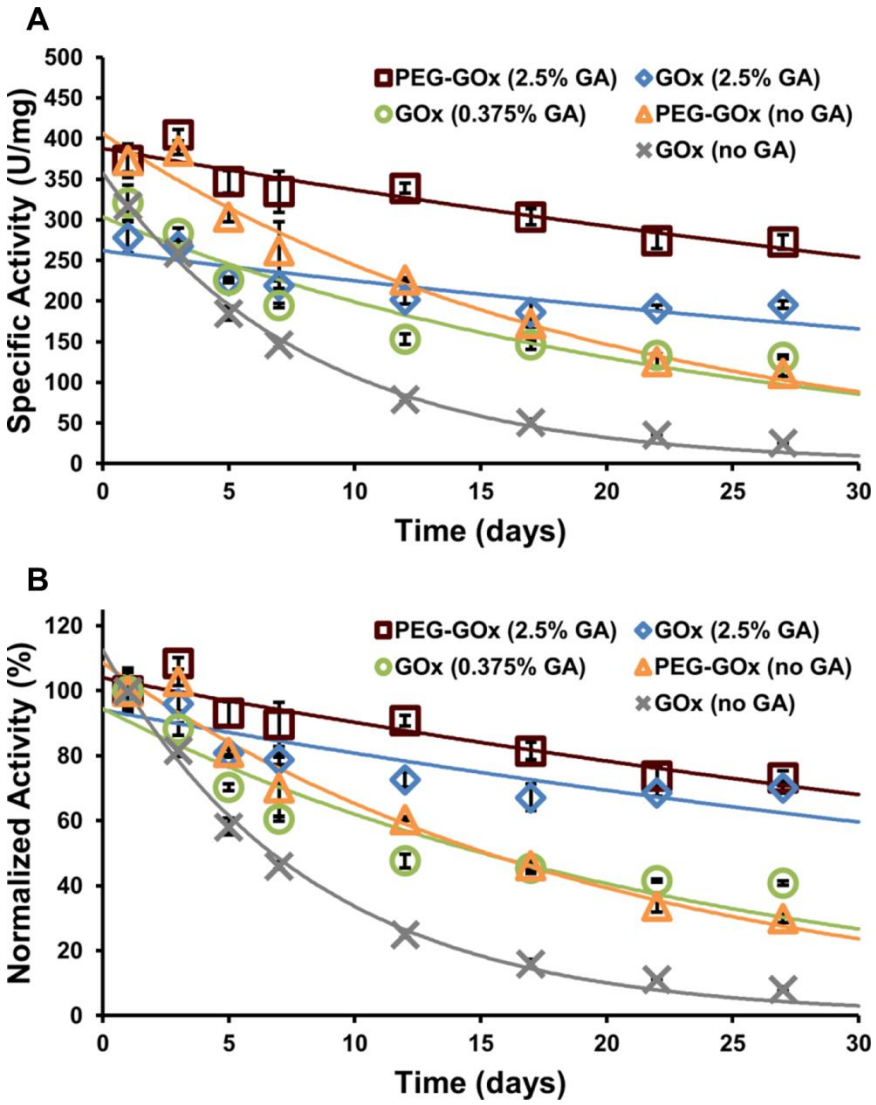

Fig. 4-8 Specific activity (A) and normalized activity (B) of GA-modified PEG-GOx and native GOx, as well as unmodified controls, in the absence of glucose over four weeks at 37 °C. PEG-GOx modified with 2.5 wt% GA (maroon squares) retained the most activity, followed by GOx modified with 2.5 wt% GA (blue diamonds), and then GOx modified with 0.375 wt% GA (green circles). Unmodified PEG-GOx (orange triangles) and GOx (gray crosses) lost the most activity over time. Error bars represent 95% confidence intervals (n = 3). The data were fit with first-order exponential decays.

For the sake of clarity, Fig. 4-8 only shows activity data for the unmodified samples and those that differ significantly from the unmodified samples. On the other

hand, the activity data for PEG-GOx and native GOx at all tested GA concentrations were fit with first-order exponential decays, and the calculated half-life values are shown in Fig. 4-9. One can see that at GA concentrations lower than 0.375 wt%, PEG-GOx is slightly more than twice as stable as native GOx (*i.e.*, half-life values of *ca.* 13.5–15 days for PEG-GOx and *ca.* 6–7 days for native GOx). However, at 0.375 wt% GA, PEG-GOx and native GOx performance are virtually identical (*i.e.*, half-life values of *ca.* 17 days and *ca.* 16.5 days, respectively), and at 2.5 wt% GA, the half-life of PEG-GOx exceeds that of native GOx by approximately 3.5 days (*i.e.*, *ca.* 49 days and *ca.* 45.5 days, respectively).

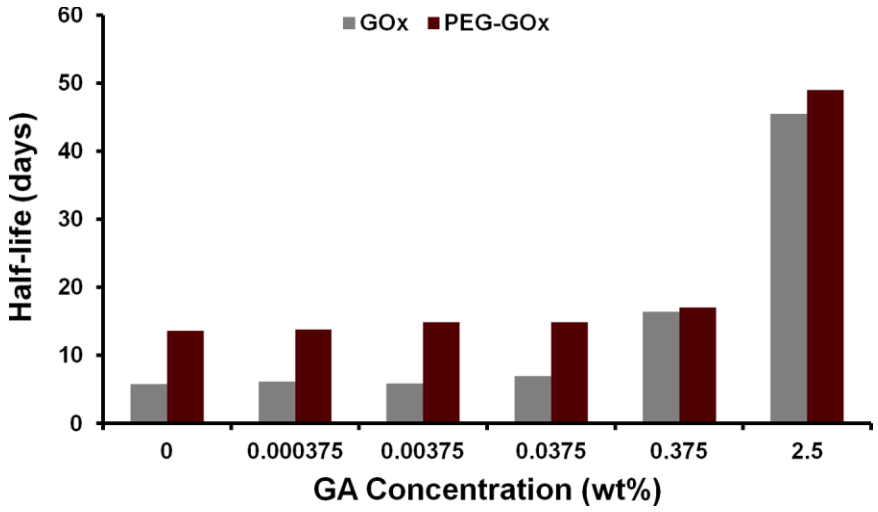

Fig. 4-9 Mean lifetime values calculated from long-term storage stability data fit with first-order exponential decays for native GOx (gray bars) and PEG-GOx (maroon bars) at various GA concentrations.

4.3.2.2. Operational Stability

It is well-known that exposure of GOx to glucose hastens its activity loss *via* production of and modification by hydrogen peroxide,[103] and we have previously reported this effect with respect to PEG-GOx.[23] Betancor and co-workers have shown that immobilization of GOx can mitigate deactivation by hydrogen peroxide to a large extent, presumably due to increased rigidity.[104] We tested for this effect on GA-modified and unmodified PEG-GOx and native GOx by continuously exposing samples to PBS containing glucose at room temperature for up to 24 h. As shown in Fig. 4-10, there were no major differences among the various samples in their response to glucose exposure; after 24 h, all samples lost approximately 75% of their initial specific activity. However, at the 6 h time point, native GOx exposed to 2.5 wt% GA had lost more activity than native GOx, and after 12 h, both of the GA-modified GOx samples (*i.e.*, 0.375 wt% GA and 2.5 wt% GA) had lost more activity than native GOx. At all tested time points, unmodified and GA-modified PEG-GOx were not significantly different from modified native GOx ($\alpha = 0.05$).

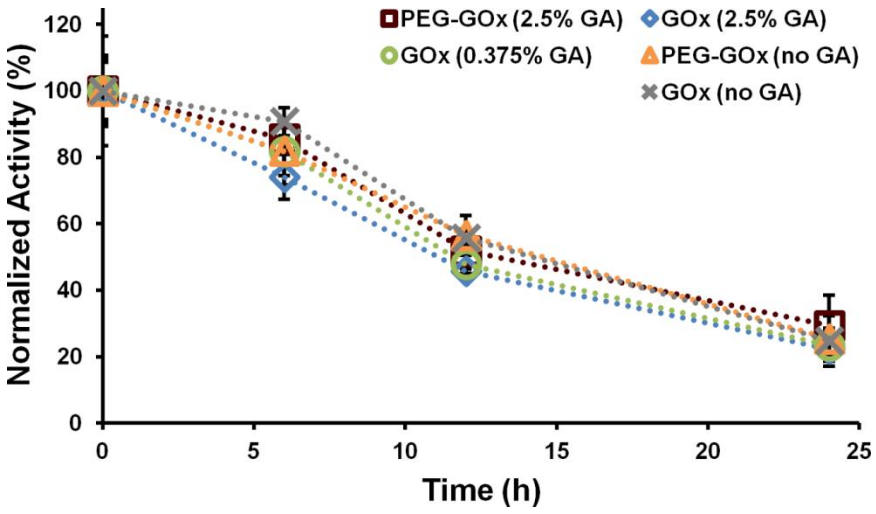

Fig. 4-10 Normalized activity of GA-modified and unmodified PEG-GOx and native GOx with exposure to glucose (PEG-GOx modified with 2.5 wt% GA, maroon squares; GOx modified with 2.5 wt% GA, blue diamonds; GOx modified with 0.375 wt% GA, green circles; PEG-GOx, orange triangles; GOx, gray crosses). Error bars represent 95% confidence intervals (n = 3), and dotted lines are intended to be a guide for the eyes.

4.3.2.3. Thermostability

For many enzymes, exposure to extreme temperature results in thermally-induced denaturation accompanied by enzymatic activity loss. For GOx specifically, thermal denaturation involves an irreversible transition to a compact denatured state, which is accompanied by dissociation of the FAD co-factor but not dissociation of the dimer into its subunits.[72] To determine if PEGylation and GA modification of the enzyme provided stability at elevated temperatures, enzymatic activity was assayed following exposure to 60 °C for up to 1 h. Interestingly, while PEGylation proved beneficial at all time points, GA modification of both native GOx and PEG-GOx appeared to have a largely deleterious effect (Fig. 4-11).

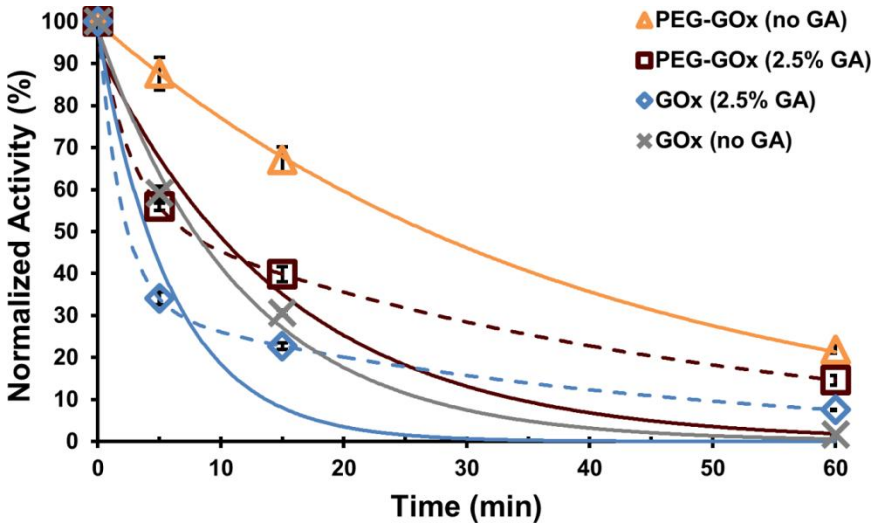

Fig. 4-11 Normalized activity of GA-modified and unmodified PEG-GOx and native GOx following heating of enzyme solutions to 60 °C. Error bars represent 95% confidence intervals (n = 3). The data for unmodified PEG-GOx (orange triangles) and unmodified GOx (gray crosses) were fit with first-order exponential decays (orange and gray solid lines, respectively); however, the data for modified PEG-GOx (maroon squares) and modified GOx (blue diamonds) were fit with both first-order (maroon and blue solid lines, respectively) and second-order exponential decays (maroon and blue dashed lines, respectively).

The data were fit with first-order exponential decays (solid lines) to allow for calculation of the half-life values. Using these decay constants, it was determined that GOx has a half-life of 8.1 min, which is reduced by half to 4.2 min upon modification with 2.5 wt% GA. Under the same conditions, PEG-GOx has a greatly improved half-life of 27 min (233% increase over native GOx), but consistent with native GOx, that half-life is reduced by a factor of 2.5 to 11 min for the GA-modified PEG-GOx.

While the first-order exponential decays fit well for the unmodified enzymes ($R^2 > 0.99$), they did not fit as well for the GA-modified enzymes ($R^2 < 0.95$). As such, the activity data for the GA-modified GOx and PEG-GOx were fit with second-order exponential decays (dashed lines), which fit quite well ($R^2 = 1$). For GA-modified PEG-

GOx, a majority of the population had a long half-life of 31 min, while the remaining 45% of the population had a short half-life of 1.8 min. On the other hand, approximately two-thirds of the GA-modified GOx population had a short half-life of 1.3 min, while only one-third of the population had a long half-life of 28 min. So while PEGylation of GOx clearly protects the enzyme during exposure to elevated temperatures, GA modification of the enzyme has a more complex outcome, with a fraction of the enzyme population receiving a protective effect and the remaining portion experiencing a deleterious effect. However, it appears that PEGylation of the enzyme prior to GA modification can help to increase the portion of the enzyme population that experiences the protective effect, translating to overall improved stability at elevated temperatures.

Seymour and Klinman have shown that PEGylation of GOx increases its melting temperature, which is in good agreement with our results.[100] The most likely explanation for the reduced thermostability observed from the GA-modified samples is an inability for these forms of the enzyme to undergo thiol-disulfide exchange. GOx, which contains two disulfide bonds and two thiol groups per homodimer, relies heavily upon thiol-disulfide exchange for stability at higher temperatures, according to Ye and Combes.[105] They have shown that blocking of the free thiols of GOx with *N*-ethylmaleimide does not affect the initial activity, but drastically reduces the enzyme's stability at 60 °C. Therefore, it is possible that GA modification prevents thiol-disulfide exchange, either through increased rigidity or creation of a microenvironment in which thiol-disulfide exchange is unfavorable; however, it would be difficult to test this hypothesis.

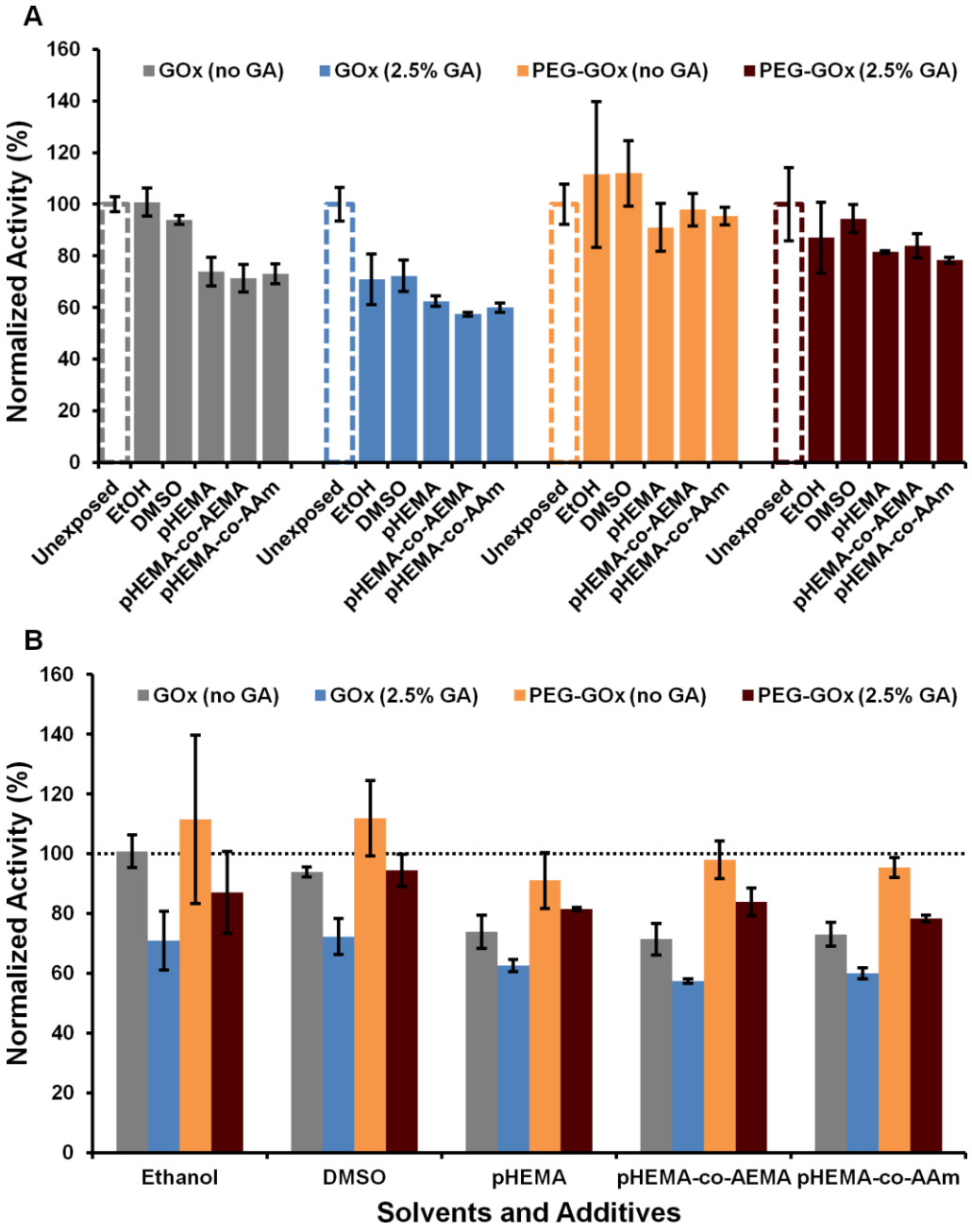

Fig. 4-12 Normalized activity of GA-modified and unmodified PEG-GOx and native GOx with exposure to various solvents and additives grouped by enzyme type (A) or exposure type (B). In all cases, samples are normalized to unexposed enzyme of the same type (*e.g.*, exposed PEG-GOx samples normalized to unexposed PEG-GOx); for grouping by exposure type (B), unexposed enzyme is indicated by the dotted horizontal line at 100%. GOx is depicted with gray bars, GA-modified GOx with blue bars, PEG-GOx with orange bars, and GA-modified PEG-GOx with maroon bars. Error bars represent 95% confidence intervals (n = 3).

4.3.2.4. Solvent/Additive Stability

Since it is expected that enzymes might come into contact with various solvents and additives throughout normal use—some of which might be harmful—modified and unmodified PEG-GOx and native GOx were exposed to a number of substances for a limited period of time, then tested for changes in enzymatic activity. Fig. 4-12 shows the specific activity of each type of enzyme after exposure to the solvents and additives, which has been normalized to the specific activity of unexposed enzyme of the same type (*e.g.*, exposed PEG-GOx samples normalized to unexposed PEG-GOx). In Fig. 4-12A, the bars are grouped by enzyme type to facilitate comparison of the effects of each solvent or additive on each type of enzyme, as well as to provide a snapshot of each enzyme type's overall stability to various solvents and additives in general. Fig. 4-12B shows the bars grouped by exposure type to permit evaluation of each enzyme's relative appropriateness in the presence of each solvent or additive.

For native GOx, exposure to 70% EtOH did not affect its specific activity, although some limited protein aggregation was observed; a slight reduction in specific activity resulted from exposure to 50% DMSO, and exposure to all of the tested polymer precursor solutions resulted in an approximate 25% reduction in specific activity. At a 95% confidence level, the specific activity of PEG-GOx following exposure to each of the tested solvents and additives was statistically equivalent to unexposed PEG-GOx. Moreover, PEG-GOx retained more of its pre-exposure activity than native GOx in all cases except the EtOH exposure, in which native GOx did not experience a statistically significant reduction in activity. Conversely, GA-modified GOx lost more of its pre-

exposure activity than native GOx in every case, with an approximate 30% reduction in the case of EtOH and DMSO and an approximate 40% reduction in the case of the polymer precursor solutions. It is worth noting that moderate aggregation of the GA-modified GOx was observed upon addition of the EtOH and led to loss of some protein during purification in two of the three samples. Finally, with the exception of exposure to the pHEMA and pHEMA-co-AAm polymer precursor solutions, the specific activity of GA-modified PEG-GOx following exposure to each of the tested solvents and additives was statistically equivalent to unexposed GA-modified PEG-GOx ($\alpha = 0.05$). Compared to native GOx, GA-modified PEG-GOx was statistically equivalent when exposed to EtOH and DMSO, and it retained only slightly more activity than native GOx when exposed to the polymer precursor solutions.

It should be clarified that a limitation of this work is that the enzyme is no longer exposed to the solvent or additive when it is tested for enzymatic activity. In one way, this is ideal because irreversible changes that occur during the enzyme's exposure to the solvent or additive are revealed (initial and final states are identical; *i.e.*, aqueous buffered solution devoid of solvent or additive). Furthermore, dissolution of the enzyme in solutions with the same composition during activity testing permits direct comparison among the various exposure types. However, one must consider the actual application in which the enzyme will be employed. For our lab's intended application (*i.e.*, incorporation into pHEMA-based hydrogels), it is expected that the enzyme might be exposed to 70% EtOH for a short period of time during sterilization. To some extent, this is also the case for the polymer precursor solutions; however, it's actually much more

complex because the solution components are transformed during hydrogel formation, which completely changes the environment of the enzyme. As such, it is necessary to perform *in situ* activity testing of the enzyme immobilized within the hydrogel. This is beyond the scope of this dissertation, but will need to be considered in future work.

4.4. Conclusions

In summary, we have demonstrated the utility of PEGylation to function as a steric stabilizer during chemical modification with GA. PEG chains do not appear to inhibit GA modification, but seem to prevent intermolecular crosslinking, which leads to irreversible aggregation. Likewise, the PEGylated enzyme appears to resist aggregation during and following heat treatment. The utility of enzymes modified in this manner is dependent upon the intended use. After one month at physiological temperature and in the absence of glucose, PEG-GOx modified with 2.5 wt% GA retains nearly an order of magnitude more of its initial activity compared to native GOx. Neither PEGylation nor GA modification imparts any significant protective effect upon exposure to glucose. Interestingly, PEGylation appears to help preserve enzymatic activity of GOx exposed to extreme temperature, especially in the short-term, but modification with GA actually has a detrimental effect. Finally, PEGylation seems to best stabilize the enzyme against the solvents and additives to which the enzyme was exposed in this study, while GA-modified native GOx was the worst; in general, PEG-GOx modified with 2.5 wt% GA performed as well as native GOx. It would be interesting to apply this technique to other glycoenzymes (or a modified version of the approach for non-glycosylated proteins), especially in cases where subunit dissociation of multimeric proteins is expected.

5. ALBUMINATION OF GLYCOENZYME

5.1. Introduction

In the previous section, an approach to enzyme stabilization was demonstrated, wherein GOx was PEGylated and subsequently modified with GA. As hypothesized, the PEG shell provided steric protection, which prevented GOx molecules from reacting with one another. Furthermore, significant stabilization was observed during storage of the GA-modified PEG-GOx for one month at physiological temperature and in the absence of glucose. However, using this combination of previous techniques, stability toward solvents and additives was only marginally improved (PEG-GOx without GA modification demonstrated superior performance overall), operational stability was not improved, and thermostability was actually reduced upon GA modification for both native GOx and PEG-GOx. Ideally, an approach would be developed that could stabilize glycoenzymes under all or most of these different conditions; however, even an approach that could provide stabilization under complimentary conditions would be beneficial.

The novel approach presented in this section involves the orthogonal covalent attachment of BSA macromolecules to the glycosylation sites of an enzyme, resulting in encasement of the glycoenzyme within an albumin shell (Fig. 5-1). This approach was inspired by a strategy commonly used in current glucose biosensors (described in Section 1); however, the latter was refined by introducing the BSA in a *controlled* manner and on the *single-enzyme level*. Beyond simple inspiration, the vast literature on

BSA supported the hypothesis that thermostability might be improved *via* albumination. Serum albumin is known to be thermostable,[106] and many groups have reported that addition of BSA to an enzyme solution improves the enzyme's thermostability.[107-110] More recently, the focus has shifted toward studying the ability of BSA to act as a molecular chaperone, inhibiting temperature-induced aggregation and deactivation.[108, 109] Therefore, it seems reasonable to expect that controlled covalent attachment of BSA to an enzyme might impart desirable characteristics similar to or even beyond those which are observed upon simple addition of albumin to an enzyme solution.

It is demonstrated herein that this technique, which can be applied to both GOx and Cat, results in dramatic thermostabilization with a moderate increase in long-term storage stability for BSA-GOx. As in previous sections, while the direct goal of this work was to stabilize GOx and Cat in a manner which permits their incorporation within our lab's optical biosensing hydrogels, this approach could be applied or adapted to stabilize a myriad of other proteins.

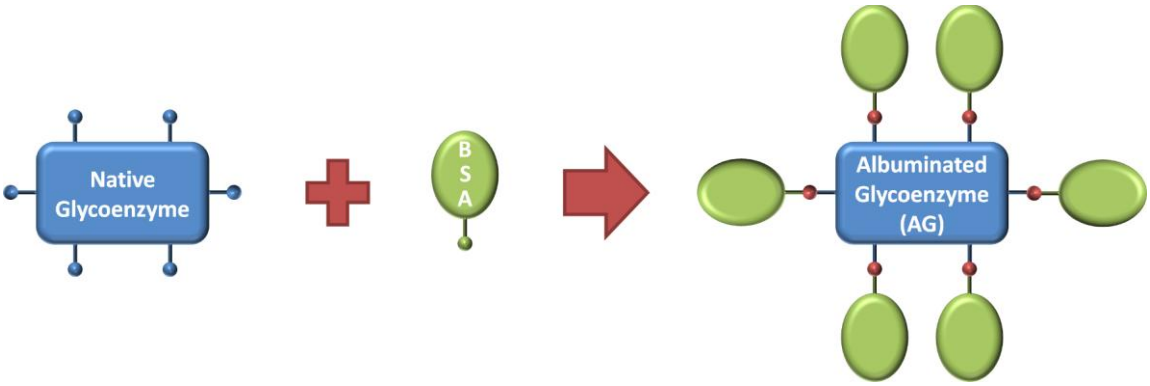

Fig. 5-1 Cartoon illustrating the orthogonal attachment of multiple BSA macromolecules to a native glycoenzyme to form an AG.

5.2. Experimental

5.2.1. Materials

GOx from *A. niger* was obtained from BBI Enzymes (GO3A, 270 U/mg solid, 75% protein by Lowry). Cat from *A. niger* was obtained from EMD Millipore (219261, 6450 U/mg solid, 37.6% protein by UV absorbance) and purified by GFC to remove contaminants. BSA (A7906) and peroxidase from *Amoracia rusticana* (type II, 188 U/mg solid) were obtained from Sigma. *N*-(β-maleimidopropionic acid) hydrazide (BMPH) was obtained from Thermo Scientific.

5.2.2. Preparation of Albuminated Glycoenzymes

The procedure used to synthesize the AGs is depicted schematically in Fig. 5-2. BSA (74.25 mg, **1**) was dissolved in 1.85 mL of 100 mM sodium phosphate containing 154 mM NaCl (pH 7.2). BMPH was dissolved in 150 µL of DMSO at a concentration of 50 mM and added to the BSA solution, yielding a 6.67 molar excess of BMPH to BSA. The reaction solution was mixed for 2 h at room temperature, followed by removal of excess BMPH using a desalting column equilibrated with 100 mM sodium phosphate containing 154 mM NaCl (pH 7.2) to yield hydrazide-functionalized BSA (**2**).

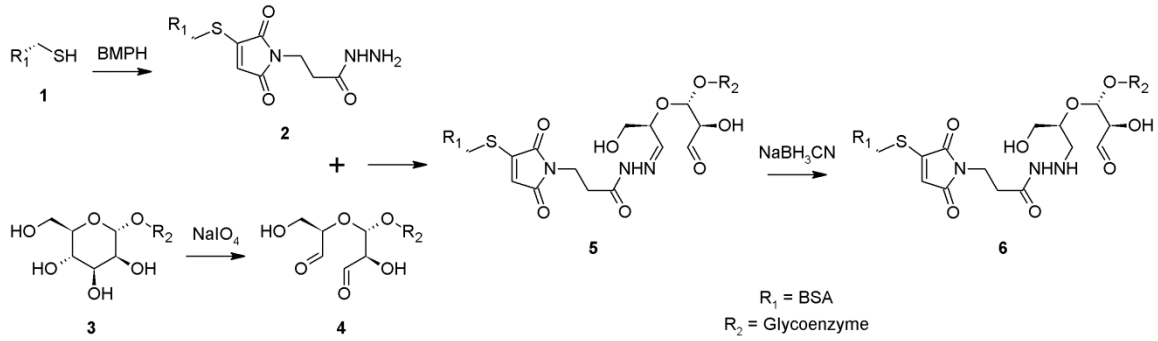

Fig. 5-2 Synthesis of BSA-modified glycoenzymes—AGs. Oxidation of multiple glycosylation sites on the glycoenzyme yields aldehydes, which are then reacted with hydrazide-functionalized BSA. The single hydrazide group of each BSA is covalently attached at the oxidized glycosylation sites, and the resulting hydrazone linkages are reduced with $NaBH_3CN$ for stability.

The glycoenzyme (**3**) was dissolved in 100 mM sodium phosphate containing 154 mM NaCl (pH 7.2) at a concentration of 3.33 mg/mL for GOx and 5.22 mg/mL for Cat. Separately, 4.3 mg of $NaIO_4$ was dissolved in 100 µL of deionized water, then immediately added to 900 µL of the glycoenzyme solution and slowly agitated in the dark for 1 h at room temperature to yield **4**. As discussed in Section 3.2.2, proteins exposed to oxidants have been reported to form higher-order oligomers in certain cases due to intermolecular crosslinking. Therefore, a small amount of aggregated glycoenzyme might be observed following oxidation, but it will be removed during subsequent desalting or purification. The reaction was quenched by the addition of excess glycerol (1.25 µL). The oxidized glycoenzyme was diluted to 1.75 mL by the addition of 750 µL of 100 mM sodium phosphate containing 154 mM NaCl (pH 7.2), then purified using a desalting column equilibrated with the same phosphate buffer to

remove excess $NaIO_4$, glycerol, and degradation products from glycerol quenching (*i.e.*, formaldehyde and formic acid).

The solutions of oxidized glycoenzyme and hydrazide-functionalized BSA were combined, yielding a *ca.* 60-fold molar excess of BSA to glycoenzyme. The mixture was reacted in the dark for 2 h at room temperature under gentle agitation to yield **5**. In a fume hood, 40 µL of 5 M $NaBH_3CN$ in 1 N NaOH was added. **Caution: $NaBH_3CN$ is extremely toxic; as such, all operations should be performed with care in a fume hood**. The $NaBH_3CN$ was reacted with the bioconjugate for 30 min at room temperature under gentle agitation to yield the AG (**6**). Finally, the conjugate was purified from low-molecular-weight contaminants by diafiltration and transferred into 10 mM sodium phosphate containing 154 mM NaCl (pH 7.2).

5.2.3. Physical Characterization

5.2.3.1. Liquid Chromatography

GFC was performed to purify the AGs and approximate their size. The crude sample was injected into a liquid chromatography system (GE Healthcare Life Sciences model ÄKTAexplorer 10) equipped with a gel-filtration column (GE Healthcare Life Sciences model HiLoad Superdex 200 PG) equilibrated with phosphate buffer (10 mM sodium phosphate, 154 mM NaCl, pH 7.2). Absorbance was monitored at 280 nm and 450 nm (for GOx) or 405 nm (for Cat), and 1 mL fractions were collected.

5.2.3.2. Particle Sizing

A photon correlation spectrometer (Malvern model Zetasizer Nano ZS) was used to acquire size distributions of the AGs, as well as the native glycoenzymes and BSA, to

determine the change in size following modification. Also, it is important to determine whether oligomerization occurred during oxidation or subsequent conjugation. Disposable 3.5 mL cuvettes were filled with 1 mL enzyme in 10 mM sodium phosphate containing 154 mM NaCl (pH 7.2).

5.2.3.3. Temperature Ramp

A photon correlation spectrometer (Malvern model Zetasizer Nano ZS) was used to determine the effect of heating on the size of AGs and native glycoenzymes (n = 3). Standard 3.5 mL glass cuvettes were filled with enzyme (1 mL, *ca.* 0.735 mg/mL) in 10 mM sodium phosphate containing 154 mM NaCl (pH 7.2). The temperature of the cuvette holder was incrementally increased from 25 °C to 90 °C in steps of 5 °C, and the enzyme solution was allowed to equilibrate to each temperature for 2 min prior to collection of sizing data.

5.2.4. Functional Characterization

5.2.4.1. Enzymatic Activity Assays

Enzymatic assays of BSA-GOx and native GOx samples were performed to determine activity following exposure to various challenges.[88] In all cases, enzymatic activity measurements were performed in triplicate at pH 5.1 and 35 °C using a UV/Vis spectrophotometer (Agilent model Cary 300) equipped with a water-thermostatted multicell holder to maintain the appropriate temperature. Absorbance data were collected at approximately 30 Hz for approximately 2.5 min. Data were fit *via* linear regression using the maximum number of points to obtain a norm of residuals less than 0.025. This

procedure was adopted to minimize the effects of nonlinearities present at later time points in absorbance data collected for samples of high catalytic activity.

5.2.4.2. Long-Term Storage Stability

To observe the effects of albumination on the spontaneous denaturation of GOx, enzymatic activity was assayed over a period of four weeks with the enzyme samples stored at 37 °C (elevated temperature to accelerate deactivation and simulate physiological conditions) in the absence of glucose. To limit sample contamination, multiple samples were prepared for each enzyme type and each time point to prevent the need for samples to be repeatedly opened; that is, samples were only opened on the day they were assayed for enzymatic activity.

5.2.4.3. Operational Stability

To test for the effect of glucose on native GOx and BSA-GOx enzymatic activity, samples were continuously exposed to PBS containing glucose at room temperature for up to 24 h. For these experiments, the dynamic dialysis system described in Section 4.2.4.3 was employed. Enzyme solutions (250 µL, *ca.* 0.25 mg/mL) were added to the wells (n = 3), and PBS containing glucose (100 mg/dL) was pumped through the dialysis chamber at 4 mL/min using a peristaltic pump. After the appropriate glucose exposure time (6 h, 12 h, or 24 h), glucose-containing PBS was removed from the dialysis chamber, and 1 L of fresh PBS (no glucose) was pumped through the system at 4 mL/min (*ca.* 4 h) to remove excess glucose and product from the sample wells. Because the samples may change volume due to osmotic and hydrostatic forces—and because there is a possibility for the membrane to be compromised during testing—the

samples were transferred to a standard microplate and concentration was determined using a multimode microplate reader (Tecan model Infinite M200 PRO series). Finally, the samples were assayed for enzymatic activity as described in Section 5.2.4.1.

5.2.4.4. Thermostability

To determine if attachment of BSA provided stabilization of the enzyme at elevated temperatures (*i.e.*, where thermally-induced denaturation dominates), enzyme samples (0.73 mg/mL) were immersed into a 60 °C water bath for up to 1 h. Separate replicate samples (n = 3) were prepared for each time point (5 min, 15 min, and 1 h). Upon removal from the water bath, samples were immediately cooled to 4 °C, then assayed for enzymatic activity as described in Section 5.2.4.1.

5.2.4.5. Solvent/Additive Stability

Solvents and additives to which BSA-GOx and native GOx might be expected to be exposed (*e.g.*, during sensor fabrication or sterilization) were tested for their effect on enzymatic activity. Enzymes (0.25 mg/mL) were exposed to 70% EtOH and 50% DMSO for 10 min. Additionally, enzymes were exposed to three multi-component polymer precursor solutions: pHEMA, pHEMA-*co*-AEMA, and pHEMA-*co*-AAm. The composition of each of the precursor solutions is provided in Table 4-1, and the final enzyme concentrations were approximately 0.215 mg/mL. Following exposures, samples were transferred back into PBS using centrifugal devices (Pall model Nanosep 30K). Samples were then transferred to a microplate and concentration was determined using a multimode microplate reader (Tecan model Infinite M200 PRO series). Finally, the samples were assayed for enzymatic activity as described in Section 5.2.4.1.

5.3. Results and Discussion

5.3.1. Physical Characterization

5.3.1.1. Liquid Chromatography

Fig. 5-3 contains the overlaid chromatograms of the native glycoenzymes (gray lines) and the AGs (maroon lines) for GOx (Fig. 5-3A) and Cat (Fig. 5-3B). In the case of both native glycoenzymes, elution of only one primary peak is detected, which has overlapping absorbance in both the UV (dashed lines) and the visible regions (solid lines) as expected. In contrast, the UV chromatograms for the crude AG samples contain three primary peaks, but only the one at the lowest elution volume overlaps with the single peak detected at the visible wavelengths; this peak corresponds to the AG, and it is sufficiently resolved from the other peaks such that purification from the other components in the crude AG sample is possible. The component which eluted at approximately 76 mL corresponds to BSA, and the peak at approximately 66 mL elution volume is believed to be dimers of BSA.[111]

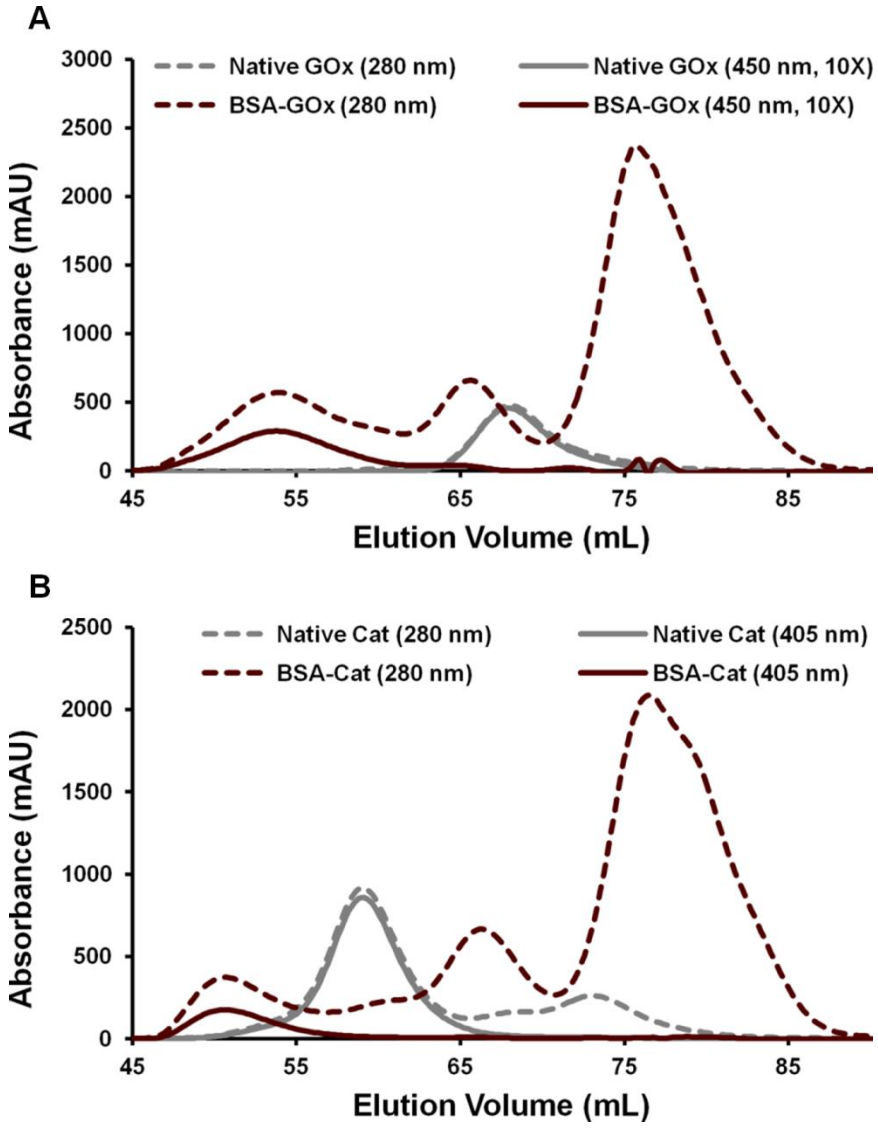

Fig. 5-3 Chromatograms of BSA-GOx and native GOx (A), as well as BSA-Cat and native Cat (B). Traces corresponding to AGs are shown in maroon, while those corresponding to native enzymes are shown in gray. Absorbance at 280 nm is indicated by a dashed line, while absorbance at 450 nm (for GOx and BSA-GOx) or 405 nm (for Cat and BSA-Cat) is indicated by a solid line. For visualization purposes, the 450 nm traces for native GOx and BSA-GOx have been multiplied by a factor of ten.

Regarding the peaks corresponding to the AGs, presence of absorbance in the visible region supports retention of the enzymes' respective cofactors, as they contribute

the absorbance in this region. Conjugation of the BSA to the glycoenzymes is supported by 1) the large shift in elution volume, which is indicative of a drastic increase in the Stokes radius; and 2) the additional UV absorbance as compared to the native glycoenzymes. Concerning the latter point, the UV:visible absorbance ratio doubled upon albumination, increasing from 10:1 for GOx and 1:1 for Cat to 20:1 for BSA-modified GOx (BSA-GOx) and 2:1 for BSA-modified Cat (BSA-Cat). As BSA absorbs at 280 nm, but does not contribute any appreciable absorbance at 405 nm or 450 nm, this increase in the UV:visible absorbance ratio supports co-elution of BSA and GOx.

5.3.1.2. Particle Sizing

DLS was used to determine the hydrodynamic sizes of BSA, the native glycoenzymes, and the AGs. Particle sizing reveals that BSA has a hydrodynamic diameter of 7.959 nm. DLS reveals that native GOx has a hydrodynamic diameter of 12.36 nm, which increases by 7.76 nm to 20.12 nm upon modification with BSA. Likewise, the hydrodynamic diameter of native Cat increases by 9.27 nm following albumination (from 15.38 nm to 24.65 nm). The relative increase (*i.e.*, percent change) in hydrodynamic size is similar for both AGs—62.8% increase for BSA-GOx and 60.3% increase for BSA-Cat.

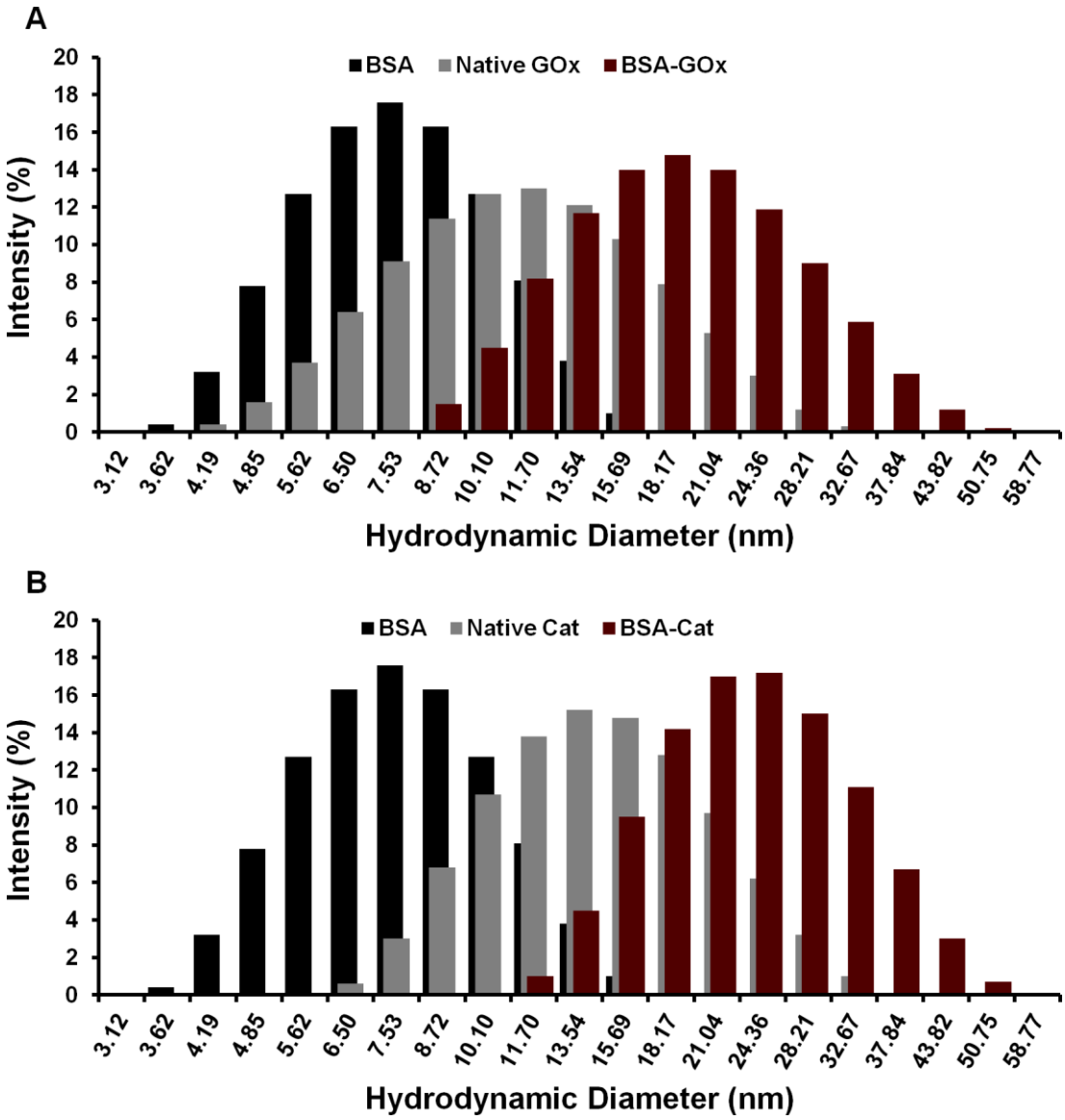

Fig. 5-4 Size distributions of BSA, native GOx, and BSA-GOx (A), as well as BSA, native Cat, and BSA-Cat (B). BSA is shown as black bars, native enzymes as gray bars, and AGs are shown as maroon bars.

5.3.1.3. Temperature Ramp

The albuminated and native glycoenzymes were characterized with DLS to investigate the effect of heating on their size distributions (n = 3). The hydrodynamic diameter of each form of enzyme was monitored while the temperature of the sample

was incrementally increased from 25 °C to 90 °C. The size distributions for the native glycoenzymes and the AGs as a function of temperature are shown in Fig. 5-5. All samples exhibit one primary peak at all tested temperatures; however, the native glycoenzymes (especially Cat) show evidence of higher-molecular-weight species at some lower temperatures. Remarkably, at all tested temperatures, the size distributions of the AGs remain relatively constant as compared to the native glycoenzymes.

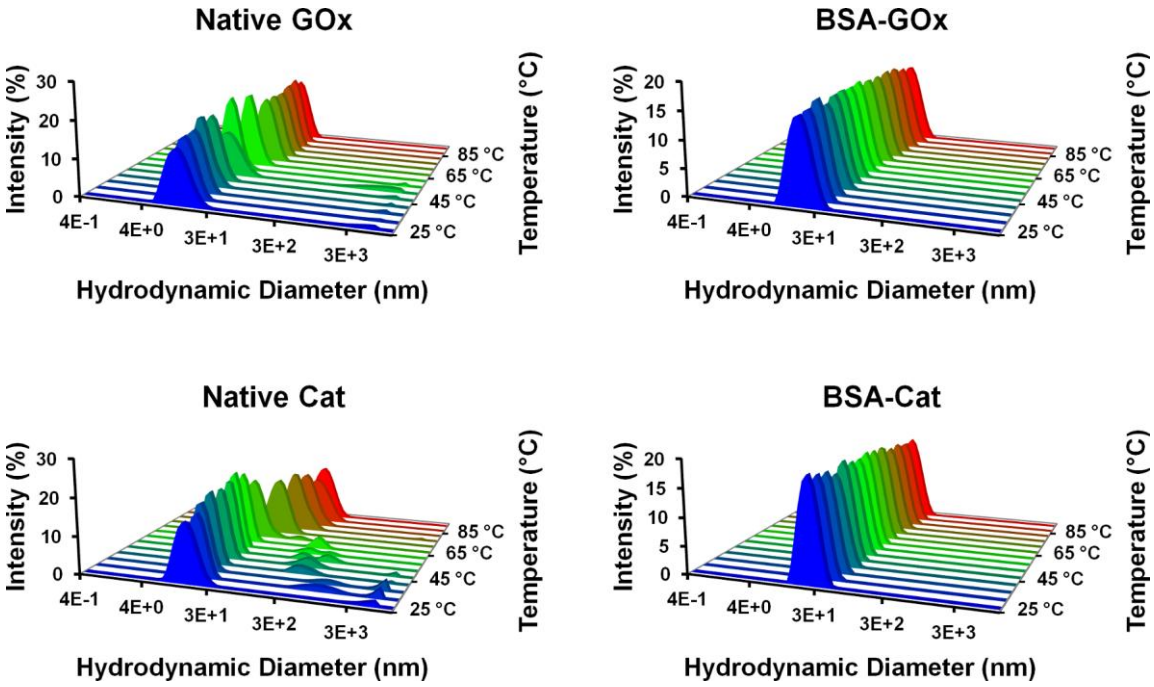

Fig. 5-5 Size distributions for native GOx and BSA-GOx, as well as native Cat and BSA-Cat, as a function of temperature (n = 3).

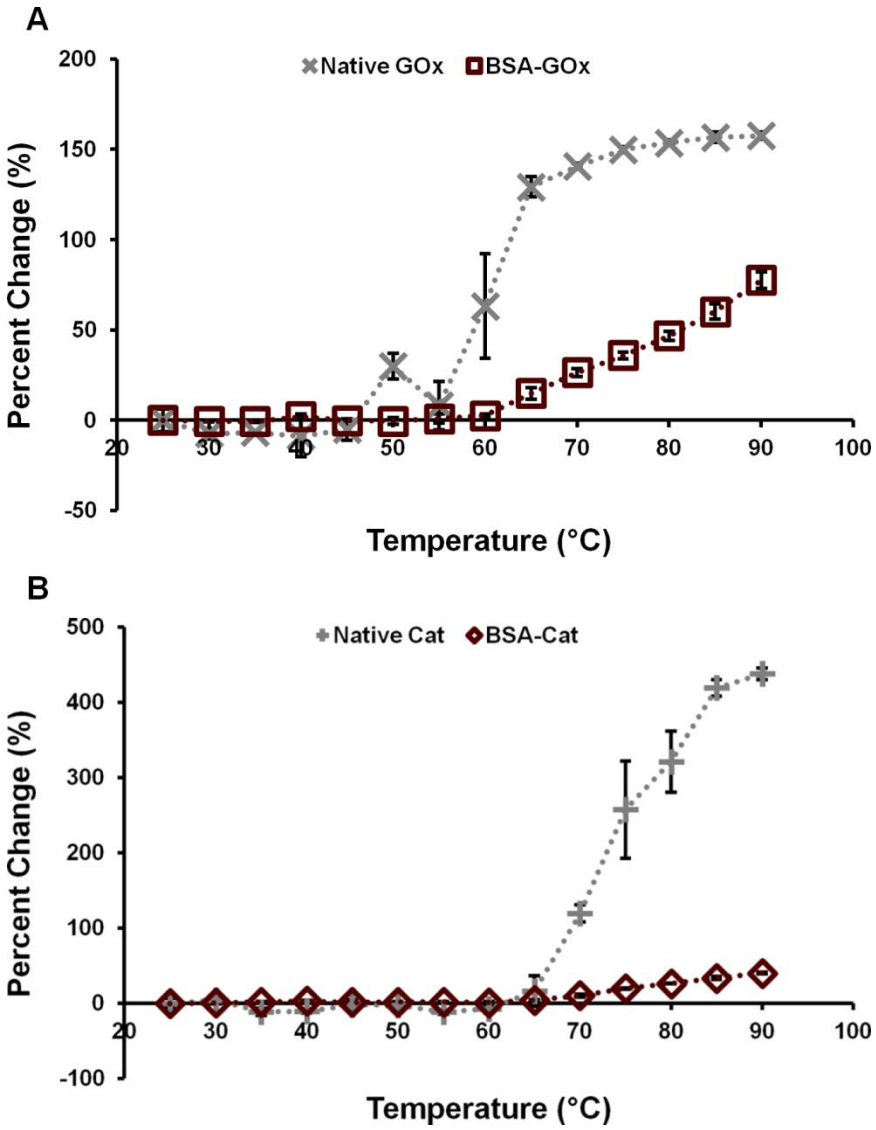

Fig. 5-6 Effect of heating on the size of BSA-GOx and native GOx (A) and BSA-Cat and native Cat (B). BSA-GOx and native GOx are indicated by maroon squares and gray crosses, respectively, while BSA-Cat and native Cat are indicated by maroon diamonds and grey plus signs, respectively. Error bars represent 95% confidence intervals (n = 3), and dotted lines are intended to be a guide for the eyes.

Fig. 5-6 shows the percent change in the size of the primary peak (from the size distributions shown in Fig. 5-5) from its initial size as a function of temperature. At 60 °C, native GOx begins to drastically increase in size, stabilizing near 150% change at 75

°C. This shift of the enzyme's size distribution toward larger size is indicative of thermal denaturation and subsequent aggregation, which is consistent with the reported melting temperature of GOx (*ca.* 56–58 °C)[72, 100, 102] as well as reports that GOx forms trimers and tetramers upon thermal denaturation.[72] Like native GOx, the size distribution for BSA-GOx begins to increase in size at approximately 60 °C; however, the rate of change is approximately 5–6 times slower than that of native GOx, and the total percent change after ramping to 90 °C is reduced by a factor of two. The results obtained for native Cat and BSA-Cat are similar to those for native GOx and BSA-GOx, but even more dramatic. Both native Cat and BSA-Cat begin to experience a shift in their size distributions toward larger size at approximately 65 °C; however, after ramping to 90 °C, native Cat increases by 440% of its initial size, whereas BSA-Cat only increases by 40% (an 11-fold difference).

These findings are consistent with reports in the literature that indicate BSA has molecular chaperone-like properties.[108, 109] Marini and co-workers were the first to recognize that BSA can act as a molecular chaperone, reporting that addition of BSA to an enzyme solution significantly reduced thermally induced aggregation.[108] Finn and others also noted that BSA inhibits aggregation and even amyloid formation,[109] consistent with the notion that BSA functions like a molecular chaperone. Therefore, similar interactions between enzyme and BSA might be conserved in the AGs.

The inhibition of aggregation shown in Fig. 5-5 and Fig. 5-6 might be an indicator that thermal denaturation (and thus, inactivation) is reduced upon albumination; however, BSA encasement might just prevent the aggregation of

thermally denatured enzyme. Further testing of functional characteristics after exposure to elevated temperatures is necessary to elucidate these findings and is the subject of Section 5.3.2.3.

5.3.2. Functional Characterization

5.3.2.1. Long-Term Storage Stability

Samples of BSA-GOx and native GOx were stored in PBS devoid of glucose for four weeks at 37 °C, and enzymatic activity was assayed at various time points to investigate the effect of albumination on long-term storage stability. As shown in Fig. 5-7A, BSA-GOx has 78.4% of the specific activity of native GOx at the initial time point. This could be due to inactivation of a fraction of the enzyme during attachment of BSA or diffusional limitations imparted by the BSA shell. Despite having a lower initial specific activity, the data show that after four weeks, BSA-GOx is approximately three times as active as native GOx (74.4 U/mg *vs.* 26.0 U/mg, respectively). The activity data were normalized and fit with exponential decays (Fig. 5-7B). For native GOx, a first-order exponential decay fits quite well ($R^2 > 0.99$) with a decay constant of 0.1206/day, corresponding to a half-life of 5.75 days. BSA-GOx is more than 2.5 times as stable, with a decay constant of 0.0453/day ($R^2 \sim 0.97$) and a half-life of 15.3 days.

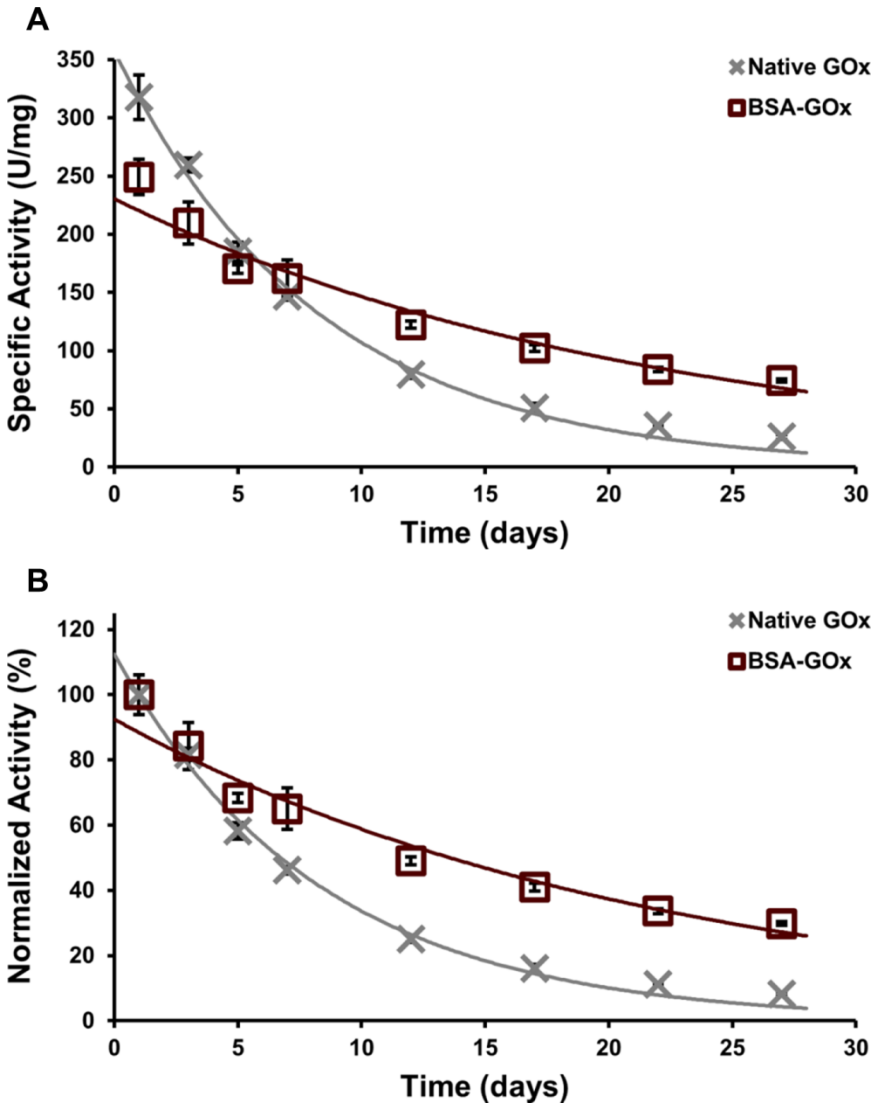

Fig. 5-7 Specific activity (A) and normalized activity (B) of BSA-GOx (maroon squares) and native GOx (gray crosses) in the absence of glucose over four weeks at 37 °C. Error bars represent 95% confidence intervals (n = 3). The data were fit with first-order exponential decays; the maroon lines corresponds to the BSA-GOx data and the gray lines corresponds to the native GOx data.

5.3.2.2. Operational Stability

As GOx reacts with glucose and oxygen, hydrogen peroxide is produced, which has been shown to deactivate the enzyme.[8] To test for any protective effect imparted by

albumination, native GOx and BSA-GOx were continuously exposed to glucose-containing PBS at room temperature for up to 24 h. As shown in Fig. 5-8, after 6 h of continuous glucose exposure, BSA-GOx retained less of its initial activity than native GOx (72.4% *vs.* 90.7%). Likewise, at the 12 h time point, BSA-GOx retained less initial activity (44.8% *vs.* 55.7%). However, after 24 h, both native GOx and BSA-GOx lost approximately 75% of their initial specific activity.

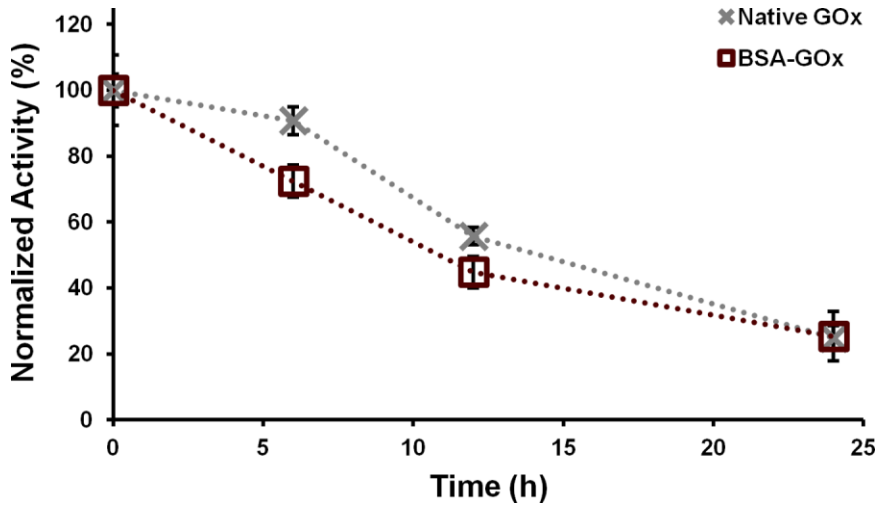

Fig. 5-8 Normalized activity of BSA-GOx (maroon squares) and native GOx (gray crosses) exposed to glucose for 24 h at room temperature. Error bars represent 95% confidence intervals (n = 3), and dotted lines are intended to be a guide for the eyes.

5.3.2.3. Thermostability

For many proteins, exposure to elevated temperature induces thermal denaturation, which is often accompanied by a loss of functional properties (*e.g.*, enzymes lose catalytic abilities). Thermal denaturation of GOx results in an irreversible transition to a compact denatured state with the enzyme's dimeric structure preserved

but dissociation of the FAD co-factor.[72] To determine whether albumination imparts stability at elevated temperatures, enzymatic activity was assayed following exposure to 60 °C for up to 1 h. Fig. 5-9 shows that BSA-GOx is remarkably more stable than native GOx. After 1 h, native GOx only retains 1.42% of its initial activity, while BSA-GOx retains 37.7% of its initial activity—a 26.5-fold improvement in stability.

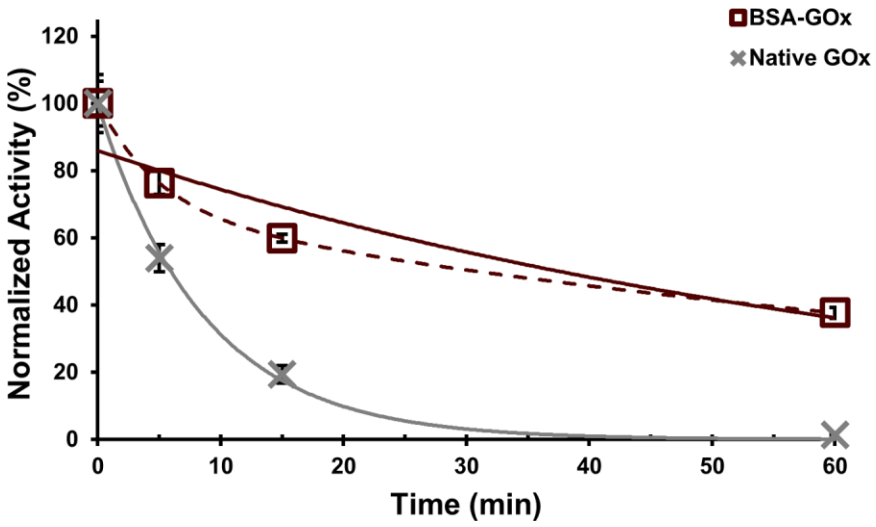

Fig. 5-9 Normalized activity of BSA-GOx (maroon squares) and native GOx (gray crosses) with exposure to extreme temperature (60 °C). Error bars represent 95% confidence intervals (n = 3). Native GOx data were fit with a first-order exponential decay (gray line), while BSA-GOx data were fit with both a first-order (maroon solid line) and second-order exponential decay (maroon dashed line).

The data were fit with first-order exponential decays (solid lines). For native GOx, a first-order exponential decay fit well ($R^2 > 0.99$) with a decay constant of 0.1157/min, corresponding to a half-life of 5.99 min. The data for BSA-GOx were also fit with a first-order exponential decay, which yielded a decay constant and half-life of 0.0144/min and 48.1 min, respectively; however, with a coefficient of determination of

approximately 0.91, it was determined that the behavior might be better described using a multi-exponential decay. As such, the activity data for BSA-GOx were fit with a second-order exponential decay (dashed line), which fit quite well as expected ($R^2 = 1$). Two-thirds of the population had a long half-life of 71.7 min, while the remaining one-third of the population had a short half-life of 3.53 min. Therefore, it appears that albumination imparts a protective effect upon a majority of the enzyme population, translating to an overall increase in the thermostability of the AG compared to the native GOx.

Serum albumin is quite thermostable,[106] and enzyme thermostabilization by BSA has been reported previously by many groups.[107-110] Chang and Mahoney showed that addition of BSA to a solution of *β*-galactosidase from *Streptococcus thermophilus* resulted in a nine-fold thermostabilization. They also proposed that hydrophobic interactions played a critical role in the stabilizing action imparted by BSA.[107] Building upon that work, Marini and co-workers recognized that BSA has molecular chaperone-like properties; that is, when added to an enzyme solution, the enzyme experienced greatly reduced thermal inactivation and aggregation. In some cases, BSA even outperformed *α*-crystallin, a recognized intracellular molecular chaperone.[108] Finally, Myung and Zhang also observed enhanced enzyme stability with the addition of BSA,[110] which they explained in the context of the macromolecular crowding effect.[112]

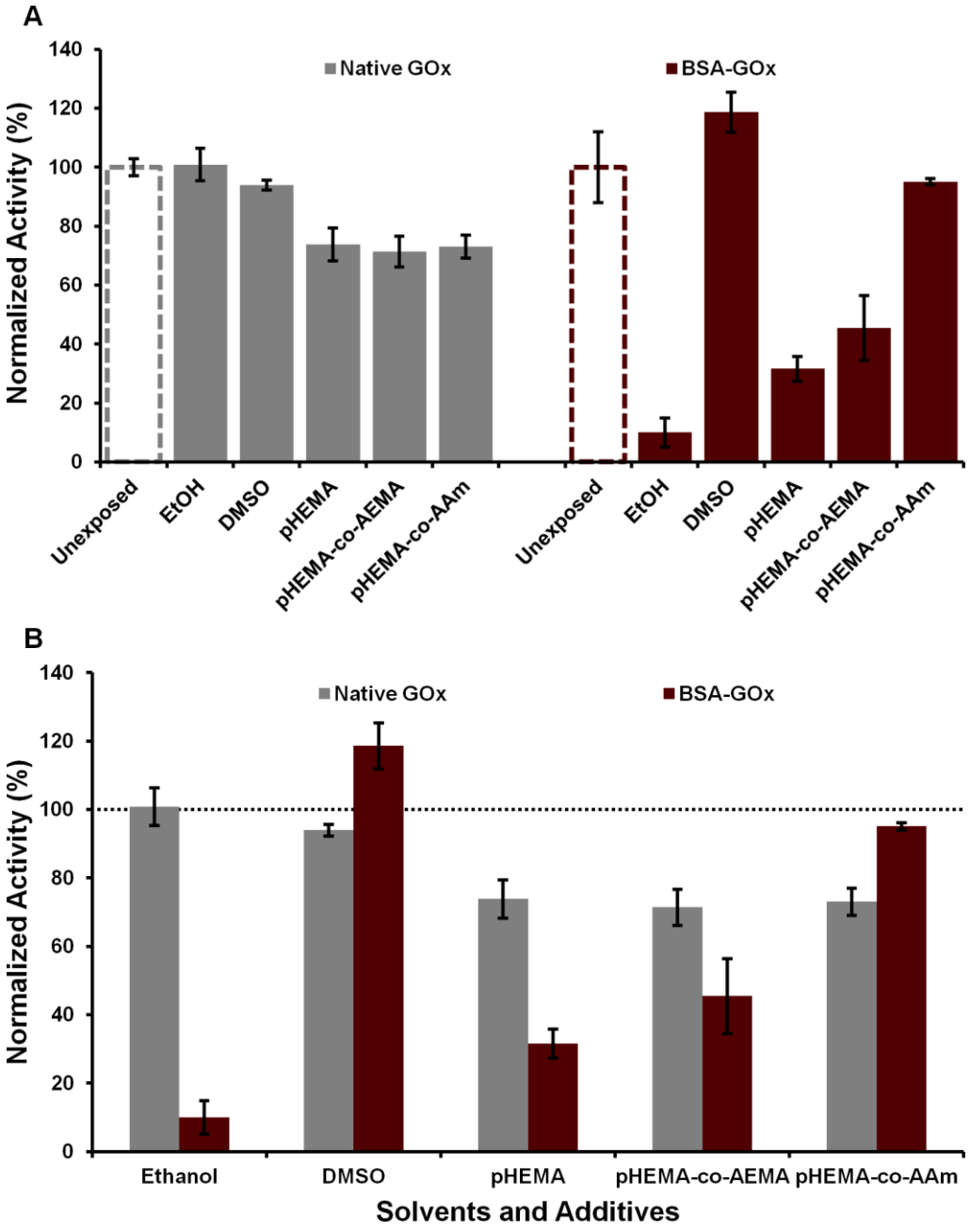

Fig. 5-10 Normalized activity of BSA-GOx (maroon bars) and native GOx (gray bars) with exposure to various solvents and additives grouped by enzyme type (A) or exposure type (B). All samples are normalized to unexposed enzyme of the same type (*e.g.*, BSA-GOx samples are normalized to unexposed BSA-GOx), which is indicated by the horizontal dotted line at 100%. Error bars represent 95% confidence intervals (n = 3).

5.3.2.4. Solvent/Additive Stability

Since it is expected that enzymes might come into contact with various solvents and additives throughout normal use—some of which might be harmful—native GOx and BSA-GOx were exposed to a number of substances for a limited period of time, then tested for changes in enzymatic activity. Fig. 5-10 shows the specific activity of native GOx and BSA-GOx after exposure to the solvents and additives, which has been normalized to the specific activity of unexposed enzyme of the same type (*e.g.*, exposed BSA-GOx samples normalized to unexposed BSA-GOx). In Fig. 5-10A, the bars are grouped by enzyme type (*i.e.*, native GOx or BSA-GOx) to facilitate comparison of the effects of each solvent or additive on each of the two enzyme types, as well as to provide a snapshot of each enzyme type's overall stability to various solvents and additives in general. Fig. 5-10B shows the bars grouped by exposure type to permit evaluation of each enzyme's relative appropriateness in the presence of each solvent or additive.

For native GOx, exposure to 70% EtOH did not affect its specific activity, although some limited aggregation was observed. Conversely, BSA-GOx experienced significant aggregation when exposed to 70% EtOH, accompanied by a severe reduction (*ca.* 90%) in specific activity. A slight reduction in specific activity resulted from exposure of native GOx to 50% DMSO, while the specific activity of BSA-GOx following the same exposure was statistically equivalent to unexposed BSA-GOx (α = 0.05). For native GOx, exposure to all of the tested polymer precursor solutions resulted in an approximate 25% reduction in specific activity. Filter clogging was noted in each of the three polymer precursor solutions to which BSA-GOx was exposed, although the

clogging was approximately twice as severe for the pHEMA and pHEMA-co-AEMA as compared to the pHEMA-co-AAm (*i.e.*, they required twice the filtration time). BSA-GOx exposed to pHEMA-co-AAm fared well, retaining approximately 95% of its specific activity following exposure. In contrast, exposure to pHEMA and pHEMA-co-AEMA resulted in the loss of approximately one-half to two-thirds of the initial specific activity of BSA-GOx.

The EtOH-induced aggregation of BSA-GOx is not surprising, as native BSA has been shown to denature and become virtually insoluble in 70% EtOH.[113] Denaturation of the albumin shell of BSA-GOx could place strain on the interior GOx, resulting in its denaturation and/or loss of FAD cofactor. To further explain the different effects of the various solvents and additives on the retention of BSA-GOx activity, one must consider the polarity of the solution, which can be approximated by the relative permittivity of the solvent or mixture of solvents. BSA-GOx exposed to DMSO (ε_r = 46.7) has the same activity as unexposed BSA-GOx stored in water (ε_r = 80.1), while EtOH (ε_r = 24.6) exposure results in retention of only about 10% of the enzymatic activity. Therefore, the greater the polarity of the solvent, the greater the retention of activity following exposure to that solvent. In the polymer precursor solutions, the water content dramatically increases from 22% and 23% in pHEMA and pHEMA-co-AEMA, respectively, to 34% in pHEMA-co-AAm. This correlates with the effect that the solution has on the retention of activity, with higher water content (*i.e.*, higher relative permittivity and polarity) corresponding to greater retention of activity.

As discussed in Section 4.3.2.4, it should be clarified that a limitation of this work is that the enzymes are no longer exposed to the solvent or additive when tested for enzymatic activity. In one way, this is ideal because irreversible changes that occur during the enzyme's exposure to the solvent or additive are revealed (initial and final states are identical; *i.e.*, aqueous buffered solution devoid of solvent or additive). Furthermore, dissolution of the enzyme in solutions with the same composition during activity testing permits direct comparison among the various exposure types. However, one must consider the actual application in which the enzyme will be employed. For our lab's intended application (*i.e.*, incorporation into pHEMA-based hydrogels), it is expected that the enzyme might be exposed to 70% EtOH for a short period of time during sterilization. To some extent, this is also the case for the polymer precursor solutions; however, it's actually much more complex because the solution components are transformed during hydrogel formation, which completely changes the environment of the enzyme. As such, it is necessary to perform *in situ* activity testing of the enzyme immobilized within the hydrogel. This is beyond the scope of this dissertation, but will need to be considered in future work.

5.4. Conclusions

In summary, we have demonstrated that two glycoenzymes, GOx and Cat, can be bioconjugated with BSA to form AGs. Liquid chromatography reveals a large shift in the elution volume accompanied by a doubling of the UV:visible absorbance ratio following albumination, which supports conjugation of the enzyme with BSA. DLS indicates that the AGs are approximately 60% larger than the respective native

glycoenzymes, which provides secondary confirmation that modification has occurred. Both BSA-GOx and BSA-Cat appear to resist aggregation during heating to 90 °C, but this effect is more profound in the latter AG. It is proposed that the previously reported molecular chaperone-like properties of BSA might be conserved in the AGs.

The response of BSA-GOx to the tested conditions, in terms of its functional characteristics, varied greatly. For instance, the thermostability of BSA-GOx is excellent compared to the native glycoenzyme, and moderate stabilization is observed with storage for one month at physiological temperature and in the absence of glucose. However, BSA-GOx experienced significant reductions in activity following exposure to solvents with relatively low relative permittivity and polymer precursor solutions with relatively low water content. Operational stability of GOx appeared to be unaffected by albumination. Therefore, careful consideration of the expected conditions is required before BSA-GOx should be utilized in a particular application.

6. CONCLUSIONS AND FUTURE WORK[*]

Enzyme deactivation is expected to be a major barrier in the realization of long-term glucose sensing with fully implantable optical glucose biosensors, and this work represents a step toward overcoming that hurdle. This dissertation presents the evaluation of three enzyme modification strategies, which have been tailored to suit the constraints of our specific application. Each strategy yields a stabilized enzyme under certain conditions, whether it be long-term storage, elevated temperature, or exposure to various solvents/additives.

In the first approach, GOx was modified using a glycosylation site-targeted PEGylation approach. Two different techniques—GFC and denaturing polyacrylamide gel electrophoresis—were utilized to provide independent approximations of the apparent molecular mass. Both techniques revealed that the PEGylated enzyme had a significantly higher apparent molecular mass as compared to native GOx, which supported successful modification of the enzyme. Moreover, both characterization techniques indicated that only one form of the modified enzyme was present following PEGylation, which simplified separation. The actual molecular mass increase was measured using MALDI-TOF mass spectrometry, and from the 15 kDa increase in mass per monomer, it was determined that six 5 kDa PEG chains were attached to each GOx dimer. To complete the physical characterization of PEG-GOx, DLS was used to

[*] Parts of this section are reprinted with permission from "Glycosylation site-targeted PEGylation of glucose oxidase retains native enzymatic activity" by D.W. Ritter, J. R. Roberts and M. J. McShane, *Enzyme Microb. Technol.*, 2013, **52**, 279-285. Copyright 2013 by Elsevier Inc.

observe a change in hydrodynamic size following modification; this also allowed for confirmation that oligomers were not present in the purified PEG-GOx sample.

Following extensive physical characterization of the PEG-GOx, its long-term storage stability and operational stability were tested. After storage in buffer for 29 days at 37 °C, PEG-GOx and native GOx had lost an equivalent amount of enzymatic activity. However, due to differing activities at intermediate time points for the two sample types, the half-life value calculated for PEG-GOx was 60% longer than native GOx. No operational stabilization was realized upon PEGylation, as native GOx and PEG-GOx had the same activity retention following glucose exposure for 24 h. Although no major improvements in storage or operational stability were observed upon PEGylation of GOx, this modified enzyme could still be employed in applications requiring increased size and near-native enzymatic activity. An example where these qualities might be desirable would be in the entrapment of GOx within a polymeric matrix that has a mesh size slightly larger than GOx. In this case, an increase in the hydrodynamic size—*via* PEGylation, for instance—would likely yield improved entrapment (*i.e.*, increased retention of the GOx over time). Therefore, while direct stabilization of the enzyme is not achieved, better entrapment of the enzyme would translate to improved apparent enzyme stability of the enzyme-containing system. Future work could incorporate PEG chains of different molecular weight (*i.e.*, other than 5 kDa) and geometry (*i.e.*, other than linear), which might better protect the GOx.

Building upon the previous approach, the second approach was intended to stabilize GOx through modification of the initially PEGylated enzyme with GA. I

hypothesized that the glycosylation site-bound PEG chains would stabilize GOx (through steric hindrance) against intermolecular crosslinking, while permitting GA modification. As expected, the amine content of the PEG-GOx, as determined by a fluorescamine assay, was reduced with increasing GA concentration; this effect was also observed with native GOx, which indicates that the presence of PEG does not appear to inhibit GA modification. Furthermore, exposure of native GOx to increasing concentrations of GA resulted in aggregation of the enzyme (significant at higher concentrations). Conversely, the hydrodynamic size of PEG-GOx was not altered across the entire range of tested GA concentrations. These findings support the hypothesis that initial deposition of PEG imparts steric stability to the enzyme during subsequent GA modification, which prevents the occurrence of irreversible, large-scale aggregation, but does not inhibit GA modification.

GA modification of PEG-GOx was shown to dramatically improve long-term storage stability. Following four weeks of storage in buffer at 37 °C, PEG-GOx modified with 2.5 wt% GA retained approximately an order of magnitude more initial activity than native GOx. PEGylation of the enzyme (with or without GA modification) appears to stabilize the enzyme against heat-induced aggregation. Interestingly, however, enzyme modification with PEG appeared to impart greater resistance to thermal deactivation as compared to modification with GA. Likewise, PEG-GOx appeared most tolerant of the panel of solvents and additives to which it was exposed in this study—even more than GA-modified PEG-GOx. Finally, neither PEGylation nor GA modification, nor the combination thereof, produced an improvement in operational

stability. In future work, the mechanism by which the enzyme is stabilized or destabilized could be further investigated, and higher GA concentrations for PEG-GOx could be evaluated. Of course, application of this technique to multimeric glycoenzymes in which subunit dissociation is expected has the potential for significant enzymatic stabilization.

The final enzyme stabilization approach replaces the synthetic polymer in the first two approaches with an inert biopolymer. In this technique, BSA is orthogonally attached to GOx or Cat at the glycosylation sites, which essentially encapsulates the glycoenzyme within an albumin shell to form the AG. A comparison of chromatograms for the native glycoenzymes and the AGs reveals a large shift in elution volume upon albumination, as well as an increase in the ratio of UV absorbance to visible absorbance. These findings are consistent with bioconjugation of BSA to the enzyme, which is confirmed by particle sizing data showing an approximate 60% increase in hydrodynamic size following modification. Both AGs are extremely resistant to heat-induced aggregation (especially in the case of Cat), which might indicate that the BSA is acting as a molecular chaperone.

BSA-GOx was shown to be much more thermostable than native GOx. Following exposure to buffer at 60 °C, BSA-GOx retained greater than 25 times more activity than native GOx. Albumination of GOx provided moderate stabilization throughout long-term storage, but no stabilizing effect was observed with continuous exposure to glucose. Lastly, BSA-GOx proved to be quite incompatible with solvents of

low relative permittivity and polymer precursor solutions with low water content, losing significant amounts of activity following exposure.

Table 6-1 Comparison of the various glycoenzyme conjugates

	Native GOx	GOx (2.5% GA)	PEG-GOx	PEG-GOx (2.5% GA)	BSA-GOx
Size by DLS (nm)	10.76	13.91	16.98	16.67	20.12
Storage Stability (half-life, days)	$t_{1/2}$ = 5.75	$t_{1/2}$ = 45.5	$t_{1/2}$ = 13.6	$t_{1/2}$ = 49.0	$t_{1/2}$ = 15.3
Operational Stability (% ret.)	24.8 ± 3.81	22.3 ± 5.22	25.4 ± 6.90	29.4 ± 9.10	25.3 ± 7.54
Thermostability (% ret. @ 1 h)	1.69 ± 0.0981	7.51 ± 0.145	21.9 ± 0.843	14.6 ± 1.13	37.7 ± 1.57
Thermostability (half-life from 1st or 2nd-order decays, min)	$t_{1/2}$ = 8.09	$t_{1/2,1}$ = 1.33 (67.1%); $t_{1/2,2}$ = 28.2 (32.9%)	$t_{1/2}$ = 27.0	$t_{1/2,1}$ = 31.2 (55.4%); $t_{1/2,2}$ = 1.78 (44.6%)	$t_{1/2,1}$ = 71.7 (67.3%); $t_{1/2,2}$ = 3.53 (32.7%)
Solvent/Additive Tolerability	Average	Below Average	Excellent	Above Average	Poor

Table 6-1 provides a summary of the physical and functional properties of the various glycoenzyme conjugates, which permits direct comparison among them. As one can see, the choice of the "best" modified glycoenzyme for a particular application will depend upon the intended use and must be considered on a case-by-case basis. The GA-modified PEG-GOx is well-suited for applications in which long-term storage is expected and stability during that time is required. If exposure to elevated temperature is expected, use of BSA-GOx or unmodified PEG-GOx would be advisable. If working with solutions of low relative permittivity or low water content, one should avoid using

BSA-GOx. None of the approaches was shown to directly improve GOx operational stability, but incorporation of Cat—stabilized using one of the appropriate stabilization strategies discussed here—is expected to prolong GOx operation.[6]

Ultimately, each of the various modified enzymes, which have been shown to be stabilized under certain isolated conditions, will need to be systematically incorporated into different candidate hydrogels and tested for long-term glucose response under simulated *in vivo* conditions. Combination systems (*i.e.*, stabilized enzymes and compatible hydrogels) that are promising under simulated *in vivo* conditions will then need to be tested *in vivo* as well. Determination of the "optimal" formulation will be largely based upon a large amount of empirical evidence, and the complexity of this work should not be underestimated. As a first step in that direction, we entrapped PEG-GOx within a pHEMA hydrogel and demonstrated that a reversible glucose response could be observed.

The same general approach was used to encapsulate and test PEG-GOx as was previously reported for the encapsulation and testing of native GOx in a pHEMA hydrogel.[7] Briefly, PEG-GOx and Pd(II) meso-tetra(4-carboxyphenyl) porphine, an oxygen-sensitive phosphor, were combined with a pHEMA precursor solution at final concentrations of 20 μM and 100 μM, respectively. The pHEMA precursor solution comprised 2-hydroxyethyl methacrylate (monomer), tetra(ethyleneglycol) diacrylate (crosslinker), and 2,2-dimethoxy-2-phenylacetophenone (photoinitiator) dissolved in an ethylene glycol/water mixture (the molar ratio of monomer/crosslinker was 98:2). Microscope slides were silanized with (trimethoxysilyl)propyl methacrylate to facilitate

binding of the pHEMA to the glass. The pHEMA precursor solution containing the PEG-GOx and phosphor was then cast into a mold placed directly on the microscope slide and photopolymerized. Four pHEMA hydrogels (*ca.* 2.5 mm in diameter and 1 mm thick) on four separate microscope slides were prepared in this manner from the same stock precursor solution.

To test each pHEMA hydrogel for a glucose response, the microscope slide was placed into a custom-built dynamic testing apparatus[7] and equilibrated in PBS until the baseline phosphorescence signal was stable. The hydrogel was then exposed to random glucose concentrations (2 h per concentration) within a range of 0–400 mg/dL by flowing glucose-containing PBS across the pHEMA hydrogel at a volumetric flow rate of 4 mL/min. A modulated green light-emitting diode (523 nm) was coupled into a bifurcated fiber optic bundle to illuminate the hydrogel, and phosphorescence from the oxygen-sensitive phosphor was captured through the same fiber bundle. Luminescence lifetime measurements were collected using a frequency-domain lifetime system (TauTheta model MFPF-100).

Fig. 6-1 shows the sensor response that was obtained by entrapping PEG-GOx and an oxygen-sensitive phosphor in a pHEMA hydrogel. As described above, four separate hydrogels were prepared by casting the pHEMA precursor solution into a mold placed on a microscope slide. Data points represent the average luminescence lifetimes at each glucose concentration, and error bars represent 95% confidence intervals ($n = 4$). The sensor response is approximately linear, and luminescence lifetime values increase by 220 ± 73% over the physiologically-relevant glucose range (*i.e.*, 0–400 mg/dL).

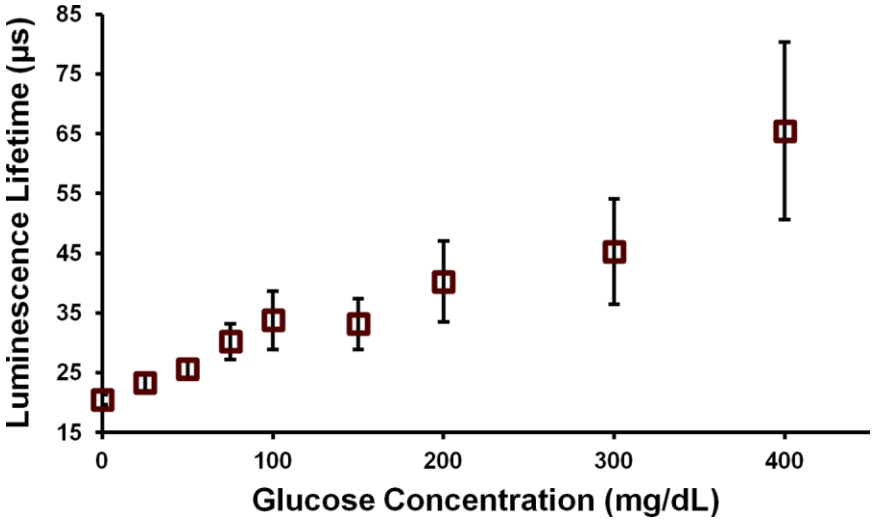

Fig. 6-1 Sensor response obtained by entrapping PEG-GOx and an oxygen-sensitive phosphor in a pHEMA hydrogel. Data represent the average luminescence lifetimes at each glucose concentration, and error bars represent 95% confidence intervals (n = 4).

We have also incorporated BSA-GOx into a pHEMA hydrogel-immobilized sensing assay to determine whether the sensor response was stabilized (compared to a pHEMA hydrogel comprising native GOx) during extended exposure to repeated glucose flight plans. BSA-GOx was entrapped within a pHEMA hydrogel and tested for a glucose response in a dynamic testing apparatus as described above. Fig. 6-2 shows that while both native glycoenzyme- and AG-containing hydrogels respond to varying glucose concentrations over a 40-hour period, those hydrogels containing BSA-GOx (red line) were shown to be nearly *three times more stable* (*i.e.*, three times slower degradation of luminescence lifetime at 400 mg/dL for BSA-GOx) than those containing native GOx (blue line). Improved thermostability of the BSA-GOx likely ensures that more enzyme remains active following the photopolymerization process; however, as the enzymes were merely entrapped and not covalently bound to the hydrogel network, the

increased hydrodynamic size resulting from albumination could have contributed to the observed increase in operational stability as well. As discussed previously, addition of Cat or BSA-Cat could even further improve this stability. These findings are encouraging and suggest that these modified enzymes hold promise for improving the long-term operational stability of optical glucose-sensing hydrogels.

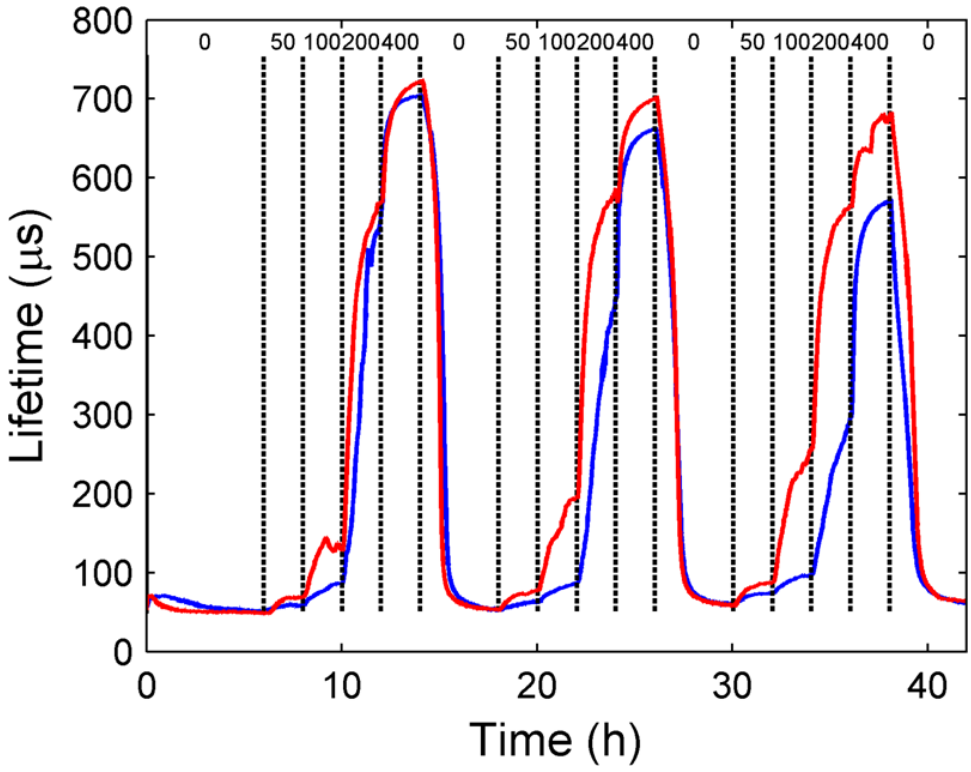

Fig. 6-2 Sensor response of glucose-sensitive hydrogels containing BSA-GOx (red line) and native GOx (blue line) during extended exposure to repeated glucose flight plans.

Despite these promising results, there are a number of intermediate steps that should be taken to facilitate incorporation of these modified enzymes into glucose-sensing hydrogels. First, the techniques used to produce the stabilized enzymes do not

yield large quantities of product, which increases the cost and time intensiveness. This also leads to secondary issues, such as loss of activity from lyophilized stock GOx due to long-term storage and multiple freeze-thaw cycles. As such, these techniques will need to be "scaled-up" such that incorporation into hydrogels and testing at the required scale becomes feasible. Alternatively, the amount of enzyme required to be immobilized within the hydrogels could be reduced, but this could have unintended consequences on sensor response and/or sensor longevity.

Development of appropriate lyophilization strategies for the modified enzymes would also be beneficial, as this would permit their storage for longer periods of time with reduced activity loss (as compared to solution-phase storage). Moreover, lyophilized (dry) product could be added to polymer precursor solutions to yield higher final enzyme concentrations in the glucose-sensing hydrogels.

Finally, while physical entrapment of the modified enzymes within the hydrogels may be sufficient for early simulated *in vivo* testing to show proof of concept, covalent attachment of the modified enzymes to the hydrogel in which they are incorporated would be ideal. Release of enzyme will lead to response degradation, leached enzyme could elicit a host response that further degrades sensor response, and most importantly, leached enzyme could have deleterious effects on the host.

Covalent attachment of BSA-GOx should be relatively straightforward, as the BSA surface presents 30–35 solvent-accessible lysine ε-amino groups and even more carboxylic acids (pI of BSA is 5.1). BSA-GOx could be directly attached to amine groups on pHEMA-*co*-AEMA using carbodiimide chemistry or a dialdehyde.

Alternatively, the surface of BSA-GOx could be decorated with amine-reactive heterobifunctional crosslinkers presenting acrylate groups on the distal end, which would permit covalent incorporation of the BSA-GOx during photopolymerization.

Because PEG-GOx and GA-modified PEG-GOx were designed to have inert surfaces, covalent attachment of these modified enzymes will be more challenging. The most obvious approach would be to replace the methoxy-terminated PEG-Hz with another heterobifunctional PEG-Hz. Unfortunately, there is not a diverse selection of commercially available heterobifunctional PEG-Hz, which might require custom synthesis of PEG derivatives. In this case, a photo-activatable distal group would be ideal, in that one could easily incorporate the PEG-GOx or GA-modified PEG-GOx during photopolymerization. Alternatively, an acid-terminated PEG-Hz could allow for enzyme attachment to a pHEMA-*co*-AEMA hydrogel *via* carbodiimide chemistry without the need for a protecting group. Lastly, the approach to prepare GA-modified PEG-GOx could be altered to employ a detachable PEG chain that could prevent aggregation during chemical modification, but allow for subsequent removal and return of the enzyme to its native size. Standard approaches, which are currently utilized to covalently bind native GOx to our current glucose-sensing hydrogels, could then be employed. These various strategies are outlined below in Table 6-2.

Table 6-2 Proposed strategies for glycoenzyme conjugate attachment to hydrogels

Target on Glycoenzyme	Target on Hydrogel(s)	Linker Chemistry	Modification to Current Design
COOH on BSA-GOx	NH_2 on pHEMA-*co*-AEMA	EDC/Sulfo-NHS	None
NH_2 on BSA-GOx	NH_2 on pHEMA-*co*-AEMA	dialdehydes	None
NH_2 on BSA-GOx	Incorporation during photopolymerization	acrylate-terminated heterobifunctional crosslinker + UV	None
COOH on PEG-GOx or GA-modified PEG-GOx	NH_2 on pHEMA-*co*-AEMA	EDC/Sulfo-NHS	Must employ acid-terminated PEG-Hz
Acrylate on PEG-GOx or GA-modified PEG-GOx	Incorporation during photopolymerization	UV	Must employ acrylate-terminated PEG-Hz
COOH on GA-modified GOx	NH_2 on pHEMA-*co*-AEMA	EDC/Sulfo-NHS	Must employ a detachable PEG

In summary, three enzyme modification strategies were developed, and the resulting glycoenzyme conjugates were thoroughly characterized physically, chemically, and functionally. This work has laid the foundation for further investigation, as well as incorporation of these stabilized glycoenzymes into optical glucose biosensing systems. Finally, it is expected that these modification strategies will have broader impacts as well, as other researchers can directly apply these modification techniques to stabilize other proteins or enzymes, or adapt the approaches presented herein as necessary.

REFERENCES

1. The Diabetes Control and Complications Trial Research Group, *N. Engl. J. Med.*, 1993, **329**, 977-986.
2. A. Heller and B. Feldman, *Chem. Rev.*, 2008, **108**, 2482-2505.
3. J. Q. Brown, R. Srivastava and M. J. McShane, *Biosens. Bioelectron.*, 2005, **21**, 212-216.
4. E. W. Stein, P. S. Grant, H. Zhu and M. J. McShane, *Anal. Chem.*, 2007, **79**, 1339-1348.
5. E. W. Stein, S. Singh and M. J. McShane, *Anal. Chem.*, 2008, **80**, 1408-1417.
6. S. Singh and M. McShane, *Biosens. Bioelectron.*, 2010, **25**, 1075-1081.
7. J. R. Roberts, J. Park, K. Helton, N. Wisniewski and M. J. McShane, *J. Diabetes Sci. Technol.*, 2012, **6**, 1267-1275.
8. P. H. S. Tse and D. A. Gough, *Biotechnol. Bioeng.*, 1987, **29**, 705-713.
9. W. L. Clarke, D. Cox, L. A. Gonder-Frederick, W. Carter and S. L. Pohl, *Diabetes Care*, 1987, **10**, 622-628.
10. F. A. Quiocho and F. M. Richards, *Proc. Natl. Acad. Sci. U. S. A.*, 1964, **52**, 833-839.
11. L. Cao, F. van Rantwijk and R. A. Sheldon, *Org. Lett.*, 2000, **2**, 1361-1364.
12. L. Cao, L. v. Langen and R. A. Sheldon, *Curr. Opin. Biotechnol.*, 2003, **14**, 387-394.

13. R. Schoevaart, M. W. Wolbers, M. Golubovic, M. Ottens, A. P. G. Kieboom, F. van Rantwijk, L. A. M. van der Wielen and R. A. Sheldon, *Biotechnol. Bioeng.*, 2004, **87**, 754-762.

14. R. A. Sheldon, R. Schoevaart and L. M. Van Langen, *Biocatal. Biotransform.*, 2005, **23**, 141-147.

15. R. Sheldon, *Appl. Microbiol. Biotechnol.*, 2011, **92**, 467-477.

16. J. I. Lopez-Cruz, G. Viniegra-Gonzalez and A. Hernandez-Arana, *Bioconjugate Chem.*, 2006, **17**, 1093-1098.

17. A. Matsushima, Y. Kodera, M. Hiroto, H. Nishimura and Y. Inada, *J. Mol. Catal. B: Enzym.*, 1996, **2**, 1-17.

18. J. A. Rodriguez-Martinez, I. Rivera-Rivera, R. J. Sola and K. Griebenow, *Biotechnol. Lett.*, 2009, **31**, 883-887.

19. F. M. Veronese, P. Caliceti, O. Schiavon and L. Sartore, in *Poly(ethylene Glycol) Chemistry: Biotechnical and Biomedical Applications*, ed. J. M. Harris, Plenum Press, New York, 1992, ch. 9, pp. 127-137.

20. C. Mateo, J. M. Palomo, G. Fernandez-Lorente, J. M. Guisán and R. Fernández-Lafuente, *Enzyme Microb. Technol.*, 2007, **40**, 1451-1463.

21. S. Zalipsky, *Adv. Drug Delivery Rev.*, 1995, **16**, 157-182.

22. S. Zalipsky, *Bioconjugate Chem.*, 1995, **6**, 150-165.

23. D. W. Ritter, J. R. Roberts and M. J. McShane, *Enzyme Microb. Technol.*, 2013, **52**, 279-285.

24. D. W. Ritter, J. M. Newton and M. J. McShane, *RSC Adv.*, 2014, **4**, 28036-28040.

25. O. Barbosa, C. Ortiz, Á. Berenguer-Murcia, R. Torres, R. C. Rodrigues and R. Fernández-Lafuente, *RSC Adv.*, 2014, **4**, 1583-1600.

26. P. V. Iyer and L. Ananthanarayan, *Process Biochem.*, 2008, **43**, 1019-1032.

27. D. Brady and J. Jordaan, *Biotechnol. Lett.*, 2009, **31**, 1639-1650.

28. R. Fernández-Lafuente, *Enzyme Microb. Technol.*, 2009, **45**, 405-418.

29. C. Garcia-Galan, Á. Berenguer-Murcia, R. Fernández-Lafuente and R. C. Rodrigues, *Adv. Synth. Catal.*, 2011, **353**, 2885-2904.

30. R. C. Rodrigues, Á. Berenguer-Murcia and R. Fernández-Lafuente, *Adv. Synth. Catal.*, 2011, **353**, 2216-2238.

31. E. T. Hwang and M. B. Gu, *Eng. Life Sci.*, 2013, **13**, 49-61.

32. R. C. Rodrigues, C. Ortiz, Á. Berenguer-Murcia, R. Torres and R. Fernández-Lafuente, *Chem. Soc. Rev.*, 2013, **42**, 6290-6307.

33. V. Stepankova, S. Bidmanova, T. Koudelakova, Z. Prokop, R. Chaloupkova and J. Damborsky, *ACS Catal.*, 2013, **3**, 2823-2836.

34. S. Cantone, V. Ferrario, L. Corici, C. Ebert, D. Fattor, P. Spizzo and L. Gardossi, *Chem. Soc. Rev.*, 2013, **42**, 6262-6276.

35. J. M. Bolivar, L. Wilson, S. A. Ferrarotti, J. M. Guisán, R. Fernández-Lafuente and C. Mateo, *J. Biotechnol.*, 2006, **125**, 85-94.

36. B. C. C. Pessela, C. Mateo, M. Fuentes, A. Vian, J. L. García, A. V. Carrascosa, J. M. Guisán and R. Fernández-Lafuente, *Enzyme Microb. Technol.*, 2003, **33**, 199-205.

37. C. Mateo, R. Monti, B. C. C. Pessela, M. Fuentes, R. Torres, J. Manuel Guisán and R. Fernández-Lafuente, *Biotechnol. Progr.*, 2004, **20**, 1259-1262.

38. C. Mateo, G. Fernández-Lorente, O. Abian, R. Fernández-Lafuente and J. M. Guisán, *Biomacromolecules*, 2000, **1**, 739-745.

39. C. Mateo, O. Abian, R. Fernandez–Lafuente and J. M. Guisan, *Enzyme Microb. Technol.*, 2000, **26**, 509-515.

40. F. López-Gallego, L. Betancor, C. Mateo, A. Hidalgo, N. Alonso-Morales, G. Dellamora-Ortiz, J. M. Guisán and R. Fernández-Lafuente, *J. Biotechnol.*, 2005, **119**, 70-75.

41. R. Axen, J. Porath and S. Ernback, *Nature*, 1967, **214**, 1302-1304.

42. K. Sarıoğlu, N. Demir, J. Acar and M. Mutlu, *J. Food Eng.*, 2001, **47**, 271-274.

43. B. Solomon and Y. Levin, *Biotechnol. Bioeng.*, 1974, **16**, 1161-1177.

44. W. Tischer and K. Volker, *Trends Biotechnol.*, 1999, **17**, 326-335.

45. C. Mateo, A. Chmura, S. Rustler, F. van Rantwijk, A. Stolz and R. A. Sheldon, *Tetrahedron: Asymmetry*, 2006, **17**, 320-323.

46. S. Dalal, M. Kapoor and M. N. Gupta, *J. Mol. Catal. B: Enzym.*, 2007, **44**, 128-132.

47. R. A. Sheldon, *Adv. Synth. Catal.*, 2007, **349**, 1289-1307.

48. J. M. González-Sáiz and C. Pizarro, *Eur. Polym. J.*, 2001, **37**, 435-444.

49. K. Won, S. Kim, K.-J. Kim, H. W. Park and S.-J. Moon, *Process Biochem.*, 2005, **40**, 2149-2154.

50. N. Munjal and S. K. Sawhney, *Enzyme Microb. Technol.*, 2002, **30**, 613-619.

51. M. T. Reetz and K.-E. Jaeger, *Chem. Phys. Lipids*, 1998, **93**, 3-14.

52. N. Bruns and J. C. Tiller, *Nano Lett.*, 2004, **5**, 45-48.

53. J. Lalonde and A. Margolin, in *Enzyme Catalysis in Organic Synthesis*, eds. K. Drauz and H. Waldmann, Wiley-VCH, Germany, 2008, ch. 6, pp. 163-184.

54. S. Ohlson, P.-O. Larsson and K. Mosbach, *Eur. J. Appl. Microbiol.*, 1979, **7**, 103-110.

55. J. Vaija, Y.-Y. Linko and P. Linko, *Appl. Biochem. Biotechnol.*, 1982, **7**, 51-54.

56. J. M. Lee and J. Woodward, *Biotechnol. Bioeng.*, 1983, **25**, 2441-2451.

57. M. Koudelka-Hep, N. F. de Rooij and D. J. Strike, in *Immobilization of Enzymes and Cells*, ed. G. F. Bickerstaff, Humana Press, New Jersey, 1997, DOI: 10.1385/0-89603-386-4:83, ch. 10, pp. 83-85.

58. S. M. Ryan, G. Mantovani, X. Wang, D. M. Haddleton and D. J. Brayden, *Expert Opin. Drug Delivery*, 2008, **5**, 371-383.

59. P. Bailon and C.-Y. Won, *Expert Opin. Drug Delivery*, 2009, **6**, 1-16.

60. C. J. Fee and J. M. van Alstine, *Bioconjugate Chem.*, 2004, **15**, 1304-1313.

61. K. Hinds, J. J. Koh, L. Joss, F. Liu, M. Baudyš and S. W. Kim, *Bioconjugate Chem.*, 2000, **11**, 195-201.

62. A. Basu, K. Yang, M. Wang, S. Liu, R. Chintala, T. Palm, H. Zhao, P. Peng, D. Wu, Z. Zhang, J. Hua, M.-C. Hsieh, J. Zhou, G. Petti, X. Li, A. Janjua, M.

Mendez, J. Liu, C. Longley, Z. Zhang, M. Mehlig, V. Borowski, M. Viswanathan and D. Filpula, *Bioconjugate Chem.*, 2006, **17**, 618-630.

63. C. Dhalluin, A. Ross, L.-A. Leuthold, S. Foser, B. Gsell, F. Müller and H. Senn, *Bioconjugate Chem.*, 2005, **16**, 504-517.

64. A. Crueger and W. Crueger, in *Microbial enzymes and biotechnology*, eds. W. M. Fogarty and C. T. Kelly, Elsevier Applied Science, London, 1990, ch. 5, pp. 177-226.

65. R. Wilson and A. P. F. Turner, *Biosens. Bioelectron.*, 1992, **7**, 165-185.

66. Q. H. Gibson, V. Massey and B. E. P. Swoboda, *J. Biol. Chem.*, 1964, **239**, 3927-3934.

67. G. Wohlfahrt, S. Witt, J. Hendle, D. Schomburg, H. M. Kalisz and H.-J. Hecht, *Acta Crystallogr. D*, 1999, **55**, 969-977.

68. H. Tsuge, O. Natsuaki and K. Ohashi, *J. Biochem.*, 1975, **78**, 835-843.

69. J. H. Pazur, K. Kleppe and E. M. Ball, *Arch. Biochem. Biophys.*, 1963, **103**, 515-516.

70. B. E. P. Swoboda and V. Massey, *J. Biol. Chem.*, 1965, **240**, 2209-2215.

71. H. J. Hecht, H. M. Kalisz, J. Hendle, R. D. Schmid and D. Schomburg, *J. Mol. Biol.*, 1993, **229**, 153-172.

72. G. Zoldák, A. Zubrik, A. Musatov, M. Stupák and E. Sedlák, *J. Biol. Chem.*, 2004, **279**, 47601-47609.

73. J. J. O'Malley and J. L. Weaver, *Biochemistry*, 1972, **11**, 3527-3532.

74. H. Tsuge and H. Mitsuda, *J. Biochem.*, 1974, **75**, 399-406.

75. O. M. Lardinois, M. M. Mestdagh and P. G. Rouxhet, *Biochim. Biophys. Acta, Protein Struct. Mol. Enzymol.*, 1996, **1295**, 222-238.

76. K. Kikuchi-Torii, S. Hayashi, H. Nakamoto and S. Nakamura, *J. Biochem.*, 1982, **92**, 1449-1456.

77. D. Scott and F. Hammer, *Enzymologia*, 1960, **22**, 229-237.

78. L. S. Kumosa, T. L. Routh, J. T. Lin, J. Y. Lucisano and D. A. Gough, *Biomaterials*, 2014, **35**, 8287-8296.

79. A. Abuchowski, T. van Es, N. C. Palczuk and F. F. Davis, *J. Biol. Chem.*, 1977, **252**, 3578-3581.

80. S. Jevševar, M. Kunstelj and V. G. Porekar, *Biotechnol. J.*, 2010, **5**, 113-128.

81. G. Pasut and F. M. Veronese, *J. Controlled Release*, 2012, **161**, 461-472.

82. F. M. Veronese, *Biomaterials*, 2001, **22**, 405-417.

83. C. J. Fee and J. M. van Alstine, *Chem. Eng. Sci.*, 2006, **61**, 924-939.

84. P. Bailon and W. Berthold, *Pharm. Sci. Technol. Today*, 1998, **1**, 352-356.

85. S. Zalipsky and S. Menon-Rudolph, in *Poly(ethylene glycol)*, eds. J. M. Harris and S. Zalipsky, American Chemical Society, Washington, D.C., 1997, vol. 680, ch. 21, pp. 318-341.

86. S. Nakamura, S. Hayashi and K. Koga, *Biochim. Biophys. Acta, Enzymol.*, 1976, **445**, 294-308.

87. B. Skoog, *Vox Sang.*, 1979, **37**, 345-349.

88. H. U. Bergmeyer, K. Gawehn and M. Grassl, *Methods of enzymatic analysis*, Academic Press, New York, 2nd edn., 1974.

89. R. P. Hartshorne and W. A. Catterall, *J. Biol. Chem.*, 1984, **259**, 1667-1675.

90. C. J. Skerrow and A. G. Matoltsy, *J. Cell Biol.*, 1974, **63**, 524-530.

91. B. Unterweger, T. Stoisser, S. Leitgeb, R. Birner-Grünberger and B. Nidetzky, *Bioconjugate Chem.*, 2012, **23**, 1406-1414.

92. Q. Chen, G. L. Kenausis and A. Heller, *J. Am. Chem. Soc.*, 1998, **120**, 4582-4585.

93. G. Fortier and D. Belanger, *Biotechnol. Bioeng.*, 1991, **37**, 854-858.

94. M. D. Gouda, S. A. Singh, A. G. A. Rao, M. S. Thakur and N. G. Karanth, *J. Biol. Chem.*, 2003, **278**, 24324-24333.

95. S. Krishnaswamy and J. R. Kittrell, *Biotechnol. Bioeng.*, 1978, **20**, 821-835.

96. S. J. Li, Y. Umena, K. Yorita, T. Matsuoka, A. Kita, K. Fukui and Y. Morimoto, *Biochem. Biophys. Res. Commun.*, 2007, **358**, 1002-1007.

97. A. Slavica, I. Dib and B. Nidetzky, *Biotechnol. Bioeng.*, 2007, **96**, 9-17.

98. L. Pollegioni, S. Buto, W. Tischer, S. Ghisla and M. Pilone, *Biochem. Mol. Biol. Int.*, 1993, **31**, 709-717.

99. K. B. Hadley and P. H. Sato, *Enzyme*, 1989, **42**, 225-234.

100. S. L. Seymour and J. P. Klinman, *Biochemistry*, 2002, **41**, 8747-8758.

101. S. J. Stocks, A. J. Jones, C. W. Ramey and D. E. Brooks, *Anal. Biochem.*, 1986, **154**, 232-234.

102. A. Haouz, J. M. Glandières and B. Alpert, *FEBS Lett.*, 2001, **506**, 216-220.

103. K. Hernandez, Á. Berenguer-Murcia, R. C. Rodrigues and R. Fernández-Lafuente, *Curr. Org. Chem.*, 2012, **16**, 2652-2672.

104. L. Betancor, F. López-Gallego, A. Hidalgo, N. Alonso-Morales, G. Dellamora-Ortiz, J. M. Guisán and R. Fernández-Lafuente, *J. Biotechnol.*, 2006, **121**, 284-289.

105. W.-N. Ye and D. Combes, *Biochim. Biophys. Acta, Protein Struct. Mol. Enzymol.*, 1989, **999**, 86-93.

106. R. Wetzel, M. Becker, J. Behlke, H. Billwitz, S. Böhm, B. Ebert, H. Hamann, J. Krumbiegel and G. Lassmann, *Eur. J. Biochem.*, 1980, **104**, 469-478.

107. B. S. Chang and R. R. Mahoney, *Biotechnol. Appl. Biochem.*, 1995, **22**, 203-214.

108. I. Marini, R. Moschini, A. D. Corso and U. Mura, *Cell. Mol. Life Sci.*, 2005, **62**, 3092-3099.

109. T. E. Finn, A. C. Nunez, M. Sunde and S. B. Easterbrook-Smith, *J. Biol. Chem.*, 2012, **287**, 21530-21540.

110. S. Myung, Y. H. P. Zhang and J. Sanchez Ruiz, *PLoS ONE*, 2013, **8**, e61500.

111. P. G. Squire, P. Moser and C. T. O'Konski, *Biochemistry*, 1968, **7**, 4261-4272.

112. S. B. Zimmerman and S. O. Trach, *J. Mol. Biol.*, 1991, **222**, 599-620.

113. H. Yoshikawa, A. Hirano, T. Arakawa and K. Shiraki, *Int. J. Biol. Macromol.*, 2012, **50**, 1286-1291.